# Reconstruction of paleo-environmental landscape characteristics of the Sarno River plain (Campania, Italy) before the volcanic eruption of Somma-Vesuvius AD 79

Dissertation of the Faculty of Science at the
Eberhard Karls University of Tübingen, Germany
for the degree of Doctor of Natural Sciences (Doctor rerum naturalium).

submitted by

Sebastian Vogel

Tübingen

2011

Day of oral qualification:

Dean: Wolfgang Rosenstiel

1st referee: Prof. Dr. Volker Hochschild,

2nd referee: Dr. Michael Märker

The photograph on the front cover is used with kind permission of Dr. Florian Seiler.

Table of contents

List of figures

Acknowledgments

First of all special thank goes to my doctoral supervisor Michael Märker for his advice, support, collegiality and friendship. He was of great help developing this project and he always had a sympathetic ear for me when he wasn't traveling the world for his various research projects. Then, I would also like to thank Florian Seiler for the initialization of this very interesting geoarchaeological research project, for introducing me into Pompeii and Italian cuisine at Leopoldo's and into the field methods of archaeological excavations. To make the research team complete a great thank goes to Pia Kastenmeier for organizing literally everything in Pompeii and for patiently dealing with all the local partners and authorities. To all three of you, I couldn't imagine to work in a better, more friendly and more inspiring working atmosphere. Furthermore, I would like to thank my second reviewer Volker Hochschild for reading and reviewing this thesis.

Last but not least deep appreciation goes to my friends and family, especially to my parents for their endless support and love during the last 33 years, to my grandparents for their continuous interest in my work and for being a good example for people that dedicate their life for science and to my partner Andrea for her unlimited warmth and love and for her infectious lust for life.

Summary

The explosive eruption of Somma-Vesuvius volcanic complex AD 79 belongs to the most well-known eruptions in history above all because it destroyed the Roman settlements of Herculaneum, Stabiae and Pompeii. During the eruption the south-eastern peri-volcanic territory, including the entire Sarno River plain, was buried with pumice lapilli fallout and pyroclastic surge/flow deposits. This resulted in a sealing and to a certain extent preservation not only of archaeological remains and artifacts but also of the pre-AD 79 paleo-topography and paleo-environmental conditions. Since the AD 79 volcanic deposits of Somma-Vesuvius show a specific stratigraphic sequence and are laterally extensive, they can be considered as a chronostratigraphic marker for the identification of the pre-AD 79 Roman period.

The present work is part of a geoarchaeological research project implemented by the German Archaeological Institute and the Heidelberg Academy of Sciences and Humanities and funded by the German Research Foundation (DFG). It is entitled "Reconstruction of the ancient cultural landscape of the Sarno River plain (Campania, Italy)" (www.salve-research.org). This geographical subproject aims at analyzing and reconstructing selected paleo-environmental landscape characteristics of the Sarno River plain to provide detailed insights into the paleo-environmental conditions before the eruption of Somma-Vesuvius AD 79. These paleo-conditions can be considered as fundamental for the understanding of ancient settlement dynamic and rural economy in the Sarno River plain, i.e. of the interactive human-environment relationship in the pre-Roman and Roman period.

To contribute to the above mentioned objectives this work draws special attention on the following three aspects:

(i)   the reconstruction of the pre-AD 79 paleo-topography and selected paleo-environmental and paleo-geomorphological features,

(ii)   the characterization of the pre-AD 79 Roman paleosol south of Pompeii and the analysis of correlations between soil parameter values and the pre-AD 79 paleo-topography, and

(iii) the analysis of post-burial soil developments of the pre-AD 79 Roman paleosol.

Zusammenfassung

Die explosive Eruption des Somma-Vesuvius' AD 79 zählt zu den bekanntesten vulkanischen Eruptionen in der Geschichte, nicht zuletzt aufgrund der Zerstörung der antiken Städte von Herculaneum, Stabiae und Pompeji. Während des Ausbruchs wurde das Gebiet südöstlich des Vulkans, darunter die gesamte Sarno-Ebene, durch den Niederschlag von Bimssteinlapilli und pyroklastischen Ascheströmen verschüttet. Das hatte zur Folge, dass nicht nur archäologische Befunde und Artefakte, sondern auch die paläo-topographischen und Paläo-Umweltbedingungen der Sarno-Ebene versiegelt und daher mehr oder weniger konserviert wurden. Da die vulkanischen Ablagerungen von AD 79 über eine spezifische stratigraphische Abfolge und eine große räumliche Ausdehnung verfügen, können sie als chrono-stratigraphischer Marker für die Identifizierung der römischen Epoche vor AD 79 verwendet werden.

Die vorliegende Arbeit ist Teil eines geoarchäologischen Forschungsprojektes mit dem Titel „Rekonstruktion der antiken Kulturlandschaft der Sarno-Ebene (Campania, Italien)" initiiert durch das Deutsche Archäologische Institut und der Heidelberger Akademie der Wissenschaften und finanziert von der Deutschen Forschungsgemeinschaft (www.salve-research.org). Das geographische Teilprojekt hat zum Ziel, ausgewählte Paläo-Umweltbedingungen der Sarno-Ebene vor dem Ausbruch des Somma-Vesuvius' AD 79 zu analysieren und zu rekonstruieren. Die Kenntnis dieser Paläo-Umweltbedingungen ist fundamental für das Verständnis der antiken ländlichen Siedlungsdynamik und Agrarstruktur der Sarno-Ebene und damit der interaktiven Mensch-Umwelt-Beziehung in vorrömischer und römischer Zeit.

Entsprechend des oben genannten Forschungsziels werden innerhalb des geographischen Teilprojektes die folgenden drei Schwerpunkte gesetzt:

(i) die Rekonstruktion der Paläo-Topographie und ausgewählter Paläo-Umweltbedingungen der Sarno-Ebene vor dem Ausbruch des Somma-Vesuvius' AD 79,

(ii)   die Charakterisierung der römischen Paläo-Böden südlich des antiken Pompejis und die Analyse der Korrelation zwischen Bodenparameter-Ausprägung und paläo-topographischer Lage,

(iii)   die Analyse pedogenetischer Veränderungen innerhalb des römischen Paläo-Bodens nach seiner Verschüttung AD 79.

1
Synopsis

1.1 Introduction

At all times in human history peri-volcanic regions have been preferred areas for human settlement above all due to their abundance of periodically replenishing natural resources. Volcanic rocks such as tuff or lava were utilized as building materials whereas the productivity of volcanic soils favored the establishment of settled agriculture. In general, volcanic ash serves as an ideal parent material for the development of fertile soils. They are characterized by (Shoji and Takahashi, 2002):

  (i)   rapid restoration of vegetation and soil environment soon after ash deposition,

 (ii)   accumulation of high amounts of organic carbon and nitrogen,

(iii)   high concentrations of micronutrients being essential for plant growth,

(iv)   high porosity and water retention capacity and

 (v)   large amounts of clay minerals due to the rapid weathering of volcanic glass.

Apart from these long-term beneficial conditions for settlement and agriculture, in the short term volcanic regions are on the other hand repeatedly subject to highly destructive natural catastrophes (e.g. volcanic eruptions, earthquakes, bradyseism, lahars) triggering transformation processes that alter the landscape morphogenetically (Seiler, 2008). Consequently, in history cultural landscapes that owe their existence to the adjacent volcanos were at the same time continuously threatened by their activity.

Amongst volcanic eruptions explosive (Plinian) eruptions are the most powerful and destructive due to the violent ejection of large amounts of pyroclastic material by means of an eruptive column that can extent some tens of kilometers high in the stratosphere. Consequently, dependent on high altitude wind direction and wind speed a large area of the peri-volcanic territory can be affected by the resulting pyroclastic fallout.

Recurring volcanic deposition and intermediate volcanic quiescence that allow for pedogenetic transformations within the substrate lead to the creation of multi-layered stratigraphies (Shoji and Takahashi, 2002). In these stratigraphies not only archaeological remains and artifacts are well preserved but also buried paleo-surfaces and paleo-strata (e.g. paleosols). They provide detailed paleo-environmental data on the conditions prior to burial, for instance in terms of paleo-topography and

paleo-pedology. In association with the archaeological findings these paleo-environmental data can be of great relevance for geoarchaeological research aiming at the reconstruction of past cultural landscapes that were buried by volcanic deposition. Moreover, by expanding our knowledge about ancient civilizations that lived in the shade of an active volcano and were affected by an explosive eruption may also allow to draw important conclusions on present-day volcanic regions. This is because the above mentioned preference of volcanic regions for human settlement is not exclusively the case for the past. In contrast, until the present day volcanic regions belong to the most densely populated and most intensely cultivated areas in world.

The general aim of the present PhD thesis is to reconstruct selected paleo-environmental landscape characteristics of the Sarno River plain before the explosive eruption of Somma-Vesuvius AD 79. It is part of the geoarchaeological research project "Reconstruction of the ancient cultural landscape of the Sarno River plain (Campania, Italy)" that was established by the German Archaeological Institute and the Heidelberg Academy of Sciences and Humanities. This work is subdevided into two parts: the synopsis and the manuscripts. The synopsis is structured as follows. Firstly, I will give an introduction into the research area and the volcanic activity of Somma-Vesuvius. Secondly, I will describe the research objectives of my work and present the three geographical subprojects including a brief introduction into the subject and a description of the methodology applied and the main results. Finally, I will give a conlusion of my research and define potential future research activities. The second part of this thesis contains the manuscripts of the four respective research papers from which two are published, one is accepted for publication and one is in the review process.

1.2 Material and methods

1.2.1 Research area

The Sarno River basin is a cultural landscape that is characterised by continuous anthropogenic activity since the Middle Bronze Age. This intramontane basin in the south of Italy is embedded between the volcanic complex of Somma-Vesuvius (1,281 m a.s.l.) in the north and the Apennine mountain range in the south (Lattari

Mountains, Monte Faito: 1,131 m a.s.l.) and in the east (Sarno Mountains). It opens to the Tyrrhenian Sea (Gulf of Naples) in the west and is drained by the Sarno River and its tributaries (Fig. 1).

The Sarno River plain has a surface area of approximately 210 km^2 and can be subdevided into the following geomorphological landscape units: (i) Tyrrhenian coast, (ii) alluvial plain, (iii) footslopes of Mount Somma-Vesuvius volcanic complex, and (iv) footslopes of the carbonatic rocks of the Lattari and Sarno Mountains (Fig 1). Geographically the Sarno River plain is part of the great graben structure of the Campanian Plain that was formed at the end of the Apennine orogenesis as a result of Plio-Pleistocene extensional tectonic phases. The Sarno River plain consists of marine, alluvial and volcanic deposits lying on top of a carbonate platform that reaches down to a maximum depth of 2 km b.s.l. (Cella et al., 2007).

Figure 1. Digital elevation model (DEM) of the Sarno River plain with the Sarno River network and sites of particular interest (white letters) (top) and different landscape units (bottom). The small scale map shows Italy with the location of the research area and the Apennine mountain ridge.
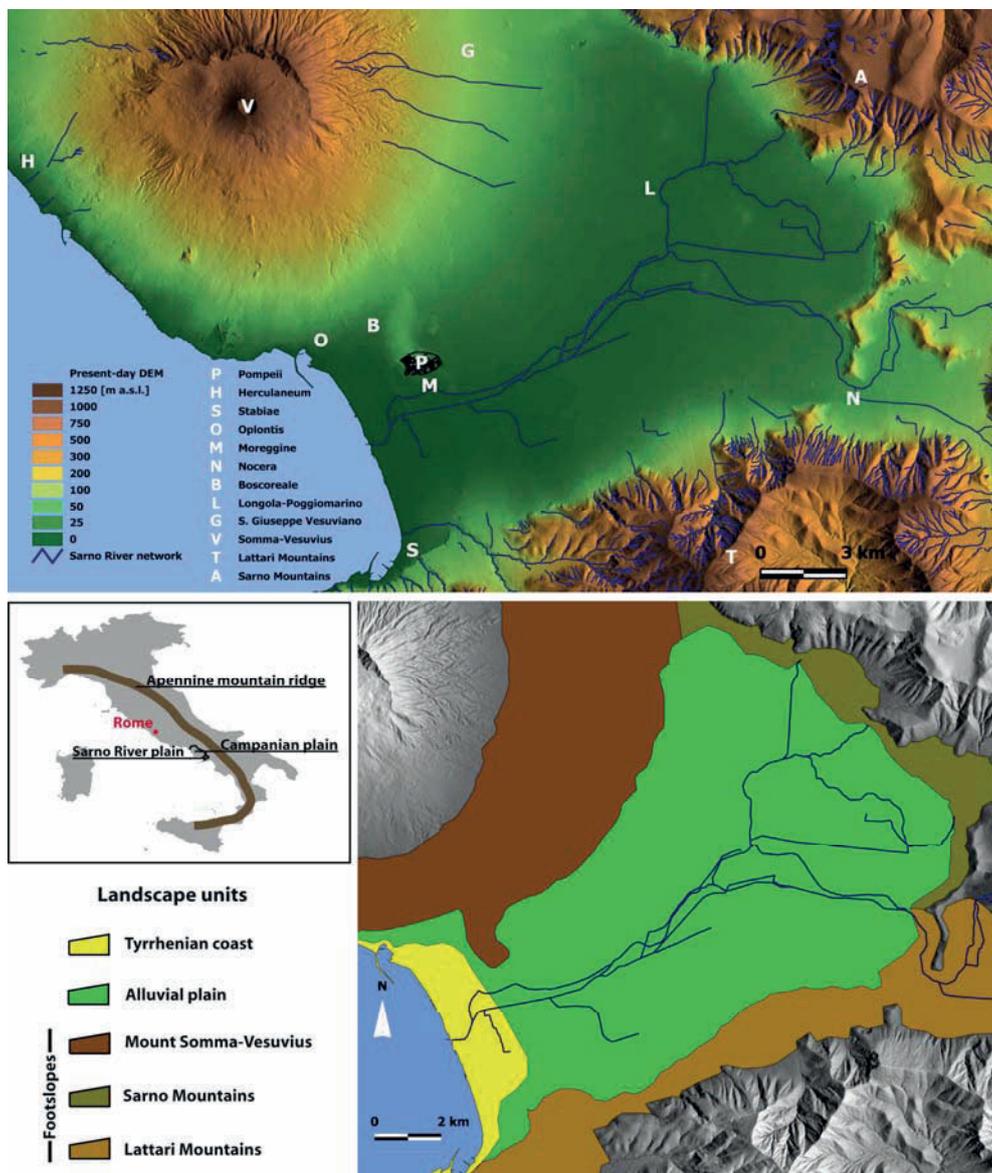
The research area is characterized by a Mediterranean climate with almost 70 % of the annual precipitation falling between October and March and a pronounced dry summer season. On a longterm average the mean annual precipitation is 865 mm whereas November is the wettest (129 mm) and July the driest month (16 mm). The mean annual temperature is 17.4 °C. With 25.7 °C August is the hottest month and January is coolest showing 9.6 °C (Osservatorio Meteorologico, Università di Napoli Federico II, from 1870 to today).

The soils of the Sarno River plain are particularly influenced by the volcanic activity of Somma-Vesuvius. They develop on ash, pumice lapilli fallout, scoria, pyroclastic surges and lava flows whereas pedogenesis especially depends on the deposition modalities of the volcanic material, the pedoclimatic conditions, anthropogenic activity and time (Lulli, 2007). Three sub-groups of soil formation can be distinguished (Di Gennaro and Terribile, 1999, modified):

 (i)   soils on old pyroclastic deposits showing weak to moderate profile differentiation and vitric, vitrandic or andic properties,

 (ii) calcareous volcanic soils with mollic features developing on pyroclastic deposits containing calcium carbonate (Lattari and Sarno Mountains) and

(iii) weakly developed soils (Regosols) on lapilli and ash from the 1944 eruption of Somma-Vesuvius.

The vegetation and landuse of the Sarno River plain can be subdevided into three different zones. The slopes of Somma-Vesuvius in the north are characterized by decideous, coniferous and mixed forests as well as mediterranean scrubland. The Apennine Mountains (Lattari and Sarno Mountains) in the south and in the east are dominated by decideous forests and mediterranean scrubland whereas the river plain is highly urbanized and intensively agronomically utilized (CORINE land cover 2000, Autorità di Bacino del Sarno). Main agricultural products are vegetables, fruits and flowers. Agriculture in the Sarno River plain is above all favoured by the high biological productivity and fertility of volcanic ash soils and the Mediterranean climate. The only limiting factor for agriculture is the lack of precipitation during the dry summer season. However, depending on the cultivated crop, under artificial irrigation approximately four to five crops can be harvested per year. Due to that favorable conditions today the Sarno River plain is one of the most densely populated regions in Italy. Especially during the last 50 years the area is subject to a vast urbanization process reaching a population density of approximately 1,822 inhabitants per km² (Regione Campania, 2001).

Large-scale geomorphogenetical transformation processes in the Sarno River plain are closely related to the periodic activity of Somma-Vesuvius volcanic complex. This includes volcanic eruptions, earthquakes or lahars. The municipalities that are

located in direct proximity to Somma-Vesuvius show a total population of almost 600,000 inhabitants (Osservatorio Vesuviano). Due to that high number of people being directly exposed to the volcano and the inadequate infrastructure that has to be used in case of an evacuation this area was identified to be at highest volcanic risk (Fig. 2, red zone). In case of an eruption this area is likely to be affected by pyroclastic flows/surges, mud flows and pyroclastic fallout (Osservatorio Vesuviano).

Figure 2. Circum-Vesuvian municipalities that belong to the zone of highest volcanic risk (Map of volcanic risk; Osservatorio Vesuviano).
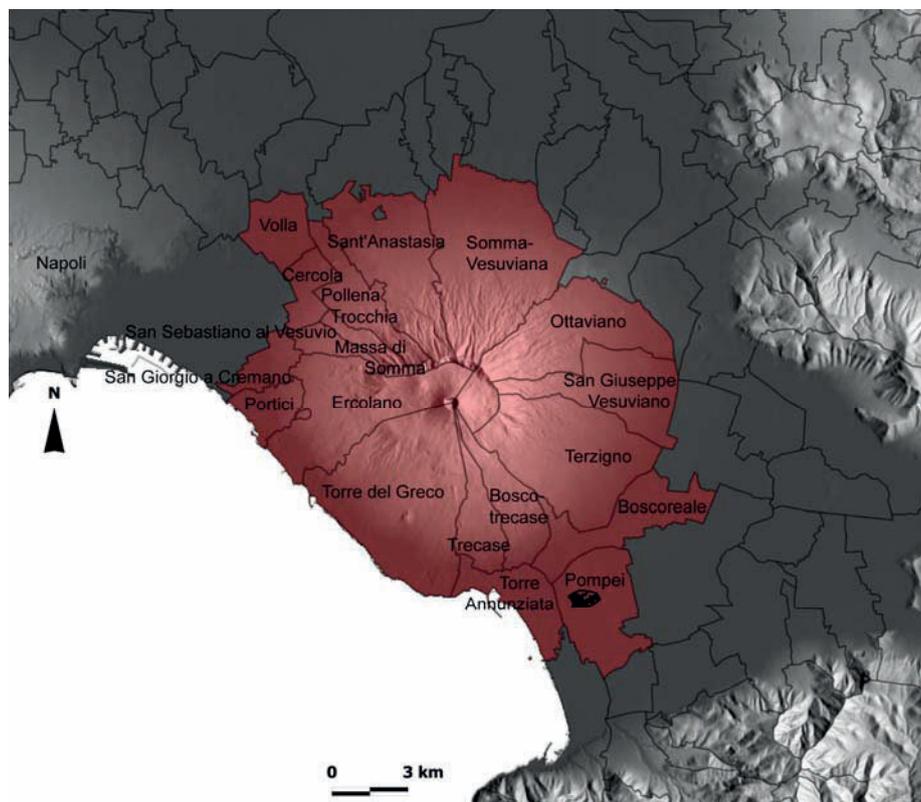
1.2.2 The volcanic activity of Somma-Vesuvius

Somma-Vesuvius volcanic complex is part of the so-called 'Roman Comagmatic Region' stretching across Italy's central and southern territory. During the last 25,000 years of Somma-Vesuvius' eruptive history the peri-volcanic region was repeatedly affected by volcanic eruptions of effusive as well as explosive type. Consequently, in the Sarno-River plain one comes across a nearly chronological appearance of archaeological presence. The volcanic activity can be subdevided into different eruptive cycles each one beginning with a Plinian eruption after a period of volcanic quiescence ranging from 1,400 to 4,000 years. Important protohistoric and

17

historic Plinian eruption of Somma-Vesuvius are Mercato/Ottaviano (7,070 – 6,770 BC), Avellino (1,890 – 1,630 BC) and Pompeii (AD 79) (Delibrias et al., 1979; Santacroce, 1987; Rolandi et al., 1993a,b; Andronico et al., 1995; Civetta et al., 1998; Sigurdsson, 2002; Cella et al., 2007).

Of these Plinian eruptions the eruption of AD 79 is the most well-known because it not only destroyed the ancient settlements of Herculaneum and Pompeii but also buried the entire Sarno River plain with volcanic deposits. Moreover, it was the first explosive eruption in history that was described in detail by the eyewitness reports of Pliny the Younger. The in-depth descriptions of the different eruptive phases in his letters to the ancient historian Cornelius Tacitus agree well with modern stratigraphic studies of the AD 79 volcanic deposits (e.g. Sigurdsson et al., 1985) as well as with observations of modern explosive eruptions (e.g. the 1902 eruption of Mount Pelee, Martinique (Lacroix, 1904)). Consequently, today Pliny became the eponym for explosive volcanic eruptions.

1.2.3   The AD 79 eruption of Somma-Vesuvius

Altogether, the AD 79 volcanic event can be subdevided into four eruptive phases (Cioni et al., 1992; Giacomelli et al., 2003):
   (i)   minor phreatomagmatic opening,
   (ii)   Plinian pumice lapilli fallout,
   (iii)   pyroclastic flows and surges and
   (iv)   phreatomagmatic closing.

The eruption began with minor phreatomagmatic explosions that were caused by an intrusion of groundwater into the vent and interactions with the magma (Sigurdsson and Carey, 2002). This was followed by the development of a high sustained eruption column reaching 14 to 32 km high into the stratosphere (Plinian phase) (Carey and Sigurdsson, 1987; Giacomelli et al., 2003; Luongo et al., 2003). Due to stratospheric winds the eruptive cloud was blown to the southeast taking a particular shape that resembled a large Mediterranean pine. The pyroclastic fallout of this second eruptive phase was dispersed more than 70 km to the southeast of the vent (Sigurdsson and Carey, 2002) and consist of two different pumiceous materials

reflecting variations in the density and chemical composition of the magma. It began with a layer of well-sorted phonolitic white pumice that was followed by a layer of phono-tephritic grey pumice (Lirer et al., 1973, 1993; Carey and Sigurdsson, 1987; Civetta et al., 1991; Cioni et al, 1992; Sigurdsson and Carey, 2002).

Figure 3. Isolines of thickness [cm] of the white (A) and gray (B) pumice fallout, dispersed during the eruption of Somma-Vesuvius AD 79 (Pfeiffer et al., 2005).
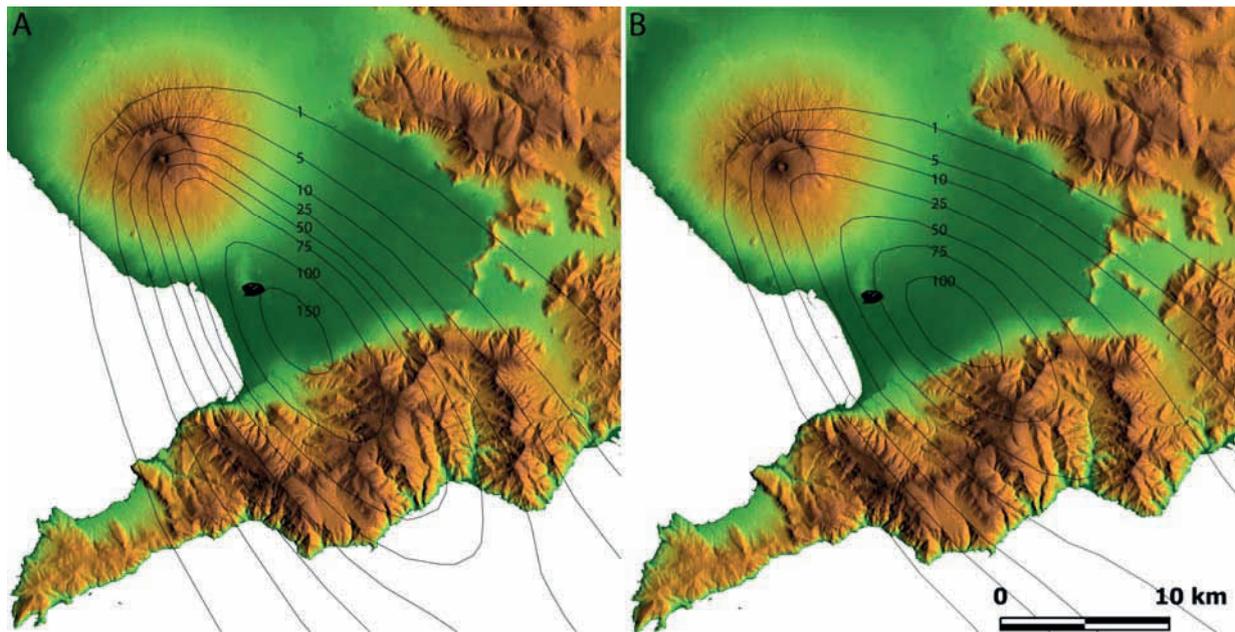
During the following third phase of the eruption the eruptive column repeatedly collapsed and recovered causing several (six to seven) destructive pyroclastic flows and surges rapidly moving down the slopes of Somma-Vesuvius and up to 10 to 15 km into the adjacent plain (Sigurdsson and Carey, 2002). The related deposits consist of thin layers of poorly-sorted ash exhibiting cross bedding and dune structures. Finally, the collapse of the magma chamber and the repeated ingression of water into the feeding system initiated the phreatomagmatic closing of the eruption embodied by silty sand beds with abundant accretionary lapilli (Sigurdsson et al., 1985, Giacomelli et al., 2003).

Due to its magnitude and destructive force the eruption of Somma-Vesuvius AD 79 caused a caesura in the existence of an entire landscape since almost the entire Sarno River plain was covered with pumice lapilli fallout and pyroclastic surge deposits. This contributed to a sealing and thus preservation not only of archaeological

structures but also of the pre-AD 79 paleo-surface and the paleo-stratum. As the AD 79 volcanic deposits show a specific and therefore easily identifiable stratigraphy and are laterally extensive, they can be considered as an ideal chronostratigraphic marker for the identification of the pre-AD 79 Roman period. The main reasons the AD 79 eruption of Somma-Vesuvius contributed to a good preservation environment are that:

(i)   a large area of the south-eastern territory of Somma-Vesuvius was buried with pyroclastic deposits, including the entire Sarno River plain,

(ii)   the Sarno River plain was buried relatively homogeneously by a distinct sequence of pumice lapilli fallout and pyroclastic surge deposits,

(iii)   the AD 79 volcanic deposits reach a high thickness of some meters which corresponds to a total volume of approximately $3.6\,km^3$ of dense rock equivalent (Sigurdsson et al., 1985),

(iv)   the process of burial was nearly isochronous, i.e. it occurred in a very short period of time of only 19 hours (Luongo et al., 2003),

(v)   the Plinian phase of the eruption consisted of 'cold' pumice lapilli fallout covering the Roman paleo-surface and hence protecting the paleo-stratum from the heating effect that was caused by the hot ash of the later occurring pyroclastic surges.

Consequently, from this point of view the volcanic eruption of Somma-Vesuvius AD 79 can be described as an 'optimal conserving catastrophe' (Marzolff, 1996).

In the Sarno River plain mechanical stratigraphical core drillings proved to be the method of choice to gain access to the pre-AD 79 paleo-surface and paleo-layer. Thus, it will be further explained in the next section.

1.2.4 Stratigraphical drillings

Nowadays, the pre-AD 79 paleo-surface of the Sarno River plain is situated underneath a 1 to 15 m thick cover of deposits not only from the AD 79 Plinian eruption but also from more recent eruptions such as that of AD 472, 1631 or 1944 (Imbo 1951, Rosi et al. 1993, Rolandi et al. 1998). Furthermore, as mentioned earlier, today the Sarno River plain is one of the most densely populated and urbanized

areas in Italy. Consequently, there are many constraints in comprehensively applying methods of stratigraphical research over the entire plain which render it very important to use a rather noninvasive or minimally invasive scientific approach. Mechanically conducted stratigraphical core drillings can be carried out with comparatively minimal technical and bureaucratic effort and costs and with a minimum of disturbance. Consequently, drillings have become a well-established and standardized method of litho-stratigraphical and pedo-stratigraphical prospection in the circum-Vesuvian region. Additionally, the methodology of stratigraphical core drillings proved to be most suitable for this particular project because it allows to approach several research questions at the same time, such as:

(i)   the identification of the AD 79 volcanic material to detect the pre-AD 79 Roman paleo-surface,

(ii)   the determination of the depth of the pre-AD 79 Roman paleo-surface to reconstruct the pre-AD 79 paleo-topography,

(iii)   the investigation and characterization of the pre-AD 79 stratum for the reconstruction of selected pre-AD 79 paleo-environmental features,

(iv)   the description and sampling of the pre-AD 79 Roman paleosol for further soil physical and chemical laboratory analyses.

Figure 3 shows the drilling apparatus and the stratigraphy of a mechanically conducted core drilling south of ancient Pompeii. The AD 79 volcanic deposits of Somma-Vesuvius, the pre-AD 79 paleo-layer and the pre-AD 79 paleo-surface are highlighted.

Figure 4. A: Apparatus for carrying out mechanical stratigraphical drillings, B: Cassette showing a part of the drilling core south of ancient Pompeii (the red rectangle shows the Roman paleosol underneath the white pumice layer of AD 79), C: Schematic diagram of the statigraphy of a self-conducted core drilling, south of Pompeii (the red line indicates the pre-AD 79 Roman paleo-surface) (Geomed s.r.l.).
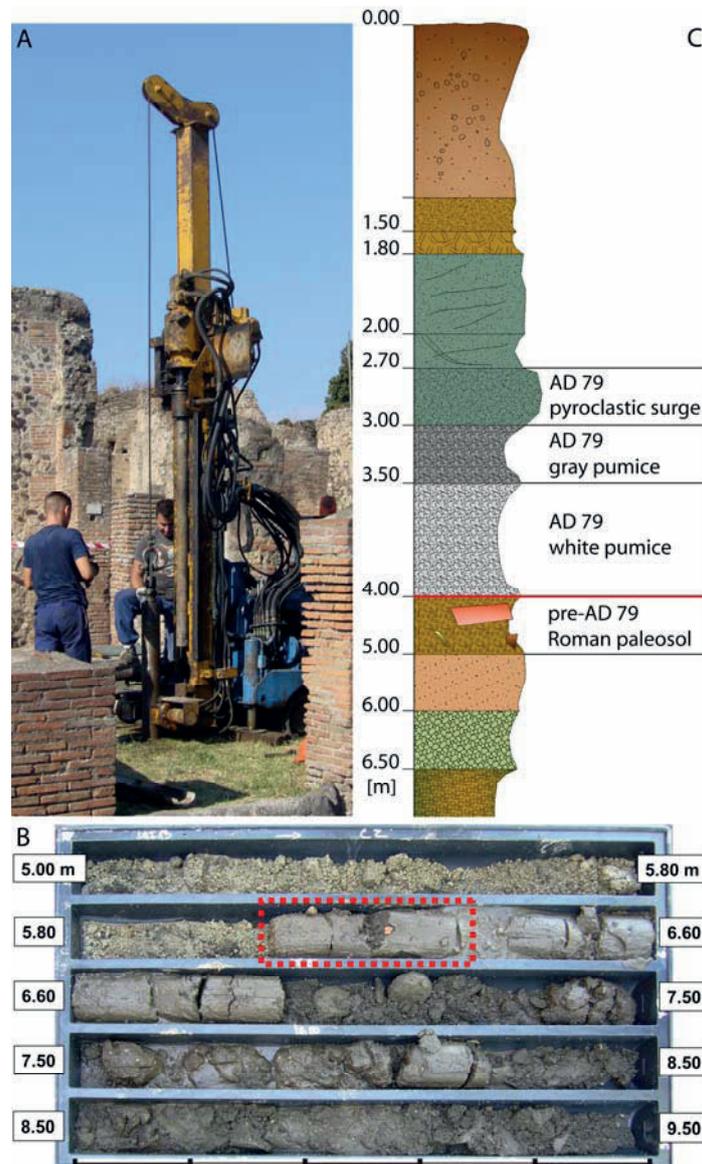
Today, stratigraphical drillings have to be carried out by law in the Sarno River plain, especially before public building projects are initiated to guarantee that no archaeologically relevant site is endangered to be overbuild (codice dei beni culturali e del paesaggio, D. Lgs. n. 42; Ferraro, 2010, oral communication). Consequently, a lot of local authorities such as planning commissions, building authorities or archaeological superintendences are in possession of numerous drilling documents. The exploitation of this huge, and as yet not scientifically utilized, data pool was of

particular importance for this project, especially for the high resolution pre-AD 79 paleo-topographical and paleo-environmental reconstruction of the Sarno River plain.

1.3   Research objectives

Until today the archaeological research activity in the Sarno River plain has particularly focused on the urban settlements like Pompeii, Nuceria and Stabiae. However, the cities cannot be considered in total isolation from their hinterland in which they were geographically, politically and culturally embedded (Seiler, 2008). To extent the Pompeiian research by aspects of the immediate environs, in 2006 a geoarchaeological research project was initiated by the German Archaeological Institute bringing together archaeology and geosciences. This project aims at reconstructing the ancient conditions of the Sarno River plain before the AD 79 eruption of Somma-Vesuvius by analyzing both the environmental and anthropogenic factors that characterize that ancient cultural landscape in Roman times (Seiler, 2008). In 2009 a one-year pilot project phase was funded by the German Research Foundation (DFG) that aimed at collecting and preprocessing the geoarchaeological data as well as testing the methodology on a smaller data set or a smaller spatial scale.

A decisive role in ancient rural life and economy in the Sarno River plain played the Roman farms *(villae rusticae)* since they were distributed within the entire plain. They were of vital importance for the utilization of natural resources and probably responsible for the supply not only of the rural areas but also of the urban centres. Thus, the Roman farms can be considered as ancient agricultural production units that are exemplary for the interactive human-environment relationship in the ancient Sarno River plain (Seiler, 2008).

The objective of this PhD thesis is to focus on geographical aspects of this above-mentioned geoarchaeological research project by reconstructing selected paleo-environmental landscape characteristics of the Sarno River plain (Campania, Italy) before the volcanic eruption of Somma-Vesuvius AD 79. These paleo-conditions can be considered as fundamental for the understanding of settlement dynamic and rural economy in the Sarno River plain, i.e. for the development of that cultural landscape

in the pre-Roman and Roman period. Special attention was drawn on the following aspects:

(i)   the reconstruction of the pre-AD 79 paleo-topography and selected paleo-environmental and paleo-geomorphological features,

(ii)   the characterization of the pre-AD 79 Roman paleosol south of Pompeii and the analysis of correlations between soil parameter values and the pre-AD 79 paleo-topography, and

(iii)   the analysis of post-burial soil developments of the pre-AD 79 Roman paleosol near Pompeii.

The above mentioned aspects were studied in detail between 2007 and 2010 and are presented as four separate research papers. They emphasize on the paleo-topographical and paleo-environmental reconstruction as well as on paleo-pedological analysis. The former can be considered fundamental for the present research project because it provides a topographical basis of the Sarno River plain before AD 79 which as yet does not exist. This is important for various further geoarchaeological applications that will be explained later on in the future research section. The latter aims at better understanding the nature of the Roman paleosol and its mode of preservation which is still unknown. This is to provide a characterization of the soil resources before AD 79 which is essential for the establishment of agriculture and rural development. In the following I will give a short résumé of these papers.

1.4   Geographical subprojects

In this chapter I will briefly decribe the three geographical subprojects mentioned above. At first, I will give an introduction. Then I will describe the methods applied and, finally, present the main research results.

1.4.1 Reconstruction of the pre-AD 79 paleo-topography and selected paleo-environmental and paleo-geomorphological features of the Sarno River plain

Initial, rather vague attempts of geoarchaeological studies in the Sarno River plain were carried out in the 19th century (Ruggiero, 1879), but it is only since the 1980s

that more standardised methodologies of geoarchaeological investigation have been developed. Since then there have been several projects to reconstruct parts of the paleo-landscape before AD 79, among them Cinque and Russo (1986), Livadie et al. (1990), Funari (1994), Pescatore et al. (1999), Di Maio and Pagano (2003) and Stefani and Di Maio (2003). These studies have mostly dealt with the delineation of the coastline in Roman times and the paleo-course of the Sarno River and its estuary mouth by using data from stratigraphical drillings and archaeological excavations. However, referring to the sometimes rather different results of previous coastline reconstructions Pescatore et al. (1999) state that from today's state of research the course of the paleo-coastline as well as the Sarno River cannot yet be clearly defined. As these past studies mostly dealt with separate aspects of the landscape before AD 79, as yet no geoarchaeological research project exists that considers the entire Sarno River plain and investigates the pre-AD 79 paleo-environmental conditions of that ancient landscape.

To reconstruct the paleo-topographical conditions of the Sarno River plain before AD 79 a methodology was developed that is based on an extensive dataset of stratigraphical core drillings, a high resolution present-day digital elevation model (DEM) and a sophisticated geostatistical approach. In this process, the thickness and spatial distribution of post-AD 79 deposits were modeled giving detailed insights into geomorphogenetic processes that took place in the peri-Vesuvian area during and after the eruption AD 79. The distribution of post-AD 79 deposits is controlled by two sets of processes: (i) the initial deposition of volcanic material during the eruptions of Somma-Vesuvius resulting in thickest deposits on the slopes of the volcano, i.e. near the source of the eruption and (ii) the subsequent remobilization and redistribution of that material by processes of erosion, transport and accumulation. This model of post-AD 79 deposits were then used to generate a high resolution pre-AD 79 DEM of the Sarno River plain.

Moreover, important pre-AD 79 paleo-environmental and paleo-geomorphological features were reconstructed by attributing the modeled paleo-topography to the paleo-environmental characteristics of the pre-AD 79 Roman statum, that are available from the drilling data. Hence, the paleo-coastline, the paleo-Sarno River

network and its associated floodplain, alluvial fans near the Tyrrhenian coast as well as abrasion terraces of historic and protohistoric coastlines were delineated.

It is the first time that the pre-AD 79 paleo-topographical and paleo-environmental conditions of the Sarno River plain were systematically reconstructed using a comprehensive database of stratigraphical information and data mining technologies. However, this reconstruction must be considered as a model of the pre-AD 79 conditions based on the hypothesis applied. The collection and conduction of additional stratigraphical drillings especially within areas only insufficiently covered as well as the combination of the pre-AD 79 DEM with archaeological findings can considerably enhance the paleo-environmental reconstruction of the Sarno River plain.

Further improvement of the paleo-environmental reconstruction is also expected by using a different topographic basis. Due to the vast urbanization process that particularly took place within the last 50 years nowadays the Sarno River basin is a highly urbanised and populated area. Consequently, the natural topography of the Sarno River plain is better reflected by the historic topography of 1944 instead of the present-day topography. Hence, a high resolution DEM of 1944 historic Italian AMI aerial photos (Autorità di Bacino del Sarno) will be generated by means of a real photogrammetric three-dimensional restitution (Heck and Vogel, 2009).

1.4.2 Characterization of the pre-AD 79 Roman paleosol south of Pompeii and the analysis of correlations between soil parameter values and the pre-AD 79 paleo-topography

Paleosols are ancient soils that have developed in the geological past under a distinct paleo-environment of soil formation. Therefore, they can contain evidence about the evolution of ancient landscapes including past land use, vegetation or geomorphological processes. Especially when an ancient land surface is preserved underneath depositional strata of volcanic ashes the ancient soilscape can be reconstructed in detail (Burggraf et al., 1981; Gerrard, 1992; Retallack, 2001, 2005; French, 2003). This will be especially relevant in relation to the Roman farms, i.e. the characterization of their spatial distribution and their ancient agricultural potential.

Pedological analyses of the pre-AD 79 Roman paleosol around Pompeii are rather scarce, among them Foss (1988), Scudder et al. (1996) and Foss et al. (2002). They investigated Roman paleosols in the Pompeii area and state that volcanic deposits such as airborne pumice and ash in general result in an excellent preservation of paleo-surfaces. Moreover, the paleosols showed little disturbance or destruction. Thus, the investigation of paleosols can provide a great deal of information for reconstructing past environments. However, Foss sampled the Roman paleosols in quarries and archaeological excavations, i.e. in outcrops that have already been open since decades. Thus, the investigated soil substrate is likely to be more or less affected by recent weathering processes.

The aim of this paper is to provide a detailed characterization of a pre-AD 79 Roman paleosol, that is in-situ preserved beneath the volcanic deposits of AD 79. Hence, mechanical core drillings were carried out along two toposequences south of ancient Pompeii to study the paleosols in natural undisturbed stratigraphies as well as to determine the pre-AD 79 paleo-topographical situation of that area. The stratigraphic sequences were macroscopically described and, where found, the paleosol substrate was sampled and analysed regarding its soil physical and chemical parameters. Furthermore, the results were confronted with the reconstructed pre-AD 79 paleo-topography and paleo-environmental features to detect interrelations between soil parameter values and paleo-topographical situation.

The results show that south of Pompeii the spatial distribution of paleosol characteristics is a function of soil development in relation to elevation and distance from the paleo-floodplain of the paleo-Sarno River network. Moreover, subsequent to the eruption AD 79 at lower elevations the buried Roman paleosols have come under the influence of a seasonally fluctuating groundwater table.

The eruption AD 79 created a good soil preservation environment since many of the original features of the Roman paleosols seem to be preserved. This is especially due to particular characteristics of volcanic soils and the influence of an increased groundwater table. However, other soil properties of the Roman paleosols do not necessarily reflect the ancient conditions because diagenetic alterations may have occurred after burial. For example, a post-burial rise of the groundwater table was identified south of Pompeii resulting in redoximorphic features in the white pumice

layer and increased amounts of sulphate in the underlying paleosols. Hence, in the next step, post-burial soil developments that may affect the Roman paleosol since AD 79 will be analysed in more detail.

1.4.3 Analysis of post-burial soil developments of the pre-AD 79 Roman paleosol near Pompeii

Paleosols are geoarchives of a past soil forming environment since diverse mechanisms of burial can contribute to a preservation of original soil properties. Consequently, paleosols can be utilized for investigating the paleo-pedological and paleo-environmental conditions before burial. However, many paleo-pedologists warn against a thoughtless and uncritical use of paleosol characteristics in interpreting paleo-environments because pronounced diagenetic processes, i.e. post-burial soil developments can take place, such as (Retallack, 1998, 2001; French, 2003):

   (i)   decomposition of soil organic matter,
  (ii)   leaching of nutrients from the overlying strata or
 (iii)   soil compaction after burial,

Hence, the present-day appearance and soil parameters of a buried paleosol can be considered as a combination of pedogenetic processes that took place prior to burial and post-burial soil alterations.

Due to the probability of post-burial soil developments in the Roman paleosol since AD 79 detailed field descriptions and laboratory analyses are necessary to understand both past and present pedogenetic processes. Consequently, soil liquid phase and soil solid phase analysis were carried out to better understand recent (post-burial) soil developments within the Roman paleosol. If the analysis of the soil solid phase provides good information about the factors and processes that influence a soil since the beginning of pedogenesis, soil liquid phase chemistry helps to estimate active pedogenic processes taking place in the Roman paleosol. Hence, for the first time a soil hydrologically monitoring was carried out within the Roman paleosol in natural, undisturbed stratification over a period of 20 months. The

objective was to detect post-burial soil water flow and nutrient transport from the overlying deposits into the paleosol.

The results show that the Roman paleosol is subject to a post-burial soil water flow and nutrient transport that is able to influence the soil parameters since AD 79. However, this soil water flow was limited to a four months period when a certain soil moisture was exceeded in the paleosol. This restricts the effect of nutrient transport from the overlying deposits to the rainy winter season.

Furthermore, to estimate post-burial soil developments that are manifested in the paleosol's solid phase the mineral soil of both the Roman paleosol and the modern soil were sampled at the same topographic location, analyzed for their physical and chemical soil properties and finally compared. Thereby, the modern soil was taken as a reference for an unburied volcanic soil hypothesizing similar pedogenetic conditions before AD 79 and today (see Foss, 1988). The results reveal distinct differences between the pre-AD 79 Roman paleosol and the modern soil at the same topographic location. Based on that differences and on the results from the soil liquid phase analysis the following post-burial soil developments of the pre-AD 79 paleosol were determined:

  (i) leaching of nutrients (Ca^{2+}, Mg^{2+}) via soil water flow from overlying deposits into the paleosol during a four months period in the rainy winter season,

  (ii) gradual transformation of former topsoil eluvial horizons into subsoil illuvial horizons due to ion accumulations within the paleosol from the overlying strata,

  (iii) ceased accumulation of soil organic matter and gradual decomposition,

  (iv) soil compaction of the paleosol as a result of the superimposed load of the overlying post-AD 79 deposits,

  (v) reduced weathering rate of the paleosol after burial.

In the future, those potential post-burial changes will be taken into account when the Roman paleosols is characterized and interpreted with respect to is ancient conditions and its ancient agricultural potential.

Moreover, a model of the present-day groundwater table of the Sarno River plain was generated and compared with the pre-AD 79 paleo-topography. It indicates that

since AD 79 the mean groundwater table has increased by approximately 1.8 m. Consequently, the Sarno River plain has to be divided into two different zones of potential post-burial soil developments: (i) the inner parts of the plain where after AD 79 the Roman paleosol has come under the influence of a rising groundwater table and (ii) the more elevated parts of the plain where the Roman paleosol is still part of the unsaturated vadose zone. Hence, the mechanism of post-burial soil development being active in the Roman paleosol strongly depends on its paleo-topographic situation. To determine the influence of the risen groundwater table on the Roman paleosol in more detail, in the next step, chemical analysis of the groundwater within the Roman paleosols should be carried out.

1.5   Conclusions

In the geographical subprojects described above selected paleo-environmental landscape characteristics of the Sarno River plain were studied before the volcanic eruption of Somma-Vesuvius AD 79. These paleo-landscape characteristics provide the basis for a comprehensive and systematic reconstruction of the ancient cultural landscape in Roman times.

For the first time a model of the pre-AD 79 paleo-topographical and paleo-environmental conditions was generated for the entire Sarno River plain. This work is unique since it allows a direct view on the pre-AD 79 paleo-surface that is buried beneath a cover of up to 15 m of post-AD 79 deposits. Consequently, it is fundamental for various future geoarchaeological research that analyzes the development of the urban settlements like Pompeii, Nuceria or Stabiae with respect to the paleo-topographical and paleo-environmental conditions. Furthermore, it provides detailed insights in the relationship between the urban centers and the rural settlements (Roman farms) in their hinterland from which they were presumably economically dependent. Hence, the ancient settlement dynamics of the entire Sarno River plain can be reconstructed including the assessment of ancient infrastructural facilities such as the road network, the water supply (aqueducts) or the marine or fluvial harbor.

As described in the methodology section of the respective research paper, in the first project phase, the paleo-topographical and paleo-environmental reconstruction was

carried out primarily from the geographical point of view by using stratigraphical data and present-day topographical terrain characteristics. However, in the Sarno River plain, plenty of archaeological findings exist that also provide important paleo-environmental information. The following three examples will illustrate this:

(i)   Roman farms for instance that are specialized on agricultural production are expected to be located in areas where the Roman layer is characterized by an unsaturated terrestrial soil that is not influenced by a high groundwater table. Consequently, Roman farms may rather be situated outside the floodplain of the paleo-Sarno River.

(ii)   During the regulation of the Sarno River in the 1850s several remains of ancient cypresses and poplars were found south of ancient Pompeii (Stefani and Di Maio, 2003). These species prefer habitats near the river and can even tolerate temporary floodings. Hence, their find spot may indicate the floodplain of the pre-AD 79 river network.

(iii) Furthermore, during 19th century excavations in the location of Bottaro, southwest of Pompeii, archaeological structures were found that may refer to the direct vicinity of the pre-AD 79 coastline. They included remains of storage buildings and shops containing amphorae, bronze coins, anchors, fishings nets and other fishing utensils. Furthermore, graffiti of seamen were found (Stefani and Di Maio, 2003).

The examples show that by systematically collecting archaeological findings in the Sarno River plain, analyzing them with respect to further paleo-environmental implications and combining them with the previous landscape reconstruction the model of the pre-AD 79 paleo-environmental conditions can be refined.

The paleo-pedological analysis around Pompeii were carried out to improve our knowledge of the pre-AD 79 Roman paleosol in the Sarno River plain. Especially its state of preservation after burial AD 79 was widely unknown. Consequently, for the first time detailed soil liquid phase and soil solid phase analysis were carried out to detect recent (post-burial) soil developments within the Roman paleosol. The knowledge of these post-burial soil developments is crucial to extract those soil parameters that have likely been preserved over time and thus may reliably

characterize the natural soil resources before AD 79. In association with the study of the Roman farms the paleo-pedological conditions are important for the reconstruction of the rural development, the establishment of agricultural production and the utilization of natural resources in the Sarno River plain in Roman times.

It must be emphasized that the study of the pre-AD 79 Roman paleosol in the Sarno River plain is still in an initial state. Consequently, more soil data from different paleo-toposequences throughout the entire Sarno River plain are needed to provide a detailed insight into the paleo-pedological conditions before AD 79. However, there are many obstacles to carry out a comprehensive analysis of the pre-AD 79 Roman paleosol. Among these are the high population density and high degree of soil sealing in the Sarno River plain as well as the thick layer of post-AD 79 deposits which makes it necessary to carry out mechanical stratigraphical core drillings.

Consequently, in the future, methodologies should be tested that are able to provide additional data on the pre-AD 79 Roman paleosols such as predictive modeling or geophysical prospections. By means of the predictive modeling approach soil data will be combined with the modeled paleo-topography. An important soil parameter for agricultural use is for example the effective soil depth (thickness) of the Roman paleosol. From the stratigraphical drilling data we have information about the thickness of a total of 445 terrestrial paleosols. Since in natural systems the soil thickness is particularly a function of the local topography the pre-AD 79 topography can be used to predict the thickness of the Roman paleosol for the entire plain. Noninvasive methods such as geophysical prospections on the other hand help to detect stratigraphical patterns and gradients as well as subsurface structures. Hence, geophysics can be utilized to validate the results of the paleo-topographical reconstruction and to detect archaeological features.

In conclusion the present work shows that an integrative interdisciplinary approach of paleo-geographical analysis and archaeological research can substantially contribute to the reconstruction of paleo-landscapes in general and, in particular, the reconstruction of the ancient cultural landscape of the Sarno River plain.

1.6　Future research and outlook

As stated above the reconstruction of pre-AD 79 paleo-environmental landscape characteristics provide important background knowledge for the understanding of settlement development and rural economy in the Sarno River plain. Consequently, it is the basis for various detailed geoarchaeological research that contributes to the reconstruction of that ancient cultural landscape before AD 79. Based on the results of the geographical subprojects future research within the Sarno River plain will focus on:

(i)　the reconstruction of the ancient rural settlement structure of Roman farms *(villae rusticae)* and its dynamics,

As mentioned earlier, representative of ancient rural settlement in the Sarno River plain are the Roman farms. Today more than two hundred Roman farms are known, apparently distributed across the entire plain (Casale, 1979; Kockel, 1985, 1986). After data collection and localization of the Roman farms by means of geographical information systems (GIS) their spatial distribution in the Sarno River plain can be combined with the modeled pre-AD 79 paleo-topography and paleo-environmental characteristics to reveal specific location patterns. Subsequently, by using GIS and spatial and predictive modeling, this preferential paleo-topographic situation can be regionalized to the entire Sarno River plain to determine the total area that may have been occupied by Roman farms and agricultural production before AD 79.

Moreover, the approximate scale of farmland surrounding a single Roman farm will be verified by applying Voronoi diagrams (Thiessen polygons) on the different clusters of aggregated Roman farms within the Sarno River plain. Subsequently, this approximate size of farmland can be applied on the preferential paleo-topographic situations of Roman farms to estimate the quantity of Roman farms that could have existed within the Sarno River plain in the Roman period.

(ii) multidisciplinary analysis of ancient agricultural soils in the surroundings of Roman farms,

Considering the identification of post-burial soil developments in the pre-AD 79 paleosol the ancient agricultural soils in the vicinity of known Roman farms will be sampled by means of trenches and stratigraphical drillings to carry out a comprehensive and multidisciplinary analysis including paleopedology, archaeo-botany, archaeozoology, and archaeology. The objectives are to:

a) provide direct evidence of the crops associated to a Roman farm (macrobotany, palynology),

b) establish the sedimentological history of the agricultural soil (molluscan analysis),

c) characterize the Roman paleosol in terms of its soil fertility and its agricultural utilization (paleopedology),

d) analyze the mode of ancient soil cultivation (tillage, e.g. plowing) and the application of fertilizer,

e) gain evidence of how the agricultural area in the immediate vicinity of the farm (part of the *fundus*), was structured by field paths, wells, fences, animal husbandry or plantings.

Furthermore, as mentioned before, the paleosol thickness taken from the drilling data will be combined with the modeled pre-AD 79 topography to systematically analyse the correlation between soil thickness and paleo-topography. This is to identify areas that were subject to erosion or accumulation processes before AD 79. Hence, taking into account the reconstructed paleo-environmental characteristic of the pre-AD 79 stratum, a zonation of the Sarno River plain will be applied determining terrestrial soils of a sufficient depth for ancient agricultural use.

(iii) the reconstruction of the ancient local road network,

Based on the locations of urban settlements and Roman farms and the pre-AD 79 paleo-topography and paleo-environmental features the ancient local road network will be reconstructed by carrying out a terrain sensitive least-cost path

analysis. We hypothesize that ancient roads that connected the Roman farms among each other and with the ancient urban centers like Pompeii, Stabiae or Nuceria followed physiographic constraints. After identifying important paleo-topographical and paleo-environmental drivers for route selection we will utilize the locations of Roman farms, ancient settlements, necropolis and other significant findings (e.g. milestones) within the Sarno River plain to determine probable routes through the ancient landscape.

(iv)   the reconstruction of the ancient water distribution system (aqueducts),

In Roman Campania multiple aqueducts ensured the supply with freshwater for instance of settlements like Pompeii or Naples. Consequently, aqueducts represent a vital part of the ancient infrastructure of Campania and the Sarno River plain. The optimal course of an aqueduct strongly considered the local topographic conditions utilizing the natural gradients of the mountains and avoiding the expensive construction of supporting structures to cross the plain. At least nine remains of the ancient aqueducts can be identified in the Vesuvian region (Ohlig, 2001, Keenan-Jones et al., 2010). By means of GIS and the pre-AD 79 DEM the exact location and elevation level of the remains of the ancient aqueducts will be determined to propose a hypothetical course of the aqueducts through the ancient topography. Finally, geophysical prospection will be utilized to detect subsurface structures that can be related to the Roman aqueduct.

(v)   the identification of potential locations of Pompeii's marine or fluvial harbor.

By means of a detailed terrain analysis of the pre-AD 79 DEM potential paleo-topographical locations of Pompeii's marine or fluvial harbor will be identified, whose exact location is still controversially debated (e.g. Stefani and Di Maio, 2003). Subsequently, further stratigraphical drillings or geophysical prospections will be carried out in that areas for verification.

The outlook shows that the present work is the beginning of an extensive and comprehensive geoarchaeological research activity in the Sarno River plain that aims at providing an in-depth reconstruction of that ancient cultural landscape before the

eruption of AD 79. However, the eruptive history of Somma-Vesuvius contains numerous other explosive eruptions. Consequently, the decribed methodology can be also applied to other chronostratigraphic markers and epochs.

1.7   References

Andronico, D., Calderoni, G., Cioni, R., Sbrana, A., Sulpizio, R., Santacroce, R., 1995. Geological map of Somma-Vesuvius volcano. Per. Mineral. 64, 77-78.

Burggraf, D.R., White, H.J., Frank, H.J. and Vondro, C.F., 1981. Hominid habitats in the Rift Valley, Part 2. In: Rapp, G., Vondra, C.F. (eds.) Hominid Sites, Their Geologic Settings. Westview Press, Boulder, 115-147.

Carey, S. and Sigurdsson, H., 1987. Temporal variations in column height and magma discharge rate during the 79 A.D. eruption of Vesuvius. Geol. Soc. Am. Bull. 99, 303-314.

Casale, A. and Bianco, A., 1979. Primo contributo alla topografia del suburbio Pompeiano. Antiqua 4, 27-56.

Cella, F., Fedi, M., Florio, G., Grimaldi, M. and Rapolla, A., 2007. Shallow structure of the Somma-Vesuvius volcano from 3D inversion of gravity data. J. Volcanol. Geoth. Res. 161, 303-317.

Cinque, A. and Russo, F., 1986. La linea di costa del 79 A.D. fra Oplonti e Stabiae nel quadro dell'evoluzione olocenica della Piana del Sarno (Campania). Boll. Soc. Geol. It. 105, 111-121.

Cioni, R., Marianelli, P. and Sbrana, A., 1992. Dynamics of the A.D. 79 eruption: Stratigraphic, sedimentological and geochemical data on the successions from the Somma-Vesuvius southern and eastern sectors. Acta Vulcanol. 2, 109-123.

Civetta, L., Galati, R. and Santacroce, R., 1991. Magma mixing and convective compositional layering within the Vesuvius magma chamber. B. Volcanol. 53, 287-300.

Civetta, L., Di Vito, M.A., De Lucia, M. and Isaia, R., 1998. Storia eruttiva del Somma-Vesuvio. In: Guzzo, P. and Peroni, R. (eds.) Archeologia e Vulcanologia in Campania. Naples, 9-16.

Di Gennaro, A. and Terribile, F., 1999. I suoli della provincia di Napoli, carta e legenda. Camera di Commercio, Ge Pro, Ter, Napoli, pp. 63.

Di Maio, G. and Pagano, M., 2003. Considerazioni sulla linea di costa e sulle modalità di seppellimento dell'antica Stabia a seguito dell'eruzione vesuviana del 79 d.C. Riv. Studi Pomp. XIV, 197-245.

Delibrias, G., Di Paola, G.M., Rosi, M. and Santacroce, R., 1979. La storia eruttiva del complesso vulcanico Somma-Vesuvio ricostruita dalle successioni piroclastiche del Monte Somma. Rend. Soc. It. Mineral. Petrol. 35, 411-438.

Foss, J.E., 1988. Paleosols of Pompeii and Oplontis. In: Curtis, R.L. (ed.) Studia Pompeiana and Classica, Aristide D. Caratzas, Publisher,New Rochelle, N.Y.

Foss, J.E., Timpson, M.E., Ammons, J.T. and Lee, S.Y., 2002. Paleosols of the Pompeii Area. In: Jashemski W.F. (ed.) The Natural History of Pompeii. Cambridge University Press, 65-79.

French, C.A.I., 2003. Geoarchaeology in action: studies in soil micromorphology and landscape evolution. Routledge, London, New York, pp. 291.

Furnari, E., 1994. Nuovi contributi all'identificazione del littorale antico di Pompei. In: AA.VV., Neapolis Temi Progettuali, Roma, II, 219-291.

Gerrard, J., 1992. Soil Geomorphology: An Integration of Pedology and Geomorphology. London, Chapman and Hall.

Giacomelli, L., Perrotta, A., Scandone, R. and Scarpati, C., 2003. The eruption of Vesuvius of 79 AD and its impact on human environment in Pompei. International Union of Geological Sciences, Episodes 26, no. 3, 234-237.

Heck, V. and Vogel, S., 2009. Rectification of Historic Royal Air Force Aerial Photos and Generation of an Aerial Image Mosaic of the Sarno River Basin, Italy. PFG, Photogrammetrie-Fernerkundung-Geoinformation, 3/2009, 245-249.

Imbo, G., 1951. L'attivita eruttiva vesuviana e relative osservazioni nel corso dell'intervalo intereruttivo 1906–1944 ed in particolare del parossimo del marzo, 1944. Ann. Ossevatorio Vesuviano, (5th series) part 1.

Keenan-Jones, D.C., 2010. The Aqua Augusta. Regional water supply in Roman and late antique Campania. Department of Ancient History, Macquarie University, Sydney.

Kockel, V., 1985. Archäologische Funde und Forschungen in den Vesuvstädten I. Archäologischer Anzeiger, 495-571.

Kockel, V., 1986. Archäologische Funde und Forschungen in den Vesuvstädten II. Archäologischer Anzeiger, 443-569.

Lacroix, A., 1904. La Montagne Pélée et ses Eruptions. Masson et Cie, Paris.

Lirer, L., Munno, R., Petrosino, P. and Vinci, A., 1993. Tephrostratigraphy of the A.D. 79 pyroclastic deposits in perivolcanic areas of Mt. Vesuvio (Italy). J. Volcanol. Geoth. Res. 58, 133-149.

Livadie, C.A., Barra, D., Bonaduce, G., Brancaccio, L., Cinque, A., Ortolani, F., Pagliuca, S. and Russo, F., 1990. Evoluzione geomorphologica, neotettonica e vulvanica della piana costiera del fiume Sarno (Campania) in relazione agli insediamenti anteriori all'eruzione del 79 d.C. Pact 25-13, 237-256.

Lulli, L., 2007. Italian volcanic soils. In: Arnalf, Ó., Bartoli, F., Buurman, P., Óskarson, H., Stoops, G. and García-Rodeja, E. (eds.), Soils of Volcanic Regions in Europe. Springer-Verlag, Berlin, Heidelberg.

Luongo, G., Perrotta, A. and Scarpati, C., 2003. Impact of the AD 79 explosive eruption on Pompeii, I. Relations amongst the depositional mechanisms of the pyroclastic products, the framework of the buildings and the associated destructive events. J. Volcano. Geoth. Res. 126, 201-223.

Lirer, L., Pescatore, T., Booth, B. and Walker, G.P.L., 1973. Two Plinian pumice-fall deposits from Somma-Vesuvius, Italy. Geol. Soc. Am. Bull. 84, 759-772.

Marzolff, P., 1996. Naturkatastrophen in der antiken Welt. In. Olshausen, E. & Sonnabend, H. (eds.) Stuttgarter Kolloquium zur historischen Heographie des Altertums. Vol. 6, 1998, Stuttgart.

Ohlig, C.P.J., 2001. De Aquis Pompeiorum. Das Castellum Aquae in Pompeji: Herkunft, Zuleitung und Verteilung des Wassers. In: De Waele, J.A.K.E. & Moormann, E.M. (eds.) Circumvesuviana. Vol. 4, 2001, pp.483.

Pescatore, T., Senatore, M.R., Capretto, G., Lerro, G. and Patricelli, G., 1999. Ricostruzione paleoambientale delle aree circostanti l'antica Città di Pompei, Campania (Italia) al Tempo dell'eruzione del Vesuvio del 79 d.C. Boll. Soc. Geol. It. 118, 243-254.

Pfeiffer, T., Costa, A. and Macedonio, G., 2005. A model for the numerical simulation of tephra fall deposits. J. Volcanol. Geoth. Res. 140, 273-294.

Retallack, G.J., 1998. Core Concepts of Paleopedology. Quaternary International, Vols. 51/52, 203-212.

Retallack, G.J., 2001. Soils of the Past, An Introduction to Paleopedology. Blackwell Science.

Retallack, G.J., 2005. Palaeosols. Soil/Palaeosols, 203-208.

Rolandi, G., Maraffi, S., Petrosino, P. and Lirer, L., 1993a. The Ottaviano eruption of Somma-Vesuvio 8000 y B.P. a magmatic alternating fall and flow-forming eruption. J. Volcanol. Geoth. Res. 58, 43-65.

Rolandi, G., Mastrolorenzo, G., Barrella, A.M. and Borrelli, A., 1993b. The Avellino plinian eruption of Somma-Vesuvio 3760 y B.P- the progressive evolution from magmatic to hydromagmatic style. J. Volcanol. Geoth. Res. 58, 67-88.

Rolandi, G., Petrosino, P. and McGeehin, J., 1998. The interplinian activity at Somma-Vesuvius in the last 3,500 years. Journal of Volcanology and Geothermal Research 82, 43-65.

Rosi, M., Principe, C. and Vecci, R., 1993. The 1631 Vesuvian eruption: A reconstruction based on historical and stratigraphical data. J. Volcanol. Geotherm. Res. 58, 151-182.

Ruggiero, M., 1879. Del sito di Pompei e dell'antico lido del mare. In: Pompei e la regione sotterata dal Vesuvio nell'anno 79. Mem. e Note pubb. dall'ufficio tecn. degli scavi delle prov. meridionali, Napoli, 5-14.

Santacroce, R., 1987. Somma-Vesuvius. C.N.R., Quaderni de 'La Ricerca Scientifica' 114, Rome, pp. 251.

Scudder, S.J., Foss, J.E. and Collins, M.E., 1996. Soil science and archaeology. Advances in Agonomy, Vol. 57, 1-76.

Seiler, F., 2008. Rekonstruktion der antiken Kulturlandschaften des Sarno-Beckens. Ein multidisziplinäres Kooperationsprojekt mit Partnern aus Naturwissenschaften und Altertumswissenschaften in Deutschland, Italien und England, In: Guzzo, P.G.; Guidobaldi M.P., (eds.) Nuove ricerche archeologiche nell'area vesuviana (scavi 2003-2006), Convegno Internazionale, Roma 1.-3. Februar 2007, 485-490.

Shoji, S. and Takahashi, T., 2002. Environmental and Agricultural Significance of Volcanic Ash Soils. Glob. Environ. Res. 6(2), 113-135.

Sigurdsson, H., 2002. Mount Vesuvius before the Disaster. In: Jashemski W.F. (ed.) The Natural History of Pompeii. Cambridge University Press, 29-36.

Sigurdsson, H. and Carey, S., 2002. The Eruption of Vesuvius in A.D. 79. In: Jashemski W.F. (ed.) The Natural History of Pompeii. Cambridge University Press, 37-64.

Sigurdson, H., Carey, S., Cornell, W. and Pescatore, T., 1985. The eruption of Vesuvius in A.D. 79. Natl. Geogr. Res. 1, 332-387.

Stefani, G. and Di Maio, G., 2003. Considerazioni sulla linea di costa del 79 d.C. e sul porto dell'antica Pompei. Riv. Studi Pomp. XIV, 142-195.

2

Manuscripts

2.1 Reconstructing the Roman topography and environmental features of the Sarno River plain (Italy) before the AD 79 eruption of Somma-Vesuvius.

Sebastian Vogel[a],* and Michael Märker[b,c]

[a] German Archaeological Institute, Podbielskiallee 69-71, D-14195 Berlin, Germany

[b] Heidelberg Academy of Sciences and Humanities c/o University of Tübingen, Rümelinstraße 19-23, D-72070 Tübingen, Germany

[c] Department of Soil Science and Plant Nutrition, University of Florence, Italy.

* Corresponding author. Tel: +49 (0)30 187 711 358, Fax: +49 (0)30 187 711 168
E-mail address: sv@dainst.de (S. Vogel)

# Reconstructing the Roman topography and environmental features of the Sarno River Plain (Italy) before the AD 79 eruption of Somma–Vesuvius

Sebastian Vogel [a,*], Michael Märker [b,c]

[a] German Archaeological Institute, Germany, Podbielskiallee 69-71, D-14195 Berlin, Germany
[b] Heidelberg Academy of Sciences and Humanities, University of Tübingen, Rümelinstraße 19-23, D-72070 Tübingen, Germany
[c] Department of Soil Science and Plant Nutrition, University of Florence, Italy

ABSTRACT

A methodology was developed to reconstruct the Roman topography and environmental features of the Sarno River plain, Italy, before the AD 79 eruption of the Somma–Vesuvius volcanic complex. We collected, localized and digitized more than 1800 core drilling data to gain a representative network of stratigraphical information covering the entire plain. Besides other stratigraphical data including the characteristics of the pre-AD 79 stratum, the depth to the pre-AD 79 surface was identified from the available drilling documentations. Instead of a simple interpolation method, we used a machine based learning approach based on classification and regression trees to reconstruct the pre-AD 79 topography. We hypothesize that the present-day topography reflects the ancient topography and related surface processes, because volcanic deposits from the AD 79 eruption coated the ancient landscape. Thus, ancient physiographic elements of the Sarno River plain are still recognizable in the present-day topography. Therefore, a high-resolution, present-day digital elevation model (DEM) was generated. A detailed terrain analysis yielded 15 different primary and secondary topographic indices. Subsequently, a classification and regression model was applied to predict the depth of the pre-AD 79 surface combining present-day topographic indices with other physiographic data. This model was calibrated with the measured depth of the pre-AD 79 surface. The resulting pre-AD 79 DEM was compared with the classified characteristic of the pre-AD 79 stratum, identified from the drilling documentations. This allowed the reconstruction of pre-AD 79 environmental features of the Sarno River plain such as the ancient coastline, the paleo-course of the Sarno River and its floodplain.
To the knowledge of the authors, it is the first time that the pre-AD 79 topography of the Sarno River plain was systematically reconstructed using a detailed database and sophisticated data mining technologies.

© 2009 Elsevier B.V. All rights reserved.

1. Introduction

The Plinian eruption of the Somma–Vesuvius volcanic complex in AD 79, which completely buried the Roman settlements of Herculaneum, Oplontis, Stabiae and Pompeii belongs to the most well-known eruptions in history. During this eruption the pumice lapilli fallout was dispersed by stratospheric winds predominantly in southeastern directions up to a distance of more than 70 km from the vent (Sigurdsson and Carey, 2002). Thus, almost the entire Sarno River plain was covered by approximately 3.6 km³ of dense rock equivalent of volcanic deposits (Sigurdsson et al., 1985) showing a specific and therefore easily identifiable stratigraphy. Since these deposits are distinctive and laterally extensive, they can be considered as an ideal chronostratigraphic marker. According to the phase of the eruption and the chemical composition and density of the magma, the Plinian volcanic deposits of AD 79 consist of white phonolitic pumice and grey tephritic–phonolitic pumice fallout deposits, interrupted as well as overlain by six ash layers of pyroclastic surge and flow deposits (Lirer et al., 1973; Sigurdsson et al., 1985; Carey and Sigurdsson, 1987; Civetta et al., 1991; Cioni et al., 1992; Pescatore et al., 1999, 2001; Sigurdsson and Carey, 2002; Luongo et al., 2003; Pfeiffer et al., 2005). Fig. 1 illustrates the approximate dispersion of the volcanic material during the eruption AD 79 as modeled by Pfeiffer et al. (2005) presuming a northwestern wind profile.

The AD 79 eruption covered a wide area of the Sarno River plain nearly isochronously (within 19 h time) with volcanic deposits of some meters. This not only caused a caesura in the existence of an entire landscape, but also contributed to the excellent preservation of the paleo-surface and the ancient paleo-environmental conditions before the eruption of AD 79 (Foss et al., 2002). Consequently, almost 2000 years later, this paleo-surface still remains in situ and is accessible for stratigraphical investigations. In the following the term pre-AD 79 refers to the conditions before the AD 79 eruption of Somma–Vesuvius.

* Corresponding author. Tel.: +49 30 187 711 358; fax: +49 30 187 711 168.
*E-mail address:* sv@dainst.de (S. Vogel).
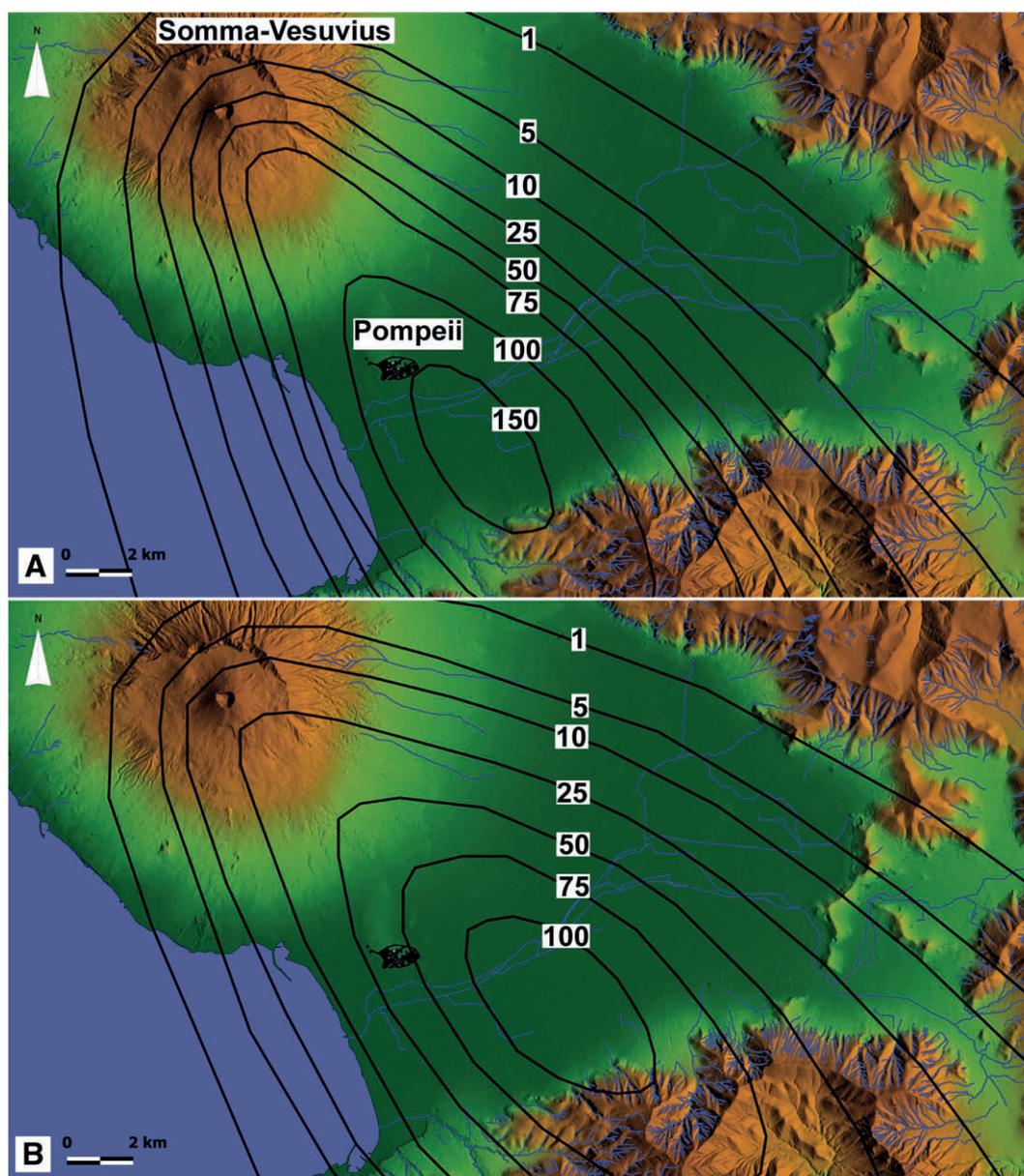
Fig. 1. Isopachs of the thickness [cm] of the white (A) and grey (B) pumice fallout, deposited during the eruption of Somma–Vesuvius AD 79. Modeled by Pfeiffer et al. (2005) (RUN V1).

Preliminary geoarchaeological studies in the Sarno River plain were carried out in the 19th century (Ruggiero, 1879). However, it is only since the 1980s that more standardized methodologies of geoarchaeological investigation have developed. Since then there have been several attempts to reconstruct the paleo-landscape before AD 79, among them Cinque and Russo (1986), Livadie et al. (1990), Furnari (1994), Pescatore et al. (1999), Di Maio and Pagano (2003) and Stefani and Di Maio (2003). These studies mostly dealt with the delineation of the coastline before AD 79 and the paleo-course of the Sarno River and its estuary mouth using data from stratigraphical drilling and archaeological excavations.

As Pescatore et al. (1999) state about previous coastline reconstructions, the results are sometimes rather different (Fig. 2). That is why the position of the paleo-coastline and the course of the paleo-Sarno cannot yet be clearly defined from today's state of research.

Barra et al. (1989) and Livadie et al. (1990) used about 50 stratigraphical drillings between Torre Annunziata and the Sarno River and archaeological data from Roman and pre-Roman times to reconstruct the pre-AD 79 topography. According to them the ancient coastline was situated approximately 1 km inland, parallel to the modern coast with lagoons that were protected from the sea. There they also assume the location of the ancient marine harbour of Pompeii. Moreover, they predicted the ancient sea level to be approximately 4 m below the modern one. In the hinterland of the ancient coastline they discovered fossil littoral dune deposits of pre-Roman times (Messigno, 5600–4500 years BP and Bottaro/Pioppaino, 3600–2500 years BP; Cinque, 1991). Furthermore they related predominantly fluvio-palustrine deposits to the paleo-course of the Sarno River whose estuary they assumed southeast of the present-day mouth between Masseria and Resinaro (Barra et al., 1989; Livadie et al., 1990).

Furnari (1994) carried out 51 stratigraphical drillings and used some data from archaeological excavations to reconstruct the pre-AD 79 topography. After identifying the pre-AD 79 stratum underneath the volcanic deposits of AD 79 in 39 of 51 drillings, he characterized it using micropaleontologic and granulometric analyses and categorized it according to its origin into four classes: (i) palustrine, (ii) alluvial, (iii) littoral and (iv) Roman paleosol. According to the location of the

43
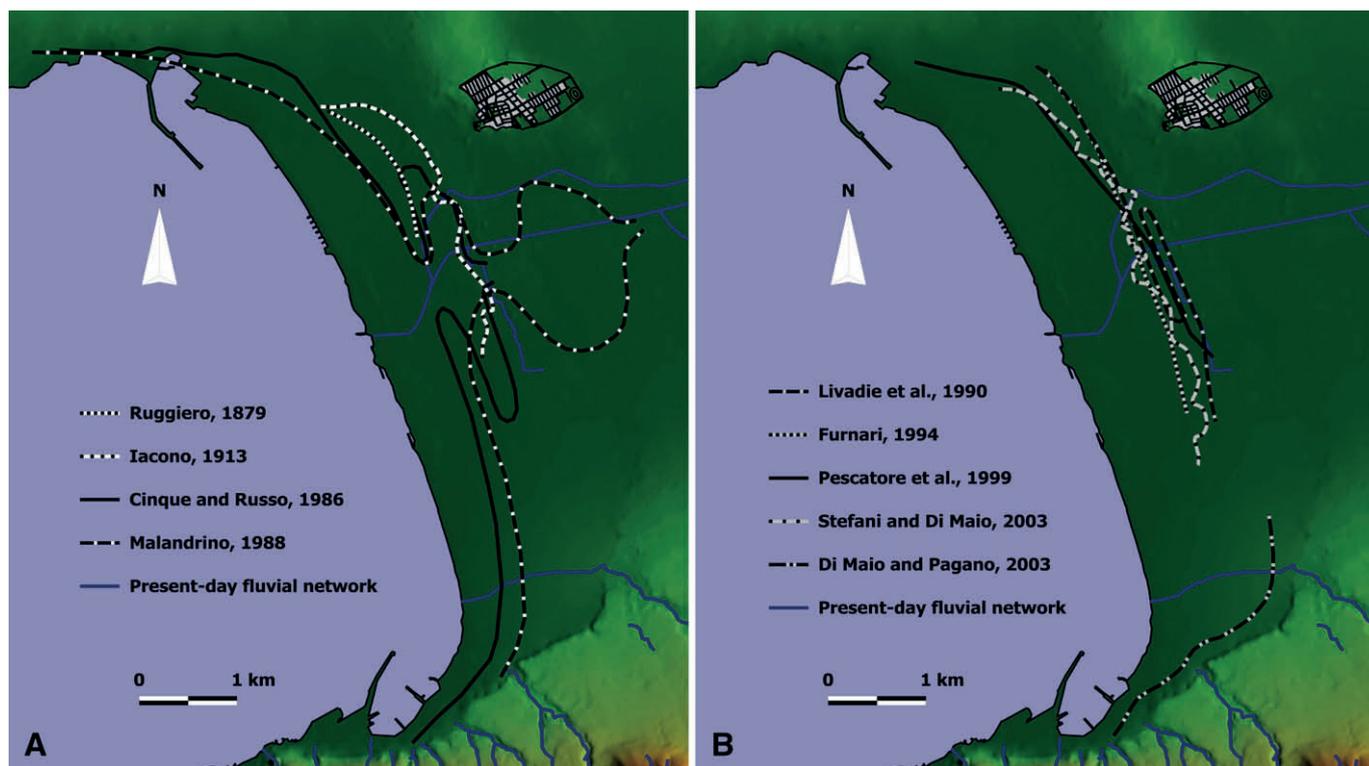
Fig. 2. Past reconstructions of the pre-AD 79 coastline of the Sarno River plain, before (A) and after (B) 1990 (Iacono, 1913; Malandrino, 1988).

drillings he could delineate the approximate position of the paleo-coastline, the paleo-Sarno and terrestrial areas of the mainland.

Pescatore et al. (1999, 2001) utilized data from 66 drillings and known archaeological sites for studying the pre-AD 79 environment around Pompeii. The stratigraphical data derived from own drillings, past construction projects, from Ruggiero (1879) and Furnari (1994). They state that the ancient shoreline may have run more or less parallel to the modern coast approximately 1 km southwest of the ancient city of Pompeii and 1 km landwards of the present-day coast. The mouth of the paleo-Sarno River they presume to be located south of the modern estuary (Pescatore et al., 1999, 2001).

Di Maio and Pagano (2003) used 15 drillings, as well as five archaeological sections and data from archaeological excavations to illustrate a 2.5 km long section of the pre-AD 79 coastline near the ancient town of Stabia (Fig. 3) north of the Lattari Mountains. According to them the coastline before AD 79 followed the terrace of San Marco at a distance of 100 to 200 m, whereas it is possible that, at this location, the Lattari Mountains represented an active cliff. The interpretation of the drilling data showed strong variation in the thickness of the AD 79 eruptive material, especially between the slopes and the adjacent Sarno River plain. Hence, they argue that shortly after their deposition, the volcanic sediments must have been mobilized by heavy rainfall and slope water, moved downslope as a mudflow and were re-deposited as an alluvial fan delta within the plain. Thereby parts of the ancient coastline propagated to the NW.

Stefani and Di Maio (2003) used a total of 78 drillings including new ones and those of Furnari (1994) as well as an extensive dataset of past archaeological excavations. They state that the eruption AD 79 coated the ancient topography with volcanic deposits up to a thickness of 3 to 6 m. Consequently the present-day topography more or less reflects the ancient topography. Despite the volcanic deposits, main physiographic elements of the Sarno River plain such as the volcanic hill of Pompeii, the prehistoric dune ridge of Bottaro/Pioppaino and the terrace of San Marco are still recognizable. Thus, the present-day topography provides valuable clues in reconstructing the ancient topography.

As these past studies mostly dealt with separate aspects of the ancient landscape pre-AD 79, there exists as yet no geoarchaeological study covering and investigating the paleo-geomorphology and paleo-environmental conditions of the entire Sarno River plain. Consequently this research project focusses on the reconstruction of the paleo-topography of the Sarno River plain before the eruption of Somma–Vesuvius in AD 79. Therefore we use a methodology that combines stratigraphical information from former and self conducted core drillings, present-day topographical data, and classification and regression methods. With this approach we expect to gain more detailed information concerning paleo-environmental features such as the position of the ancient coastline and the course of the paleo-river network before AD 79.

2. Study area

The Sarno River plain situated south of the Somma–Vesuvius volcanic complex is a cultural landscape characterized by continuous anthropogenic activity since the Middle Bronze Age. It stretches across an area of 210 km² and is drained by the Sarno River and its tributaries. In the west it opens to the Tyrrhenian Sea, whereas in the south and in the east, the plain is flanked by the Mesozoic calcareous rocks of the Lattari and Sarno Mountains that are part of the Southern Apennine chain (Fig. 3). The Sarno River plain belongs to the great graben structure of the Campanian Plain which was formed during Plio-Pleistocene extensional tectonic phases at the end of the Apennine orogenesis and is filled with marine, alluvial and volcanic deposits lying on a carbonate platform (Cinque et al., 1987; De Vita and Piscopo, 2002; Cella et al., 2007).

During the last 25,000 years of Somma–Vesuvius' eruptive history, several Plinian eruptions have occurred, each one marking the beginning of a new eruptive cycle after a period of quiescence ranging from 1400 to 4000 years, such as Mercato/Ottaviano (7070–6770 BC), Avellino (1890–1630 BC) and Pompeii (AD 79) (Delibrias et al., 1979; Santacroce, 1987; Rolandi et al., 1993a,b; Andronico et al., 1995; Civetta et al., 1998; Sigurdsson, 2002; Cella et al., 2007). Among them
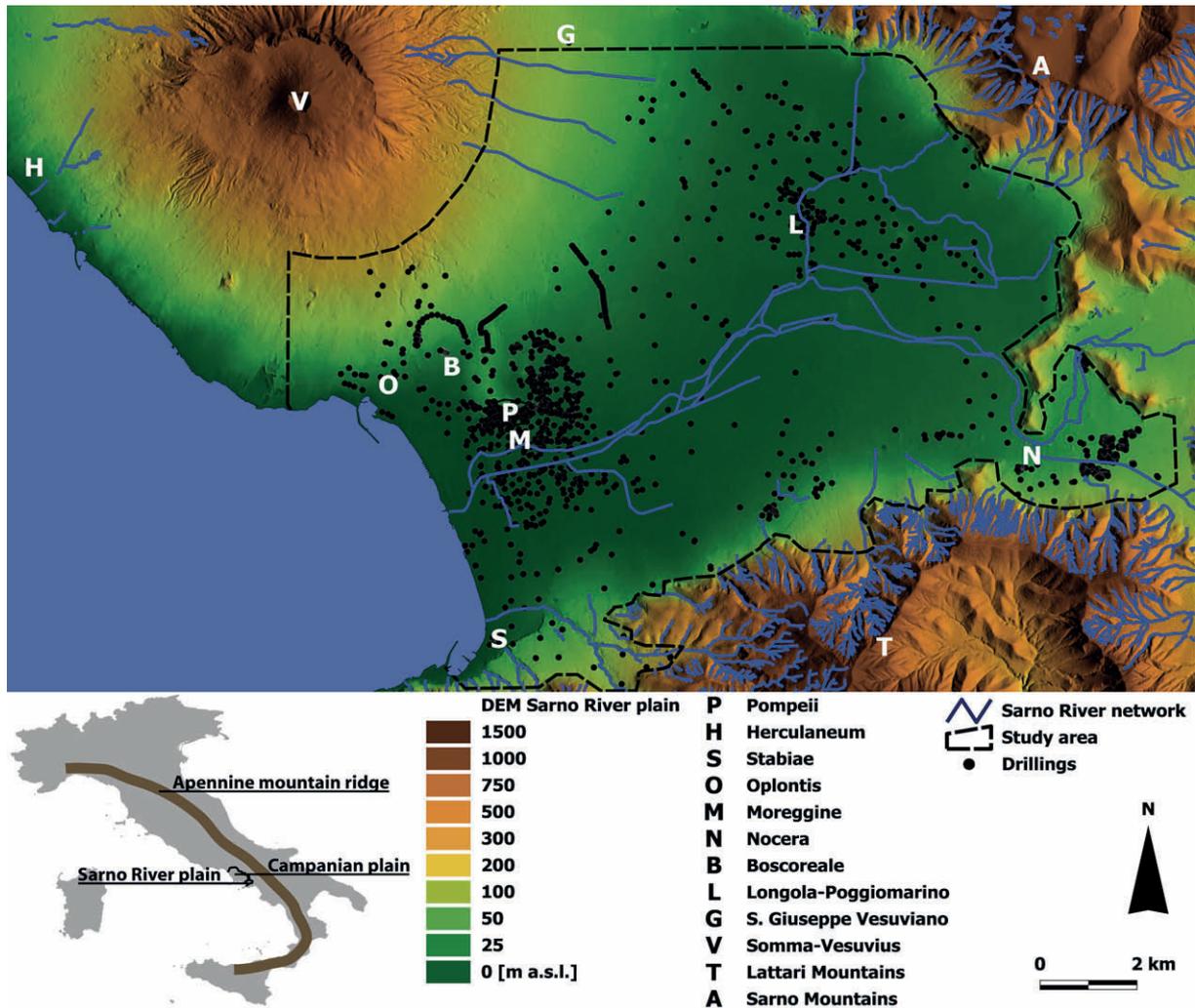
Fig. 3. Present-day digital elevation model (DEM) and fluvial network of the Sarno River plain with the location of more than 1800 stratigraphical core drillings. Letters indicate sites of interest. The small scale map of Italy shows the Campanian plain, the Sarno River plain and the Apennine mountain ridge.

the eruption of AD 79 is the most well-known thanks to the detailed written records of Pliny the Younger.

3. Materials and methods

Since today the Sarno River plain is one of the most densely populated and urbanized areas in Italy, there are many constraints in comprehensively applying methods of stratigraphical research over the entire plain. Consequently it is very important to use a rather non-invasive or minimally-invasive scientific approach. Stratigraphical core drillings have become a well-established and standardized method of geoarchaeological prospection in this region since it can be carried out with comparatively minimal technical and bureaucratic effort and costs.

To reconstruct the pre-AD 79 geomorphology and paleo-environmental features of the Sarno River plain, the documentation of more than 1800 drillings from construction works, as well as from past archaeological and geological studies, were collected to gain a representative network of stratigraphical information for the entire Sarno River plain. The drillings were localized and digitized using geographic information systems (GIS) (Fig. 3). Furthermore, 20 new core drillings were conducted south and northwest of Pompeii at Moreggine and Boscoreale (Fig. 3). The drillings were carried out mechanically to a maximum depth of 10 to 18 m to extract a core of

approximately 15 cm in diameter. By means of the drilling cores the stratigraphy was determined, the volcanic deposits of AD 79 and the pre-AD 79 surface underneath were identified, and the pre-AD 79 stratum was characterized.

For this project the most relevant data taken from the drilling documentation were:

(i) *x–y*-coordinates of each drilling point,
(ii) elevation of the present-day surface,
(iii) thickness of the volcanic deposits related to AD 79 eruption,
(iv) depth to the pre-AD 79 surface which is the difference between the present-day surface and pre-AD 79 surface, and
(v) characteristics of the pre-AD 79 stratum underneath the volcanic deposits of the AD 79 eruption.

The characteristics of the pre-AD 79 stratum allow the reconstruction of the paleo-environmental conditions. The pre-AD 79 stratum was characterized on the basis of lithofacies distinguishing five different classes:

(i) terrestrial deposits,
(ii) fluvial deposits,
(iii) palustrine deposits,
(iv) littoral deposits, and
(v) marine deposits.

45

In case the pre-AD 79 stratum could not be clearly related to one of these five classes, mixed classes were proposed to comprise intermediate forms of deposits.

Instead of using simple interpolation methods as in former studies, we reconstruct the pre-AD 79 topography with a sophisticated geostatistical methodology based on a high-resolution present-day digital elevation model (DEM). This methodology considers the statement by Stefani and Di Maio (2003) that the AD 79 eruption caused a coating of the ancient topography of the Sarno River plain which left ancient physiographic elements still recognizable in the present-day topography. Consequently the present-day topography provides valuable hints for reconstructing the ancient conditions. The following hypotheses can be outlined:

(i) geomorphic transport processes are related to topographic terrain characteristics (slope, curvature, etc.),
(ii) the pre-AD 79 topography controlled volcanic deposition, erosion and transport processes,
(iii) For pre-AD 79 and today, similar relief-forming processes have been active, and
(iv) tectonic activities and resulting landforms before AD 79 are taken into account in this modeling approach. Recent tectonic activities are considered via pre-AD 79 stratigraphic information (e.g. elevation of the ancient coastline).

Since the recent topography will be utilized to deduce the pre-AD 79 topography, a hydrologically correct present-day DEM of the Sarno River plain was generated using the interpolation method 'Topo to Raster' by Hutchinson (1988, 1989) implemented in ArcGIS 9.2. The DEM is based on digitized topographic points and contour lines in vector format of the SIT 1:5000 (Sistema Informativo Territoriale) (Provincia di Napoli, by courtesy of S.I.A.V., Soprintendenza Archeologica di Pompei). The resulting present-day DEM was postprocessed to eliminate all evident man-made structures such as dams, motorways, quarries and embankments of the Sarno River which was regulated in the 1850s (Stefani and Di Maio, 2003). After the sink drainage route detection and sink removal of the present-day DEM, 15 different primary and secondary topographic indices were delineated using the terrain analysis module of SAGA GIS (Table 1).

Based on the hypotheses stated above, a classification and regression tree approach was used to reconstruct the pre-AD 79

Table 1
Predictor variables used for the modeling process in TreeNet (Salford Systems).

Predictor variables	Method/reference
Elevation	Topo to Raster (ArcGIS 9.2)/SIT 1:5000
Altitude above channel network	SAGA terrain analysis module (Olaya and Conrad, 2008)
Aspect	SAGA terrain analysis module (Zevenbergen and Thorne, 1987)
Catchment area	SAGA terrain analysis module (Olaya and Conrad, 2008)
Channel network	SAGA terrain analysis module (Olaya and Conrad, 2008)
Channel network base level	SAGA terrain analysis module (Olaya and Conrad, 2008)
Convergence index	SAGA terrain analysis module (Köthe and Lehmeier, 1993)
Curvature	SAGA terrain analysis module (Zevenbergen and Thorne, 1987)
Curvature classification	SAGA terrain analysis module (Dikau, 1988)
Plan curvature	SAGA terrain analysis module (Zevenbergen and Thorne, 1987)
Profile curvature	SAGA terrain analysis module (Zevenbergen and Thorne, 1987)
LS-factor	SAGA terrain analysis module (Olaya and Conrad, 2008)
Slope	SAGA terrain analysis module (Zevenbergen and Thorne, 1987)
Stream power	SAGA terrain analysis module (Olaya and Conrad, 2008)
Watershed subbasins	SAGA terrain analysis module (Olaya and Conrad, 2008)
Wetness index	SAGA terrain analysis module (Olaya and Conrad, 2008)
Geology	Digitized geological map 1:10,000 (Autorità di Bacino del Sarno, 2003)
Land use	CORINE land cover 2000 (Autorità di Bacino del Sarno)
Mean annual ground water table	Interpolated (kriging) water well data (Autorità di Bacino del Sarno)

topography. Classification and Regression Trees (CARTs) is an algorithm used for exploratory data analysis and predictive modeling to discover features and understand structural patterns in large databases by describing the correlation between predictor variables and a response variable (Breiman et al., 1984; Myles et al., 2004). This algorithm can handle nominally scaled (categorical) data as well as continuously scaled (metric) data by applying either classification or regression trees. CARTs are based on binary recursive partitioning, i.e. a decision tree is generated by partition of a dataset into two subsets (binary) where each of the subsets is the basis for a further partition (recursive). This process is carried out until a partition of a subset is no longer reasonable, i.e. the elements of a subset are homogenous with respect to the response variable or if the number of elements of a subset has become too small. Eventually CARTs generate a model taking into account the combination of predictor variables with the highest correlation to explain the response variable (Dannegger, 1997; Schillinger, 2002).

The software that was applied in the present study using the CARTs algorithm is TreeNet by Salford Systems. We utilized 16 present-day topographic indices and other physiographic data as predictor variables (Table 1) and the depth to the pre-AD 79 surface as response variable to predict the pre-AD 79 topography. TreeNet is based on Friedman's stochastic gradient boosting (Friedman, 1999). Gradient boosting constructs additive regression models by sequentially fitting a simple parameterized function to current 'pseudo' residuals by least squares at each iteration. The pseudo residuals are the gradient of the loss function being minimized, with respect to the model values at each training data point, evaluated at the current step (Friedman, 1999). Practically, the method derives several hundreds to thousands of small trees each typically containing six nodes. Each tree is devoted to contributing a small portion of the overall model whereas the final model prediction is constructed by adding up each of the individual tree contributions. This methodology has a variety of advantages:

(i) it is not sensitive to data errors in the input variables,
(ii) it is resistant to overtraining, and
(iii) it is very fast even with large sets of trees.

For the modeling process we used a TreeNet regression model with the Huber-M loss function. The maximum number of trees to use is 3000. Internal model validation is performed by selecting a sample of cases at random from the model data. Here we selected a fraction of 0.2 of the entire dataset ($N = 1811$) to train the regression tree at each iteration.

The model is subsequently used to regionalize the depth to the pre-AD 79 surface for the entire Sarno River plain. To get the absolute elevation above sea level of the pre-AD 79 surface, the predicted depth is thereafter subtracted from the present-day DEM. For additional external model validation we compare the resulting pre-AD 79 DEM with the stratigraphical point type information taken from the drilling data, which is not included in the model. To specify the paleo-geomorphological and paleo-environmental characteristics of the study area and its dynamics, we perform a terrain analysis with SAGA GIS on the resulting pre-AD 79 DEM. The approximate location of the ancient coastline, the paleo-Sarno and its flood plain were already predefined by the littoral and the fluvial/palustrine deposits of the Roman stratum, respectively. We expect a more precise approximation of the ancient coastline and the paleo-Sarno from the adaptation of the existing drilling data to the modeled pre-AD 79 topography by deducing contour lines and depth contours from the pre-AD 79 DEM.

4. Results and discussion

Table 2 shows the predictor variables used for the generation of the model arranged according to their particular importance to predict the pre-AD 79 surface. For the final model not all of the

Table 2
Ranking of importance of predictor variables used for the model generation.

Variable	Importance [%]	
Elevation	100.0	||||||||||||||||||||||||||||||||||
Watershed subbasins	98.1	|||||||||||||||||||||||||||||||||
Aspect	78.3	||||||||||||||||||||||||||
Channel base level	66.9	||||||||||||||||||||||
Stream power	66.5	||||||||||||||||||||||
Depth groundwater table	58.4	|||||||||||||||||||
Slope	57.3	|||||||||||||||||||
Altitude above channel network	56.0	||||||||||||||||||
Elevation groundwater table	55.8	||||||||||||||||||
Curvature classification	49.7	||||||||||||||||
Wetness index	48.4	||||||||||||||||
Curvature	47.5	|||||||||||||||
LS-factor	46.3	|||||||||||||||
Catchment area	45.0	|||||||||||||||
Convergence index	42.5	||||||||||||||
Profile curvature	41.2	||||||||||||||
Plan curvature	40.7	||||||||||||||
Channel network	22.2	|||||||

available predictor variables were entered into TreeNet. The categorical variables geology and land use turned out to be of rather minor suitability for the modeling process since preliminary results showed that their areal distribution had a strong artificial impact on the regionalized pre-AD 79 surface. Fig. 4A illustrates the model performance with an attained minimum mean absolute error of the training dataset of 0.92 m and of the test dataset of 1.64 m. The smallest test mean absolute deviation is based on 2115 grown trees. The overall performance of the regression model on the given dataset is reported in Fig. 4B. The gain chart illustrates the percentage of population (x-axis) in relation to the percentage of the target variable (y-axis). The higher the percentage of the target variable with respective low population percentages, the better the model. In this case the model performance shows a fairly good correlation.

Fig. 5 illustrates the modeled depth to the pre-AD 79 surface of the Sarno River plain which shows a distinct spatial distribution of the volcanic deposits since the AD 79 eruption. The modeled depth to the pre-AD 79 surface ranges from > 0 to 15 m whereas the average depth is 5.7 m. In this study the Sarno River plain was only reconstructed northwards up to the modern town of S. Giuseppe Vesuviano (Fig. 3). From that location the drilling cores no longer contained AD 79 volcanic material which means that the pre-AD 79 surface could not be clearly identified anymore.

The importance of the predictor variables illustrates that the spatial distribution of volcanic deposits since and including the AD 79 eruption is most notably controlled by the absolute elevation being the result of all relief-forming geomorphic processes. Of secondary importance are the aspect and hydrological variables such as watershed subbasins, channel base level and stream power. The aspect represents the direction in which the volcanic material was spread over the territory during the eruption. Originating from the Somma–Vesuvius volcanic complex, the pumice lapilli fallout was

dispersed concentrically towards the southeast which fits well with the dispersion of the volcanic material during the AD 79 eruption as modeled by Sigurdsson and Carey (2002) and Pfeiffer et al. (2005) (Fig. 1). Consequently, on the southeastern flanks of Somma–Vesuvius, near the source of the eruption the volcanic deposits are thicker.

The hydrological parameters represent the redistribution of the volcanic deposits after the eruption by erosion, transport and accumulation processes. Thus, greater thicknesses of the volcanic deposits along the Tyrrhenian coast most likely indicate re-deposited material that was mobilized by the Sarno River and its tributaries and transported towards the Tyrrhenian Sea. This corresponds with thinner deposits in the central part of the Sarno River plain.

It is striking that along the southeastern foot slopes of Somma–Vesuvius the volcanic deposits are much thicker than in the river plain. Three main reasons may be responsible for the spatial distribution of the deposits:

(i) As mentioned above the deposition of volcanic material is generally thicker close to the vent of Somma–Vesuvius being the source of the eruption.
(ii) Apart from the white and grey pumice lapilli fallout the slopes of Somma–Vesuvius were also subject to pyroclastic surge and flow deposits of AD 79. They are concentrated at the foot slopes of Somma–Vesuvius since they did not reach far into the plain (Di Vito et al., 1998; Di Maio and Pagano, 2003).
(iii) On the slopes of Somma–Vesuvius the volcanic deposits of AD 79 are overlain by pyroclastic material and lava flows from more recent eruptions that were less powerful to reach more distant areas. Thickest deposits most notably could be related to the eruptions of 1631, 1742–1761 and 1944 (see geological map 1:10,000, Autorità di Bacino del Sarno, 2003).

An accumulation of volcanic deposits at the foot of the Lattari and Sarno Mountains may result from slope deposits being mobilized by mountain torrents or lahars after intense rainfall events. Debris flows or hyperconcentrated flows are known phenomena in the mountain areas adjacent to the Sarno River plain. The mountains are mantled by irregular layers of pyroclastic materials such as tephra and pumice fallout deposits which are intercalated with buried soils. Especially due to the presence of allophane, volcanic soils generally have a high water retention and low bulk density, which means that the weight of retained water can exceed the dry weight of the soil (Terribile et al., 2007). Due to this irregular cover of different strata which is characterized by a strong vertical variability of physical–mechanical properties, intense rainfall events can trigger slope instabilities, mass movements and thick submontane accumulations. These processes are still active today as the catastrophic landslide events of Sarno in 1998 have shown (Rao, 1995; Terribile et al., 2000; De Vita and Piscopo, 2002; Crosta and Dal Negro, 2003; Fiorillo and Wilson, 2004; Zanchetta et al., 2004; Terribile et al., 2007).

Slightly thicker deposits in the southwestern area of Pompeii running NW–SE fit well with the ancient dune ridge of Bottaro–
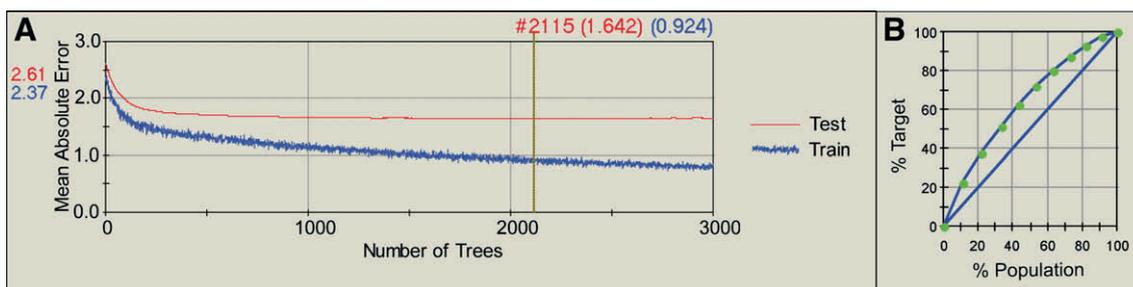

Fig. 4. Mean absolute error [m] of the depth to the pre-AD 79 surface versus number of trees of the training and test dataset (A) and gain chart of the training dataset (B) (TreeNet). The minimum mean absolute error of the training dataset of 0.92 m and of the test dataset of 1.64 m was attained at 2115 grown trees.

47
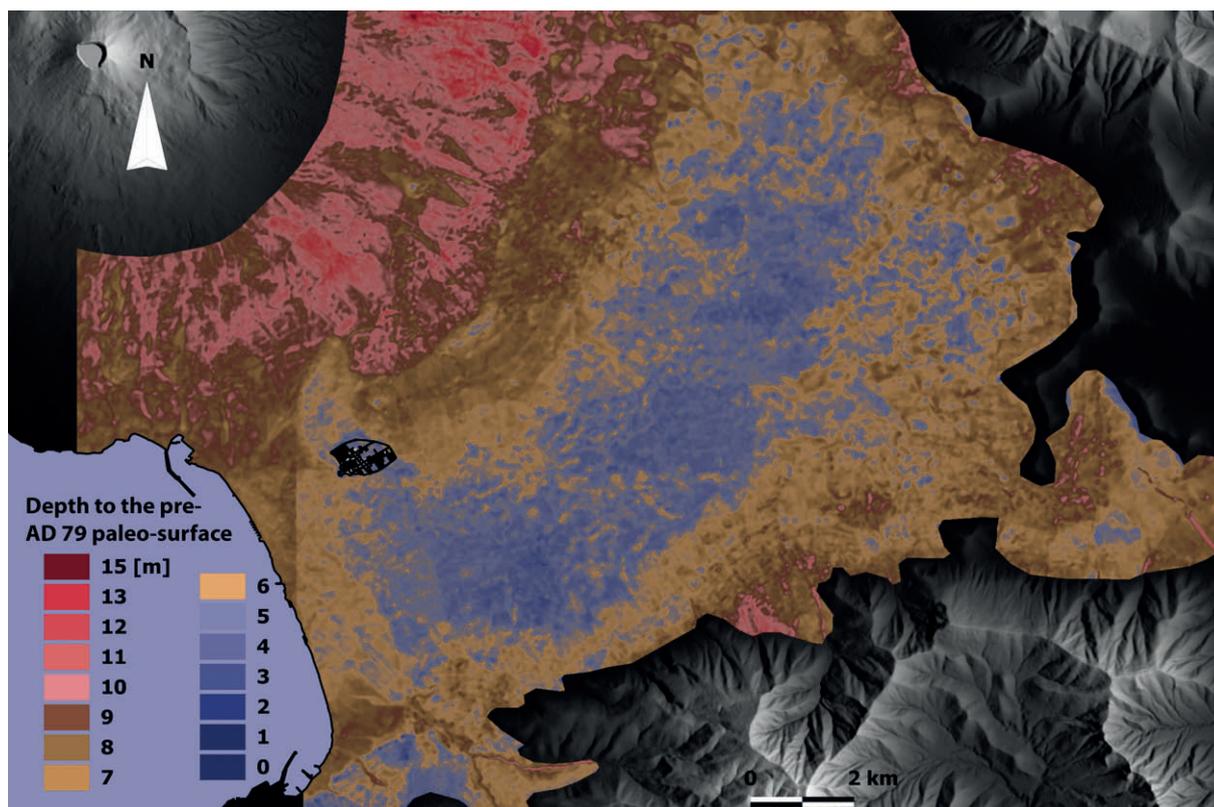
Fig. 5. Modeled depth to the pre-AD 79 surface of the Sarno River plain.

Pioppaino. This may result from the fact that the dune ridge itself shows a slightly higher elevation than the surrounding terrain. Thus, the effects of fluvial and coastal erosion processes are limited. Moreover, the surface of the dune ridge is relatively flat, for instance in comparison to the Pompeiian hill, with low slope gradients and related erosion processes. Rather thin deposits on the Pompeiian hill on the other hand indicate that after deposition AD 79 volcanic material was eroded from the ridge and accumulated in the adjacent plain due to higher slope gradients.

Fig. 6A and B compares the present-day topography with the predicted pre-AD 79 topography. Even though main physiographic elements appear on both DEMs, several differences can be identified. Most evident is that the pre-AD 79 surface is approximately 5.7 m deeper than the modern surface. Consequently the entire coastal area is lying below the recent sea level.

Comparing the present-day Sarno River (Fig. 6A) with the modeled fluvial network before AD 79 (Fig. 6B) it is striking that the main elements seem to have preserved over time and are still visible in the present-day river network, i.e. the streams from the slopes of Somma–Vesuvius, the stream from Nocera and the intersections near the Sarno Mountains. However, in comparison to the canalized present-day Sarno River, the paleo-Sarno River, which follows the depth contours of the pre-AD 79 DEM, shows meander type fluvial patterns.

In the southern section of the Tyrrhenian coast at the base of the Lattari Mountains a big fan delta can be clearly identified on both the present-day DEM and the pre-AD 79 DEM (Fig. 6). In the present-day geomorphological map of Cinque (1991) it is called 'conoide Muscariello'. It is orientated towards the main discharge of this part of the Lattari Mountains, the 'Fosso di Gragnano'. The fan delta on the modeled pre-AD 79 DEM indicates that this landform already existed in Roman times. This corresponds with Cinque (1991) and Cinque et al. (1987, 1997) who identified fan deltas of a first and second generation which they dated to the Middle and Late Pleistocene, respectively. Di Maio and Pagano (2003) also detected strong

variations in the thickness of the AD 79 eruptive material between the slopes and the adjacent Sarno River plain which they related to the formation of fan deltas due to heavy rainfall after the AD 79 eruption. However, in their reconstruction of the paleo-coastline near the ancient town of Stabia, they state that the fan delta did not exist at the moment of the AD 79 eruption. Consequently they delineated the coastline between 100 and 200 m parallel to the terrace of San Marco (Fig. 2).

The external validation of the pre-AD 79 DEM was performed using the stratigraphical information from the core drillings (see Materials and Methods). Furthermore by comparing the categorized character of the pre-AD 79 stratum with the pre-AD 79 DEM we reconstructed some paleo-environmental features before AD 79 (Fig. 7A and B).

The results show that the littoral deposits before AD 79 are distributed nearly parallel to the present-day coastline at a horizontal distance of 1000 to 1500 m (Fig. 7A). In the north of the Tyrrhenian coast, most of the littoral deposits are located between the -3 and -2 m contour lines, and near the Sarno River and in the south of the bay, between the -1 and 0 m contour lines. This matches with findings of Sigurdsson et al. (1985) and Livadie et al. (1990) who state that after AD 79 a northwards dipping subsidence of the Roman littoral deposits to approximately -4 m occurred. Near the mouth of the Sarno River the same deposits could be found at -1 m. Pescatore et al. (2001) state that a more rapid subsidence appears near Somma–Vesuvius in comparison with more distant areas. This subsidence is related to the collapse of the graben structure of the Campanian plain of approximately 2 mm year^{-1} during the entire Quaternary. In the Sarno River plain subsidence is compensated by the constant accumulation of volcanic deposits due to the activity of Somma–Vesuvius which finally resulted in a westward propagation of the coastline (Cinque et al., 1987; Livadie et al., 1990; Cinque, 1991).

Converging contour lines at the foot of Somma–Vesuvius, the Lattari Mountain and the Pompeiian hill that are orientated towards
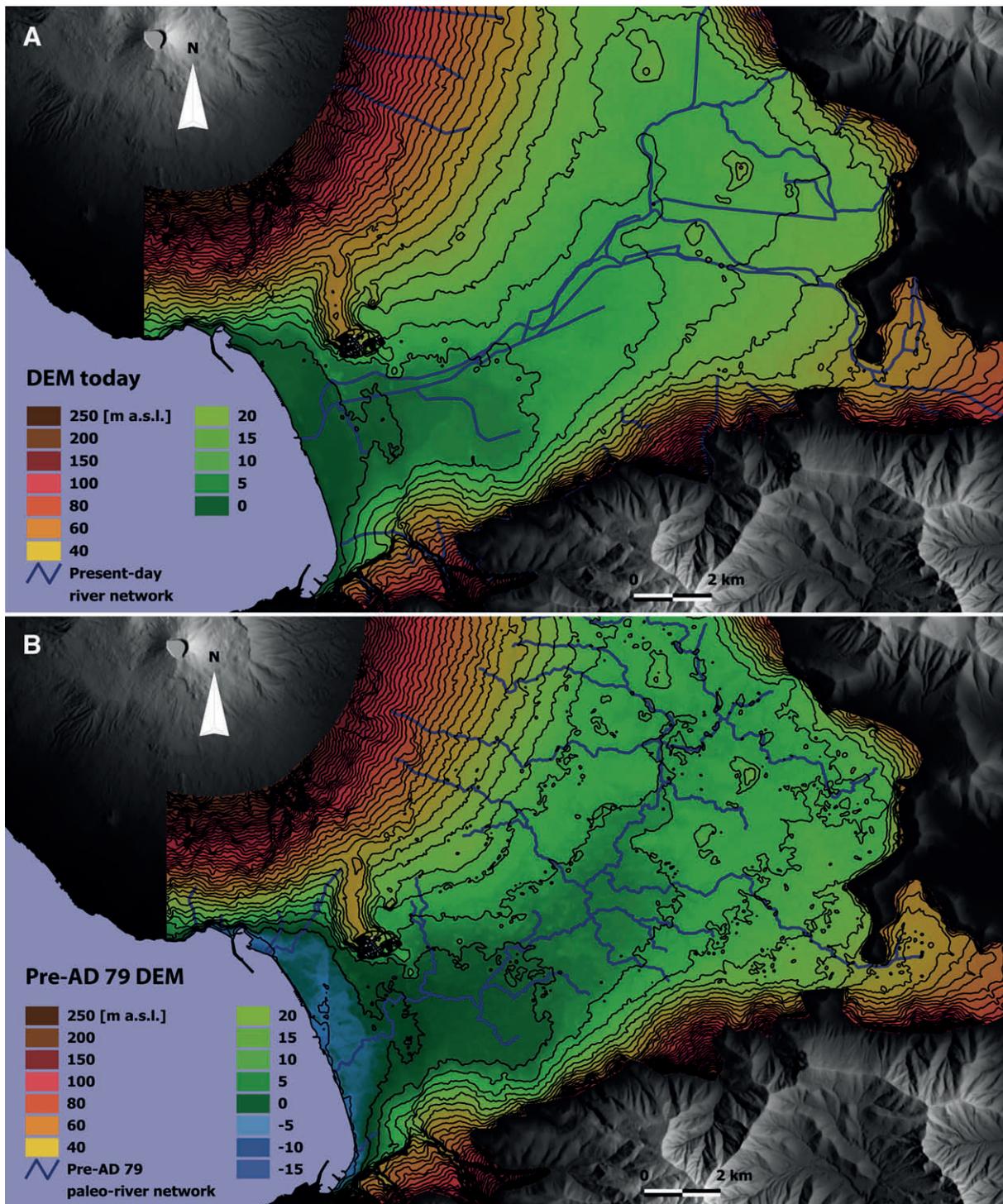
Fig. 6. Present-day DEM (A) and modeled pre-AD 79 DEM (B) of the Sarno River plain with 5-m contour lines and fluvial network.

the sea reveal escarpments that may have derived from abrasion action of the sea related to previous coastlines (Fig. 8). The protohistorical dune ridges of Messigno and Bottaro/Pioppaino could be delineated by confronting their location from the geological map (Autorità di Bacino del Sarno, 2003) with both the modeled pre-AD 79 topography and the distribution of marine/littoral deposits from the drilling data that were found inland from the ancient shoreline (Figs. 7 and 8).

The distribution of fluvial/palustrine deposits taken from the drilling data correlates well with the modeled paleo-river network.

Especially around the mouth of the paleo-Sarno River and near Longola–Poggiomarino, these deposits are characterized by the 1 to 2 m isolines of the 'vertical distance to channel network' index from the SAGA terrain analysis module. This area contains 71% of all fluvial/palustrine deposits found in the drilling data. Consequently, this area can be identified as the flood area in which the paleo-Sarno River most likely had its ancient riverbed. Near Pompeii the paleo-Sarno River bends southwards, approximately 1 km away from its present-day river bed to flow around the more elevated proto-historical dune ridges of Messigno and Bottaro/Pioppaino. This agrees
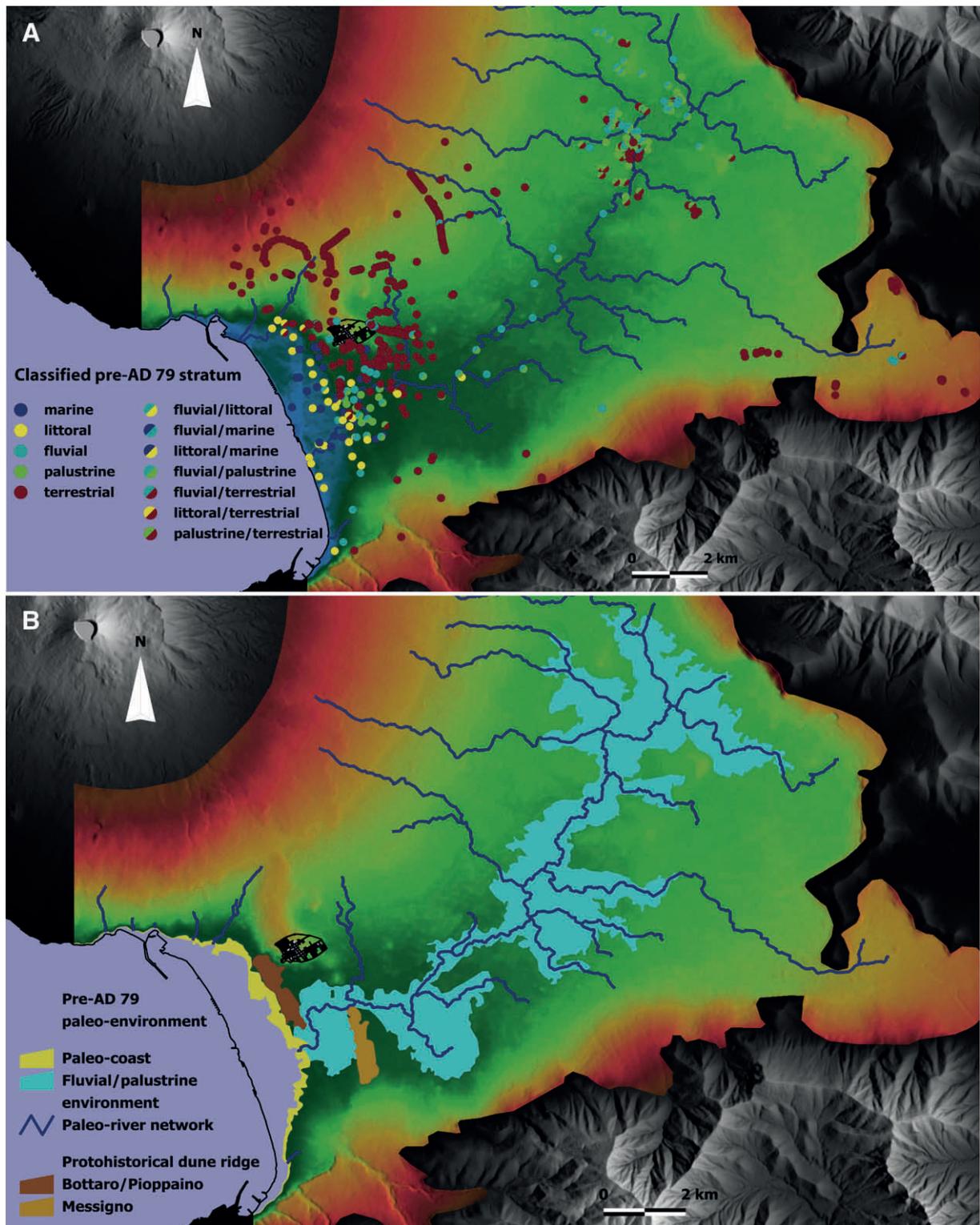
Fig. 7. Pre-AD 79 DEM with the drilling data on the pre-AD 79 stratum (A) and inferred reconstruction of pre-AD 79 environmental features (B).

well with the paleo-Sarno River of Stefani and Di Maio (2003) and the geological map (Autorità di Bacino del Sarno, 2003). Due to the plain relief, this area will most likely be characterized by meanders, backwaters and an extensive flood area. The approximate mouth of the paleo-Sarno can be localized around 1500 m east of its present-day mouth which coincides with a noticeable inland propagation of the −3 and −2 m contour lines. This location corresponds well with

the findings of Barra et al. (1989) and Livadie et al. (1990) stated above.

Based on deeper littoral deposits in the northern coastal area, the pre-AD 79 DEM revealed an elevation discontinuity southwest of the excavation of Pompeii (Figs. 5 and 8). The discontinuity is more than 3 km long and oriented N–S. It includes several elevation levels from 1 to −5 m a.s.l. and has a vertical offset from east to west of −0.5 to
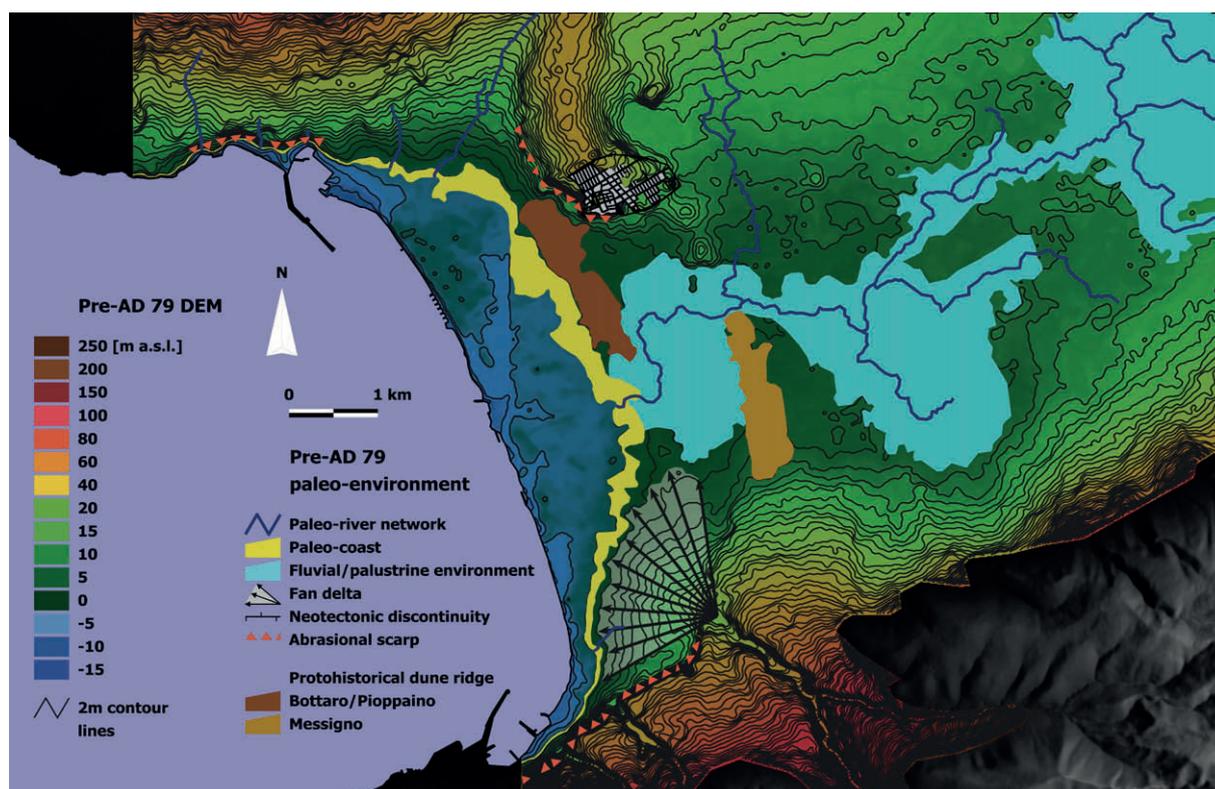
Fig. 8. Pre-AD 79 environmental reconstruction of the Tyrrhenian coast of the Sarno River plain.

−1.5 m. Thus, relative to the western part, the eastern part of this discontinuity is displaced towards the south indicating a horizontal transversal fault. Neotectonic deformations of the Apennines are predominantly oriented SW–NE or NW–SE. However, reactivated faults of an E–W or N–S orientation can sometimes be found (Nicotera and Civita, 1969a,b; Ortolani and Aprile, 1978; Aprile and Ortolani, 1979; Cinque et al., 1987). This discontinuity seems to be overprinted by recent deposition as it cannot be identified on the present-day DEM. This implies that it was formed before AD 79 possibly associated with the seismic activity preceding the AD 79 eruption, such as the big earthquakes of AD 62 and AD 64. Marturano (2008) and Marturano et al. (2009) proposed a ground uplift of Pompeii of around 2 m prior to the AD 79 eruption which fits well with the modeled discontinuity. The crustal deformations are presumably caused by the inflation of magma bodies underneath the Somma–Vesuvius volcanic complex.

5. Conclusions

The pre-AD 79 topography and paleo-environmental features of the entire Sarno River plain were reconstructed for the first time using sophisticated geostatistical methods. The estimated pre-AD 79 topography and the derived paleo-river network fit well with the stratigraphical data from the drilling documentation. In addition to the internal validation, the semantic validation also yielded good results. Nevertheless this reconstruction is only a model of the pre-AD 79 conditions based on the hypothesis stated above. Consequently the modeled paleo-river network is only approximate and cannot be considered as the exact paleo-course of the Sarno River before AD 79, since it is derived from the regionalized pre-AD 79 DEM. However, the deduced contour lines enclosing the fluvial/palustrine and littoral deposits from the drillings data more reliably indicate the approximate location of the paleo-Sarno and the paleo-coastline, respectively.

In future studies the pre-AD 79 DEM will be used to identify zones of particular interest for carrying out additional stratigraphical drillings. The pre-AD 79 DEM will be utilized to determine potential locations of Pompeii's marine or fluvial harbour, whose exact location is still debated (e.g. Stefani and Di Maio, 2003). Moreover, the combination of the pre-AD 79 DEM with archaeological findings enhances the paleo-environmental reconstruction of the Sarno River plain.

In the next project phase the pre-AD 79 DEM will be used to determine the paleo-topographic setting of the known 'villae rusticae' of the Sarno River plain (Casale and Bianco, 1979; Kockel, 1985, 1986). In addition to paleo-pedological analyses, we will use the pre-AD 79 topography to reconstruct soil and land use characteristics. These data will help us to simulate the ancient cultural landscape of the Sarno River plain. In summary, the modeled pre-AD 79 DEM has a great potential for future geoarchaeological investigations.

51

References

Andronico, D., Calderoni, G., Cioni, R., Sbrana, A., Sulpizio, R., Santacroce, R., 1995. Geological map of Somma–Vesuvius volcano. Period. Mineral. 64, 77–78.

Aprile, F., Ortolani, F., 1979. Sulla struttura profonda della Piana Campana. Boll. Soc. Nat. Napoli 88.

Autorità di Bacino del Sarno, 2003. Cartografia Geologica, scala 1:10000. Progetto CARG, Regione Campania.

Barra, D., Bonaduce, G., Brancaccio, L., Cinque, A., Ortolani, F., Pagliuca, S., Russo, F., 1989. Evoluzione geologica olocenica della piana costiera del fiume Sarno (Campania). Mem. Soc. Geol. Ital. 42, 255–267.

Breiman, L., Friedman, J., Olshen, R., Stone, C., 1984. Classification and Regression Trees. Chapman and Hall, New York.

Carey, S., Sigurdsson, H., 1987. Temporal variations in column height and magma discharge rate during the 79 A.D. eruption of Vesuvius. Geol. Soc. Amer. Bull. 99, 303–314.

Casale, A., Bianco, A., 1979. Primo contributo alla topografia del suburbio Pompeiano. Antiqua 4, 27–56.

Cella, F., Fedi, M., Florio, G., Grimaldi, M., Rapolla, A., 2007. Shallow structure of the Somma–Vesuvius volcano from 3D inversion of gravity data. J. Volcanol. Geotherm. Res. 161, 303–317.

Cinque, A., 1991. La trasgressione versiliana nella piana del Sarno, Campania. Geogr. Fis. Din. Quat. 14, 63–71.

Cinque, A., Russo, F., 1986. La linea di costa del 79 A.D. fra Oplonti e Stabiae nel quadro dell'evoluzione olocenica della Piana del Sarno (Campania). Boll. Soc. Geol. Ital. 105, 111–121.

Cinque, A., Alinaghi, H.H., Laureti, L., Russo, F., 1987. Osservazioni preliminari sull'evoluzione geomorfologica della piana del Sarno Campania, Appennino Meridionale. Geogr. Fis. Din. Quat. 10, 161–174.

Cinque, A., Aucelli, P.P.C., Brancaccio, L., Mele, R., Milia, A., Robustelli, G., Romano, P., Russo, F., Russo, M., Santangelo, N., Sgambati, D., 1997. Volcanism, tectonics and recent geomorphological change in the bay of Napoli. I.A.G. IV Int. Conf. on Geomorphology: Geogr. Fis. Dinam. Quat., vol. III (T2), pp. 123–141.

Cioni, R., Marianelli, P., Sbrana, A., 1992. Dynamics of the A.D. 79 eruption: stratigraphic, sedimentological and geochemical data on the successions from the Somma–Vesuvius southern and eastern sectors. Acta Vulcanol. 2, 109–123.

Civetta, L., Galati, R., Santacroce, R., 1991. Magma mixing and convective compositional layering within the Vesuvius magma chamber. Bull. Volcanol. 53, 287–300.

Civetta, L., Di Vito, M.A., De Lucia, M., Isaia, R., 1998. Storia eruttiva del Somma–Vesuvio. In: Guzzo, P., Peroni, R. (Eds.), Archeol. Vulcanic. Campania, pp. 9–16. Naples.

Crosta, G.B., Dal Negro, P., 2003. Observations and modelling of soil slip-debris flow initiation processes in pyroclastic deposits: the Sarno 1998 event. Nat. Hazards Earth Syst. Sci. 3, 53–69.

Dannegger, F., 1997. Tree stability diagnostics and some remedies against instability. Institute of Statistics, Ludwig-Maximilians-University of Munich, Sonderforschungsbereich. 386.

Delibrias, G., Di Paola, G.M., Rosi, M., Santacroce, R., 1979. La storia eruttiva del complesso vulcanico Somma–Vesuvio ricostruita dalle successioni piroclastiche del Monte Somma. Rend. Soc. Ital. Mineral. Petrol. 35, 411–438.

De Vita, P., Piscopo, V., 2002. Influences of hydrological and hydrogeological conditions on debris flows in peri-vesuvian hillslopes. Nat. Hazards Earth Syst. Sci. 2, 27–35.

Dikau, R., 1988. Entwurf einer geomorphographisch-analytischen Systematik von Reliefeinheiten. Heidelb. Geogr. Baust. 5, 1–45.

Di Maio, G., Pagano, M., 2003. Considerazioni sulla linea di costa e sulle modalità di seppellimento dell'antica Stabia a seguito dell'eruzione vesuviana del 79 d.C. Riv. Studi Pompei. XIV, 197–245.

Di Vito, M.A., Sulpizio, R., Zanchetta, G., Calderoni, G., 1998. The geology of the South Western Slopes of Somma–Vesuvius, Italy, as inferred by borehole stratigraphies and cores. Acta Vulcanol. 10, 383–393.

Fiorillo, F., Wilson, R.C., 2004. Rainfall induced debris flows in pyroclastic deposits, Campania (southern Italy). Eng. Geol. 75, 263–289.

Foss, J.E., Timpson, M.E., Ammons, J.T., Lee, S.Y., 2002. Paleosols of the Pompeii area. In: Jashemski, W.F. (Ed.), The Natural History of Pompeii. Cambridge University Press, Cambridge, pp. 65–79.

Friedman, J.H., 1999. Stochastic gradient boosting. Technical Report. Department of Statistics, Stanford University, USA. http://www.salford-systems.com/treenet.html.

Furnari, E., 1994. Nuovi contributi all'identificazione del littorale antico di Pompei. AA. VV., Neapolis Temi Progettuali, Roma, vol. II, pp. 219–291.

Hutchinson, M.F., 1988. Calculation of hydrologically sound digital elevation models. Third International Symposium on Spatial Data Handling, Sydney. International Geographical Union, Columbus, Ohio.

Hutchinson, M.F., 1989. A new procedure for gridding elevation and stream line data with automatic removal of spurious pits. J. Hydrol. 106, 211–232.

Iacono, L., 1913. Note di archeologia marittima. In Neapolis I, f. III–IV, pp. 353–371.

Kockel, V., 1985. Archäologische Funde und Forschungen in den Vesuvstädten I. Archäol. Anz. 495–571.

Kockel, V., 1986. Archäologische Funde und Forschungen in den Vesuvstädten II. Archäol. Anz. 443–569.

Köthe, R., Lehmeier, F., 1993. SARA — Ein Programmsystem zur Automatischen Reliefanalyse. Z. Angew. Geogr. 4, 11–21.

Lirer, L., Pescatore, T., Booth, B., Walker, G.P.L., 1973. Two Plinian pumice-fall deposits from Somma–Vesuvius, Italy. Geol. Soc. Amer. Bull. 84, 759–772.

Livadie, C.A., Barra, D., Bonaduce, G., Brancaccio, L., Cinque, A., Ortolani, F., Pagliuca, S., Russo, F., 1990. Evoluzione geomorphologica, neotettonica e vulvanica della piana costiera del fiume Sarno (Campania) in relazione agli insediamenti anteriori all'eruzione del 79 d.C. Pact 25–13, 237–256.

Luongo, G., Perrotta, A., Scarpati, C., 2003. Impact of the AD 79 explosive eruption on Pompeii, I. Relations amongst the depositional mechanisms of the pyroclastic products, the framework of the buildings and the associated destructive events. J. Volcanol. Geotherm. Res. 126, 201–223.

Malandrino, C., 1988. Il "Pagus" Marittimo di Pompei. Note di topografia antica. In: D'Amelio (Ed.), Torre Annunziata, p. 40.

Marturano, A., 2008. Sources of ground movements at Vesuvius before the AD 79 eruption: evidence from contemporary accounts and archaeological studies. J. Volcanol. Geotherm. Res 177, 959–970.

Marturano, A., Aiello, G., Barra, D., Fedele, L., Grifa, C., Morra, V., Berg, R., Varone, A., 2009. Evidence for Holocenic uplift at Somma–Vesuvius. J. Volcanol. Geotherm. Res. doi:10.1016/j.jvolgeores.2009.05.020..

Myles, A., Feudale, R., Liu, Y., Woody, N., Brown, S., 2004. An introduction to decision tree modelling. J. Chemom. 18, 275–285.

Nicotera, P., Civita, M., 1969a. Indagine idrogeologiche per la captazione delle sorgenti S. Marina di Lavorate Sarno). Mem. Note Ist. Geol. Appl. Univ. Napoli 11, 25–44.

Nicotera, P., Civita, M., 1969b. Ricerche idrogeologiche per la realizzazione delle opere di presa delle sorgenti Mercato e Palazzo Sarno). Mem. Note Ist. Geol. Appl. Univ. Napoli 11, 1–63.

Olaya, V., Conrad, O., 2008. Geomorphometry in SAGA. In: Hengl, T., Reuter, H.I. (Eds.), Geomorphometry: Concepts, Software, Applications. Elsevier, Amsterdam, pp. 293–308.

Ortolani, F., Aprile, F., 1978. Nuovi dati sulla struttura profonda della Piana Campana a SE del Fiume Volturno. Boll. Soc. Geol. Ital. 97, 591–608.

Pescatore, T., Senatore, M.R., Capretto, G., Lerro, G., Patricelli, G., 1999. Ricostruzione paleoambientale delle aree circostanti l'antica Città di Pompei Campania, Italia) al Tempo dell'eruzione del Vesuvio del 79 d.C. Boll. Soc. Geol. Ital. 118, 243–254.

Pescatore, T., Senatore, M.R., Capretto, G., Lerro, G., 2001. Holocene coastal environments near Pompeii before the A.D. 79 eruption of Mount Vesuvius, Italy. Quat. Res. 55, 77–85.

Pfeiffer, T., Costa, A., Macedonio, G., 2005. A model for the numerical simulation of tephra fall deposits. J. Volcanol. Geotherm. Res. 140, 273–294.

Rao, S.M., 1995. Mechanistic approach to the shear strength behavior of allophanic soils. Eng. Geol. 40, 215–221.

Rolandi, G., Maraffi, S., Petrosino, P., Lirer, L., 1993a. The Ottaviano eruption of Somma–Vesuvio 8000 y B.P. a magmatic alternating fall and flow-forming eruption. J. Volcanol. Geotherm. Res. 58, 43–65.

Rolandi, G., Mastrolorenzo, G., Barrella, A.M., Borrelli, A., 1993b. The Avellino plinian eruption of Somma–Vesuvio 3760 y B.P— the progressive evolution from magmatic to hydromagmatic style. J. Volcanol. Geotherm. Res. 58, 67–88.

Ruggiero, M., 1879. Del sito di Pompei e dell'antico lido del mare. Pompei e la regione sotterrata dal Vesuvio nell'anno, vol. 79. Mem. e Note pubb. dall'ufficio tecn. degli scavi delle prov. meridionali, Napoli, pp. 5–14.

Santacroce, R., 1987. Somma–Vesuvius. C.N.R., Quaderni de 'La Ricerca Scientifica' 114, Rome, 251 pp.

Schillinger, M.P., 2002. Flächenhafte Schätzung mit Classification and Regression Trees und robuste Gütebestimmung ökologischer Parameter in einem kleinen Einzugsgebiet. Doctoral Thesis, Faculty of Biology, Chemistry and Geo Sciences, University of Bayreuth.

Sigurdsson, H., 2002. Mount Vesuvius before the Disaster. In: Jashemski, W.F. (Ed.), The Natural History of Pompeii. Cambridge University Press, Cambridge, pp. 29–36.

Sigurdsson, H., Carey, S., 2002. The eruption of Vesuvius in A.D. 79. In: Jashemski, W.F. (Ed.), The Natural History of Pompeii. Cambridge University Press, Cambridge, pp. 37–64.

Sigurdsson, H., Carey, S., Cornell, W., Pescatore, T., 1985. The eruption of Vesuvius in A.D. 79. Natl. Geogr. Res. 1, 332–387.

Stefani, G., Di Maio, G., 2003. Considerazioni sulla linea di costa del 79 d.C. e sul porto dell'antica Pompei. Riv. Studi Pompei. XIV, 142–195.

Terribile, F., Basile, A., De Mascellis, R., di Gennaro, A., Mele, G., Vingiani, S., 2000. I suoli delle aree di crisi di Quindici e Sarno: proprietà e comportamenti in relazione ai fenomeni franosi del 1998. Quad. Geol. Appl. 7 (1), 59–95.

Terribile, F., Basile, A., De Mascellis, R., Iamarino, M., Magliulo, P., Pepe, S., Vingiani, S., 2007. Landslide processes and andosols: the case study of the Campania region, Italy. In: Arnalf, Ó., Bartoli, F., Buurman, P., Óskarson, H., Stoops, G., García-Rodeja, E. (Eds.), Soils of Volcanic Regions in Europe. Springer-Verlag, Berlin, Heidelberg, pp. 545–563.

Zanchetta, G., Sulpizio, R., Pareschi, M.T., Leoni, F.M., Santacroce, R., 2004. Characteristics of May 5–6, 1998 volcaniclastic debris flows in the Sarno area Campania, southern Italy. relationships to structural damage and hazard zonation. J. Volcanol. Geotherm. Res. 133, 377–393.

Zevenbergen, L.W., Thorne, C.R., 1987. Quantitative analysis of land surface topography. Earth Surf. Process. Landf. 12, 47–56.

2.2 Revised modeling the post-AD 79 volcanic deposits of Somma-Vesuvius to reconstruct the pre-AD 79 topography of the Sarno River plain (Italy).

Sebastian Vogel[a,c]*, Michael Märker[a,b], and Florian Seiler[c]

[a] Heidelberg Academy of Sciences and Humanities c/o University of Tübingen, Rümelinstraße 19-23, D-72070 Tübingen, Germany

[b] Department of Vegetation, Soil, Environment and Agroforestry Sciences, University of Florence, P.zza S.Marco 4, I-50121 Florence, Italy

[c] German Archaeological Institute, Podbielskiallee 69-71, D-14195 Berlin, Germany

* Corresponding author. Tel: +49 (0)30 187 711 358, Fax: +49 (0)30 187 711 168
E-mail address: sv@dainst.de (S. Vogel), www.salve-research.org

Abstract

In this study the methodology proposed by Vogel and Märker (2010) to reconstruct the pre-AD 79 topography and paleo-environmental features of the Sarno River plain (Italy) was considerably revised and improved. The methodology is based on an extensive dataset of stratigraphical information of the entire Sarno River plain, a high-resolution present-day digital elevation model (DEM) and a classification and regression tree approach. The dataset was re-evaluated and 32 additional stratigraphical drillings were collected in areas that were not or insufficiently covered by previous stratigraphic data. Altogether, an assemblage of 1,840 drillings, containing information about the depth from the present-day surface to the pre-AD 79 paleo-surface (thickness of post-AD 79 deposits) and the character of the pre-AD 79 paleo-layer of the Sarno River plain was utilized. Moreover, an improved preprocessing of the input parameters attained a distinct progress in model performance in comparison to the previous model of Vogel and Märker (2010). Subsequently, a spatial model of the post-AD 79 deposits was generated. The modeled deposits were then used to reconstruct the pre-AD 79 topography of the Sarno River plain. Moreover, paleo-environmental and paleo-geomorphological features such as the paleo-coastline, the paleo-Sarno River and its floodplain, alluvial fans near the Tyrrhenian coast as well as abrasion terraces of historical and protohistorical coastlines were identified. This reconstruction represents a qualitative improvement of previous work of Vogel and Märker (2010).

Introduction

When Somma-Vesuvius volcanic complex explosively erupted AD 79 its adjacent south-eastern territory was covered by volcanic deposits of some meters thickness in a very short period of time. Consequently, not only the Roman settlements of Pompeii and Herculaneum but also almost the entire ancient landscape of the Sarno River plain were buried and thereby preserved to a certain extent. Since the laterally extensive volcanic deposits of AD 79 show a specific and therefore readily identifiable stratigraphy they can be used as a chronostratigraphic marker. This stratigraphy consists of white phonolitic and grey tephritic phonolitic pumice lapilli fallout on top

of the pre-AD 79 Roman surface. The grey pumice are interrupted and overlain by several ash layers of pyroclastic surge and flow deposits (Sigurdsson et al., 1985; Carey and Sigurdsson, 1987; Civetta et al., 1991; Cioni et al., 1992; Lirer et al., 1993; Luongo et al., 2003).

Vogel and Märker (2010) made a detailed review of past paleo-environmental studies in the Sarno River plain among them Cinque and Russo (1986), Livadie et al. (1990), Furnari (1994), Pescatore et al. (1999), Di Maio and Pagano (2003) and Stefani and Di Maio (2003). These studies mostly focussed on the delineation of the coastline before AD 79 and the paleo-course of the Sarno River and its estuary mouth. Vogel and Märker (2010) demonstrated that the pre-AD 79 paleo-surface of the entire Sarno River plain can be reconstructed by using sophisticated geostatistical methods. This methodology is based on an extensive dataset of stratigraphical information, a high-resolution present-day digital elevation model (DEM) and a classification and regression tree approach.

The objective of this paper is to revise and improve the spatial model of post-AD 79 deposits established by Vogel and Märker (2010) as well as the deduced pre-AD 79 paleo-topography and selected paleo-environmental features by using an increased number of stratigraphical data and further preprocess the input parameter.

Study area

The Sarno River plain is located south of the volcanic complex of Somma-Vesuvius and belongs to the southern part of the Plio-Pleistocene graben structure of the Campanian plain. It has a surface area of approximately 210 km² and is drained by the Sarno River and its tributaries. In the south and in the east the basin is flanked by the Lattari and Sarno Mountains belonging to the Apennine Mountain chain. In the west it has an approximately 10 km long coast line with the Tyrrhenian Sea. The Sarno River plain consists of marine, alluvial and volcanic deposits lying on top of a carbonate platform that reaches down to a maximum depth of 2 km b.s.l. (Cella et al., 2007). During the last 25,000 years the Sarno River plain has been repeatedly influenced by the periodic activity of Somma-Vesuvius volcano. Several explosive (Plinian) eruptions have occurred, each one marking the beginning of a new eruptive cycle after a certain period of quiescence that can last some thousand years (Delibrias

et al., 1979; Santacroce, 1987; Rolandi et al., 1993a,b; Andronico et al., 1995; Civetta et al., 1998; Sigurdsson, 2002; Cella et al., 2007). Among those Plinian eruptions the event of AD 79 was one of the most destructive ones and today it is one of the most well-known and most studied volcanic eruptions in history.

Methodology

The methodology applied to reconstruct the pre-AD 79 topography of the Sarno River plain was described in detail by Vogel and Märker (2010). Most fundamentally, it is based on an extensive dataset of stratigraphic cross-sections from a total of 1,840 core drillings to gain a representative network of stratigraphical information for the entire Sarno River plain (Fig. 1). The collected core drillings were carried out during construction works, as well as past archaeological and geological studies. Compared to the previous model of Vogel and Märker (2010) 32 additional sections from drillings were collected in the area of Boscoreale, Stabiae, Angri and Longola-Poggiomarino. The new drillings north of Angri, but also in Boscoreale, cover an area where stratigraphical data were so far missing. Additionally, between 2007 and 2009 we conducted 24 further core drillings in areas with insufficient stratigraphical information and included them in the modeling.

A characteristic feature of the AD 79 explosive eruptions of Somma-Vesuvius is a thick layer of white phonolitic pumice that was deposited upon a dark Roman paleosol. Moreover, no former or later eruption of Somma-Vesuvius is comparable with that of AD 79 in terms of magnitude, stratigraphic appearance and spatial distribution. Consequently, the stratigraphic position of the Roman paleo-surface can be easily identified and measured even though some drillings were carried out without strict scientific control but during construction works.

The core drillings were collected, localized and digitized using geographic information systems (GIS). The stratigraphy of the drillings was determined, above all identifying the volcanic deposits of the AD 79 eruption, the pre-AD 79 paleo-surface underneath and measuring the depth from the present-day surface to the pre-AD 79 surface (thickness of post-AD 79 deposits). Furthermore, the pre-AD 79 layer was characterized and categorized distinguishing five different environmental

classes which later on allows the reconstruction of some important paleo-environmental features of the Sarno River plain (Vogel and Märker, 2010):

(i)   terrestrial deposits:

Roman paleosol of loamy sand that is characterized by the formation of a dark humus A horizon and sometimes by an initial A/Bw weathering horizon. It is composed of fine weathered ash, rounded pumice, lapilli and lithic clasts. Sometimes traces of agricultural use and former vegetation as well as fragments of ceramics can be found.

(ii)   fluvial deposits:

Fluvial deposits consist of conglomerates of black fluvial gravel within a sandy or loamy matrix. They contain rounded pumice and lithic clasts mostly sorted in thin layers of different deposition cycles. Sometimes also fragments of travertine can be found. They identify the alluvium of rivers, mainly of the Sarno River network.

(iii)   palustrine deposits:

Palustrine deposits consist of loamy substrate interconnected with dark greyish peaty layers rich in organic matter and plant remains. They are often characterized by hydromorphic features indicating pedogenetic processes of gleyzation that are caused by the presence of a high ground water table. Furthermore they can contain pumice, travertine plates and shells of fresh water gastropods. These deposits represent wetlands (bogs and swamps) that are mainly linked to the floodplain of the Sarno River.

(iv)   littoral deposits:

Littoral deposits are associated with the ancient coastline. They contain well-sorted grey littoral gravel and sand with rounded pumice and lithic clasts.

(v)   marine deposits:

Marine deposits consist of grey marine gravel and sand that can contain remains of marine organisms (e.g. shells of saltwater gastropods). They indicate the presence of the Tyrrhenian Sea or lagoons that are separated from the active shore by littoral deposits.

Since both, fluvial and palustrine deposits are closely related to the paleo-Sarno River the two classes were finally merged to identify the floodplain of the paleo-Sarno River. If the pre-AD 79 layer could not be clearly related to one of these five classes, additionally, mixed classes were built to incorporate intermediate forms of deposits.

Figure 1. Present-day digital elevation model (DEM) and fluvial network of the Sarno River plain with the location of 1,840 stratigraphical core drillings. New collected or conducted drillings are indicated in red. Letters mark sites of interest.
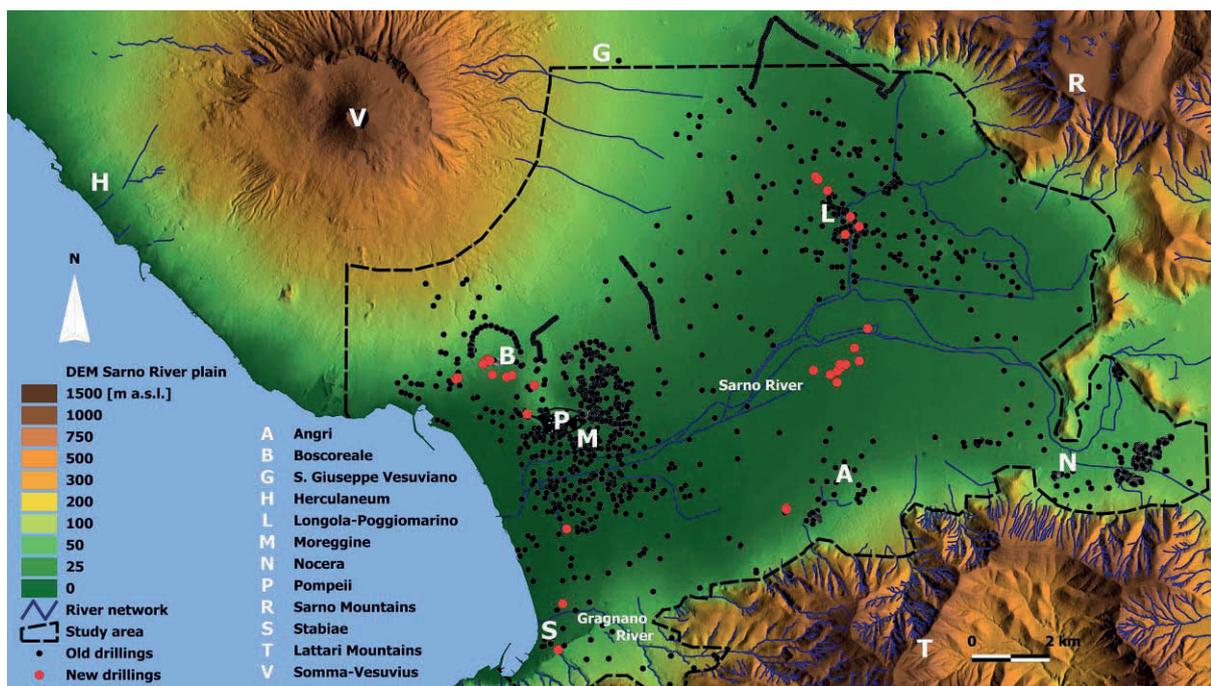
Our approach is based on the hypothesis that the eruption AD 79 mantled the ancient topography of the Sarno River plain leaving ancient physiographic elements still recognizable in the present-day topography (Sigurdsson and Carey, 2002, Stefani and Di Maio, 2003, Vogel and Märker, 2010). Consequently, the present-day topography can be utilized for reconstructing the ancient conditions. This is supported by Ohlig (2001) who states that the general structure of the Pompeiian hill must have remained constant after the eruption AD 79 apart from a different absolute altitude.

To model the pre-AD 79 topography of the Sarno River plain a classification and regression tree approach was applied using a high-resolution present-day digital elevation model (DEM) and 16 deduced primary and secondary topographic indices. Neotectonic phenomena that occurred before AD 79 are taken into account in this

modeling approach because their resulting landforms are incorporated into the present-day topography. However, the present-day DEM can also contain structures of recent neotectonic activities (after AD 79) which may by mistake be transferred to the reconstructed pre-AD 79 topography. By means of the stratigraphical information from the drilling data, e.g. the elevation of the pre-AD 79 littoral deposits, major elevation discrepancies can be identified.

Classification and regression trees is an algorithm used for exploratory data analysis and predictive modeling to discover features and structural patterns in large databases by determining the correlation between predictor variables and a response variable (Breiman et al., 1984; Myles et al., 2004). For the model generation we used the TreeNet software (Salford Systems). As predictor variables we used the present-day DEM and 16 deduced primary and secondary topographic indices and as response variable the depth to the pre-AD 79 surface (thickness of post-AD 79 deposits) (Tab. 1). Before entering the input parameters into TreeNet the quality of all 1,840 stratigraphical drilling data were re-evaluated. Plausibility checks were carried out on every drilling point by comparison with the surrounding nearest neighbors to identify drillings where the AD 79 volcanic deposits were not correctly determined and by that also the pre-AD 79 paleo-surface. Furthermore, the original drilling documentations were double-checked for drillings whose location was incorrect. By means of a statistical evaluation of the stratigraphical data outliers among the drilling points were detected and eliminated. Moreover, the aspect (A) was transformed according to Beers et al. (1966) following $A' = \cos(45 - A) + 1$. Instead of the common range of the aspect where 0° and 360° represent identical values the aspect was transformed to range of values between 0 and 2. However, it turned out to not significantly improve the model performance. Several preliminary model runs were performed with different presettings, such as number of grown trees and by leaving out different predictor variables. Thus, the sensitivity of a particular predictor variable with respect to the model performance was tested to optimize the prediction.

In order to determine the pre-AD 79 topography of the Sarno River plain the modeled thickness of post-AD 79 deposit was subtracted from the present-day DEM. The pre-AD 79 Sarno River network was reconstructed by delineation of linear

thalweg features of the pre-AD 79 topography using the SAGA terrain analysis module (Olaya and Conrad, 2008). The reconstruction of specific paleo-environmental features of the pre-AD 79 surface such as the ancient coastline or the floodplain of the paleo-Sarno River was done by attributing the classified environmental character of the pre-AD 79 paleo-layer to the modeled pre-AD 79 topography (Vogel and Märker, 2010).

Table 1. Predictor variables used for the modeling process in TreeNet (Salford Systems).

Predictor variables	Method/Reference
Elevation	Topo to Raster (ArcGIS 9.2)/SIT 1:5 000
Altitude above channel network	SAGA terrain analysis module (Olaya and Conrad, 2008)
Analytical hillshading	SAGA terrain analysis module (Olaya and Conrad, 2008)
Aspect	SAGA terrain analysis module (Zevenberg and Thorn, 1987)
Catchment area	SAGA terrain analysis module (Olaya and Conrad, 2008)
Channel network	SAGA terrain analysis module (Olaya and Conrad, 2008)
Channel network base level	SAGA terrain analysis module (Olaya and Conrad, 2008)
Convergence index	SAGA terrain analysis module (Köthe and Lehmeier, 1993)
Curvature	SAGA terrain analysis module (Zevenbergen and Thorne, 1987)
Curvature classification	SAGA terrain analysis module (Dikau, 1988)
Plan curvature	SAGA terrain analysis module (Zevenbergen and Thorne, 1987)
Profile curvature	SAGA terrain analysis module (Zevenbergen and Thorne, 1987)
LS-factor	SAGA terrain analysis module (Olaya and Conrad, 2008)
Slope	SAGA terrain analysis module (Zevenbergen and Thorne, 1987)
Stream power	SAGA terrain analysis module (Olaya and Conrad, 2008)
Watershed subbasins	SAGA terrain analysis module (Olaya and Conrad, 2008)
Topographic wetness index	SAGA terrain analysis module (Olaya and Conrad, 2008)

Results and discussion

The statistical evaluation of the thickness of post-AD 79 deposits of the drilling dataset reveals a range of values of between 0 and 19 m (Fig. 2). Drillings having a thickness of more than 19 m can be statistically considered as outliers which apply to 10 of the 1,840 drillings. Disregarding the outliers the arithmetic mean thickness of post-AD 79 deposits is 5.8 m, the median is at 5.3 m and the standard deviation is 3.1 m. Furthermore, 95 % of the drilling data are covering a range between 1.25 and 15 m.

Figure 2. Histogram of the drilling data regarding the depth to the pre-AD 79 surface
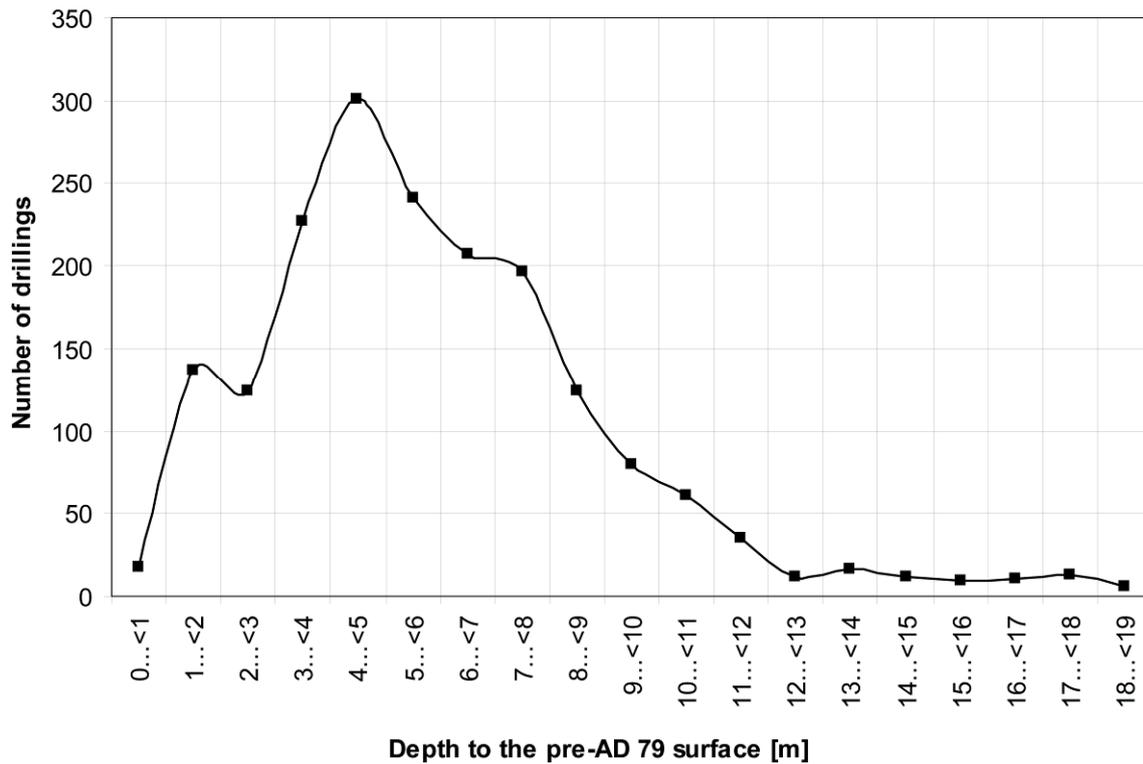
Figure 3. A: Mean absolute error [m] of the depth to the pre-AD 79 surface versus number of trees of the training and test dataset. The minimum mean absolute error of the training dataset of 0.98 m and of the test dataset of 1.68 m was attained at 2,094 grown trees. B: Gain chart of the training dataset. C: Gain chart of the test dataset (TreeNet).
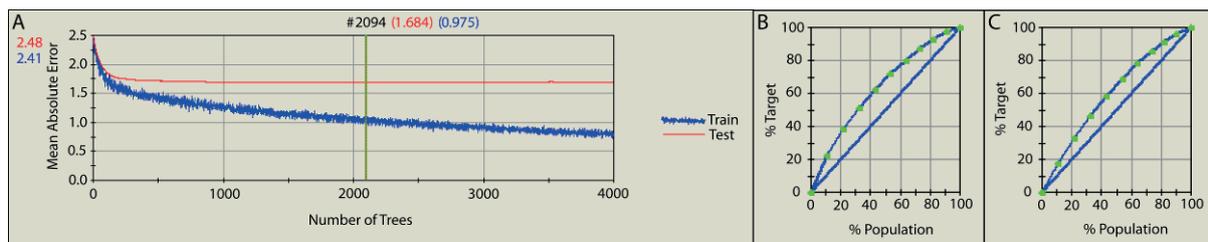
During preliminary model runs the sensitivity test of the predictor variables pointed out that the topographic index 'watershed subbasins' (SAGA terrain analysis module) produced a lot of artifacts on the regionalized thickness of the post-AD 79 deposits. Consequently, it was left out of the modeling process. Fig. 3 shows the performance of the obtained regression model. The minimum mean absolute error of the training dataset is 0.98 m and that of the test dataset 1.68 m, which is similar to the previous model of Vogel and Märker (2010). 2,094 trees were grown to achieve

the smallest test mean absolute error (Fig. 3A). The general model performance of the training and test dataset is illustrated in Figs. 3B and C, respectively. The gain charts show the percentage of population (x-axis) related to the percentage of the target variable (y-axis). The higher the percentage of the target variable with respective low population percentages, the better is the model. In this case the current model performance shows a clear positive correlation similar to the previous model (Vogel and Märker, 2010).

The modeled thickness of the post-AD 79 deposits of the Sarno River plain is illustrated in Fig. 4A. It shows a distinct spatial distribution of post-AD 79 deposits ranging from 1.1 to 15.6 m. This range of values corresponds well with the calculated range of 95 % of the drilling data.

Apart from the internal model validation that is performed by TreeNet an external validation of the model results was carried out by comparing the modeled thickness of the post-AD 79 deposits with the real thickness given by the 1,840 drilling data (Fig. 4B). Figure 4B documents an improvement of the new prediction in respect to Vogel and Märker (2010). It shows that 79 % of the drilling points match the modeled thickness with an accuracy of less than 2 m and 50 % of the drilling points with less than 1 m. The respective percentages of the previous model were 44 % and 24 %. The mean thickness of modeled post-AD 79 deposits is 5.6 m (6.5 m in Vogel and Märker, 2010) which lies exactly between the arithmetic mean of 5.8 m and the median of 5.3 m obtained from the drilling data. Best agreement between model and drilling data was attained for the plain areas where the post-AD 79 deposits are rather thin. However, with increasing thickness of post-AD 79 deposits and with increasing relief towards the slopes of Somma-Vesuvius and the Apennine Mountains the difference between real and modeled thickness is also increasing (Fig. 4B).

From 144 drilling points at the northern boundary of the Sarno River plain it turned out that with the present methodology the thickness of post-AD 79 deposits can only be reconstructed northwards up to the modern town of S. Giuseppe Vesuviano (Fig. 1). There the spatial limit of the area of deposition of the AD 79 eruption is reached. Hence, the volcanic material from the AD 79 eruption is missing in the drilling cores and the pre-AD 79 paleo-surface cannot be clearly identified anymore.

Figure 4. A: Modeled depth to the pre-AD 79 surface (thickness of post-AD 79 deposits) of the Sarno River plain. B: Combination with the actual depth to the pre-AD 79 surface at the drilling points.
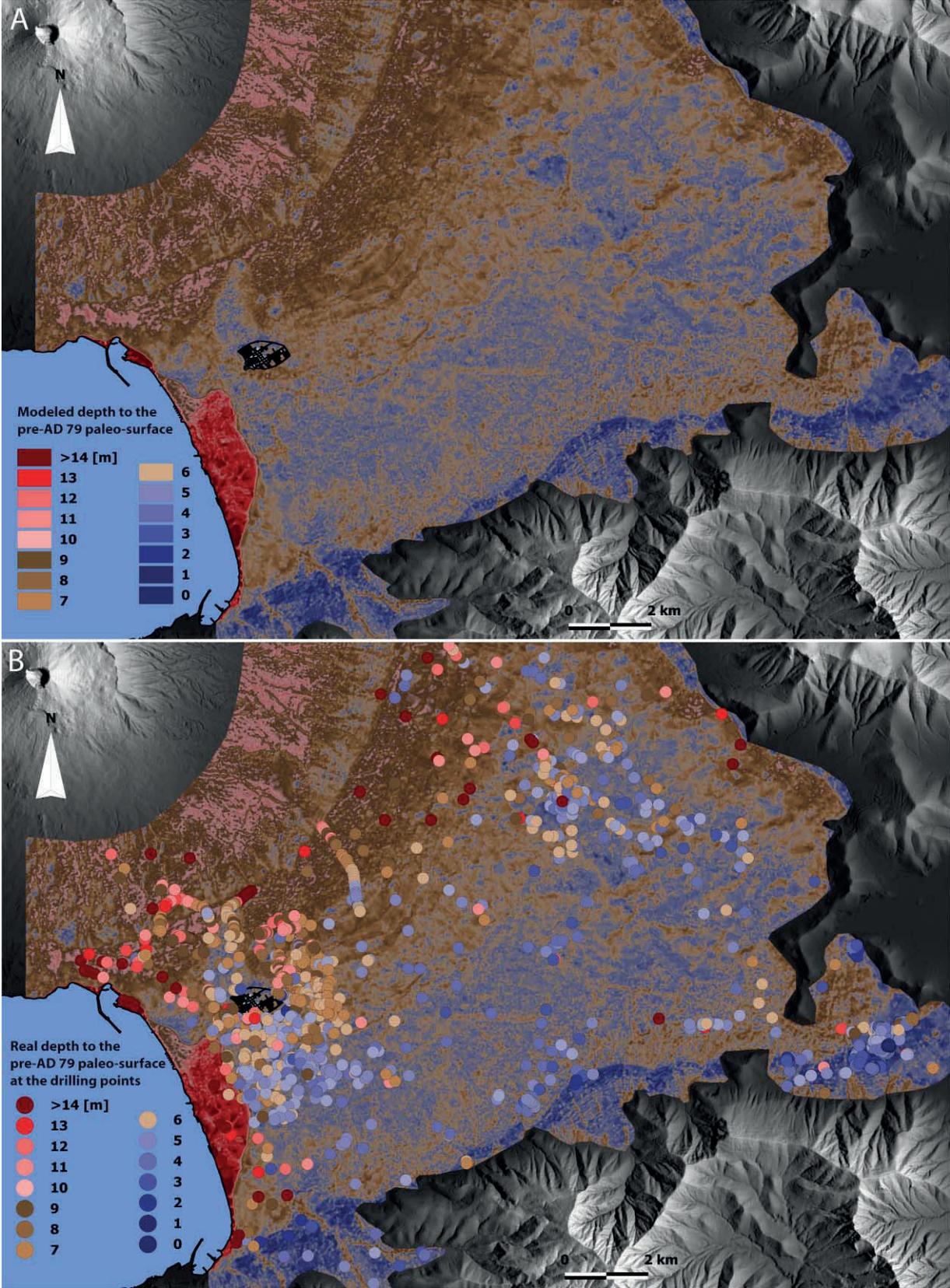
Table 2. Ranking of importance of the predictor variables used for the model generation.

Variable	Importance [%]	
Elevation above sea level	100.0	|||||||||||||||||||||||||||||||||
Aspect	93.1	|||||||||||||||||||||||||||||||
Channel base level	81.6	|||||||||||||||||||||||||||||
Altitude above Channel network	59.0	||||||||||||||||||||
Slope	52.8	||||||||||||||||||
Analytical hillshade	50.6	|||||||||||||||||
LS-factor	48.6	||||||||||||||||
Curvature classification	46.7	||||||||||||||||
Convergence index	45.9	||||||||||||||||
Profile curvature	44.3	|||||||||||||||
Topographic wetness index	44.1	|||||||||||||||
Stream power	43.8	|||||||||||||||
Curvature	43.2	|||||||||||||||
Plan curvature	41.9	|||||||||||||||
Catchment area	38.5	||||||||||||||
Channel network	9.8	|||

From the modeled depth to the pre-AD 79 surface (Fig. 4A) and the importance of the predictor variables for the model generation (Tab. 2) it can be observed that the distinct spatial distribution of post-AD 79 volcanic deposits is most notably controlled by two sets of processes: (i) the initial deposition of pyroclastic material during the eruption of Somma-Vesuvius volcanic complex and (ii) the subsequent redistribution of the volcanic material by processes of erosion, transport and redeposition (Vogel and Märker, 2010). It is noticeable that within the Sarno River plain there is a gradient of post-AD 79 deposits from the slopes of Somma-Vesuvius in the northwest to the actual plain in the southeast. Thicker deposits at the southwestern slopes of Somma-Vesuvius can be explained as follows (see also Vogel and Märker, 2010):

(i)   Originating from the vent of Somma-Vesuvius, AD 79 the pumice lapilli fallout was dispersed concentrically towards the southeast resulting in thickest deposits in the perivolcanic areas, near the source of the eruption. This corresponds with isopachs of the thickness of the AD 79 pumice fallout as reconstructed by Sigurdsson and Carey (2002) or Pfeiffer et al. (2005).

(ii)   The pumice fallout is overlain by pyroclastic surge and flow deposits of the AD 79 eruption that are especially concentrated at the slopes of Somma-Vesuvius and gradually decrease in thickness towards the plain (Di Vito et al., 1998; Rossano et al., 1998; Di Maio and Pagano, 2003). However, along the

south-eastern slope of Somma-Vesuvius a band of thinner deposits can be noticed (Fig. 4A) that extents concentrically between 50 and 70 m a.s.l. (present-day elevation). This band may be caused by a downslope acceleration of the pyroclastic surge due to the steepness of the slope temporarily compensating the deceleration of the surge with increasing travel distance. Hence, the erosive power of the surge is temporarily increased before deposition prevails towards the toeslope of Somma Vesuvius (see Rossano et al., 1998).

(iii)   Additionally, the slopes of Somma-Vesuvius are covered by pyroclastic material and lava flows from more recent eruptions such as AD 472, 1631 or 1944 (Geological map 1:10,000, Autorità di Bacino del Sarno, 2003).

Greater thickness of volcanic deposits in the coastal area on the other hand can be attributed to mobilization of initially deposited material by the paleo-Sarno River and its tributaries, transportation out of the plain and finally re-deposition in shallow water along the Tyrrhenian coast. This coincides with rather thin deposits in the central and southern parts of the Sarno River plain. Steep slopes of 3 to 4 m in height near the Tyrrhenian Sea give a first idea on the approximate position of the coastline before AD 79 (Fig. 4A).

An accumulation of deposits at the foot slopes of the Sarno and Lattari Mountains result from initially deposited volcanic material that was eroded by mountain streams or lahars, e.g. after intense rainfall events (Lirer et al., 2001; Fiorillo and Wilson, 2004). Accordingly, the mountain slopes from where this material was eroded show relative thin post-AD 79 deposits. Likewise, the volcanic material on the Pompeiian hill is rather thin on top and thicker along its foot slopes because after the deposition of the AD 79 volcanic material it was eroded from the ridge and accumulated in the adjacent plain.

It is noticeable that on the western slopes of the Lattari Mountains thicker deposits appear within the deeply incised river valleys such as the 'Fosso di Gragnano' draining this part of the mountains whereas the adjacent slopes show rather thin deposits. This is supported by Rossano et al. (1998) who state for the Vesuvius area that the movement and deposition of ash flows, lahars or debris avalanches

accompanying volcanic eruptions strongly follow topographic irregularities such as river channels. Furthermore, due to the redistribution of the volcanic material subsequent to the AD 79 eruption paleo-river valleys were filled with volcanic material that was initially deposited on the mountain slopes.

The improved digital elevation model (DEM) of the Sarno River plain before AD 79 was calculated by subtracting the modeled thickness of the post-AD 79 deposits from the present-day surface. The pre-AD 79 paleo-river network was deduced by deriving the linear thalweg features of the pre-AD 79 DEM (Fig. 5). Finally, the reconstruction of specific paleo-environmental features before AD 79 was done by attributing the classified environmental characteristic of the pre-AD 79 layer taken from the drilling data to the pre-AD 79 topography (Fig. 6A). Hence, the approximate course of the coastline before AD 79 and the floodplain of the paleo-Sarno River were delineated by means of the littoral and the fluvial-palustrine environmental information from the drilling data. Marine and littoral deposits that were found rather inland from the ancient coastline identified the approximate location of the protohistorical dune ridges of Messigno (5,600-4,500 yr BP) and Bottaro/Pioppaino (3,600-2,500 yr BP) (Cinque, 1991) (Fig. 6B) (Vogel and Märker, 2010).

Figure 5. Present-day (A) and modeled pre-AD 79 digital elevation model (DEM) (B) of the Sarno River plain with fluvial network (A: regulated and canalized present-day Sarno River, B: modeled pre-AD 79 Sarno River) and 5m-contour lines (10m lines: solid, 5m lines: thin; white numbers indicate the elevation [m a.s.l.]).
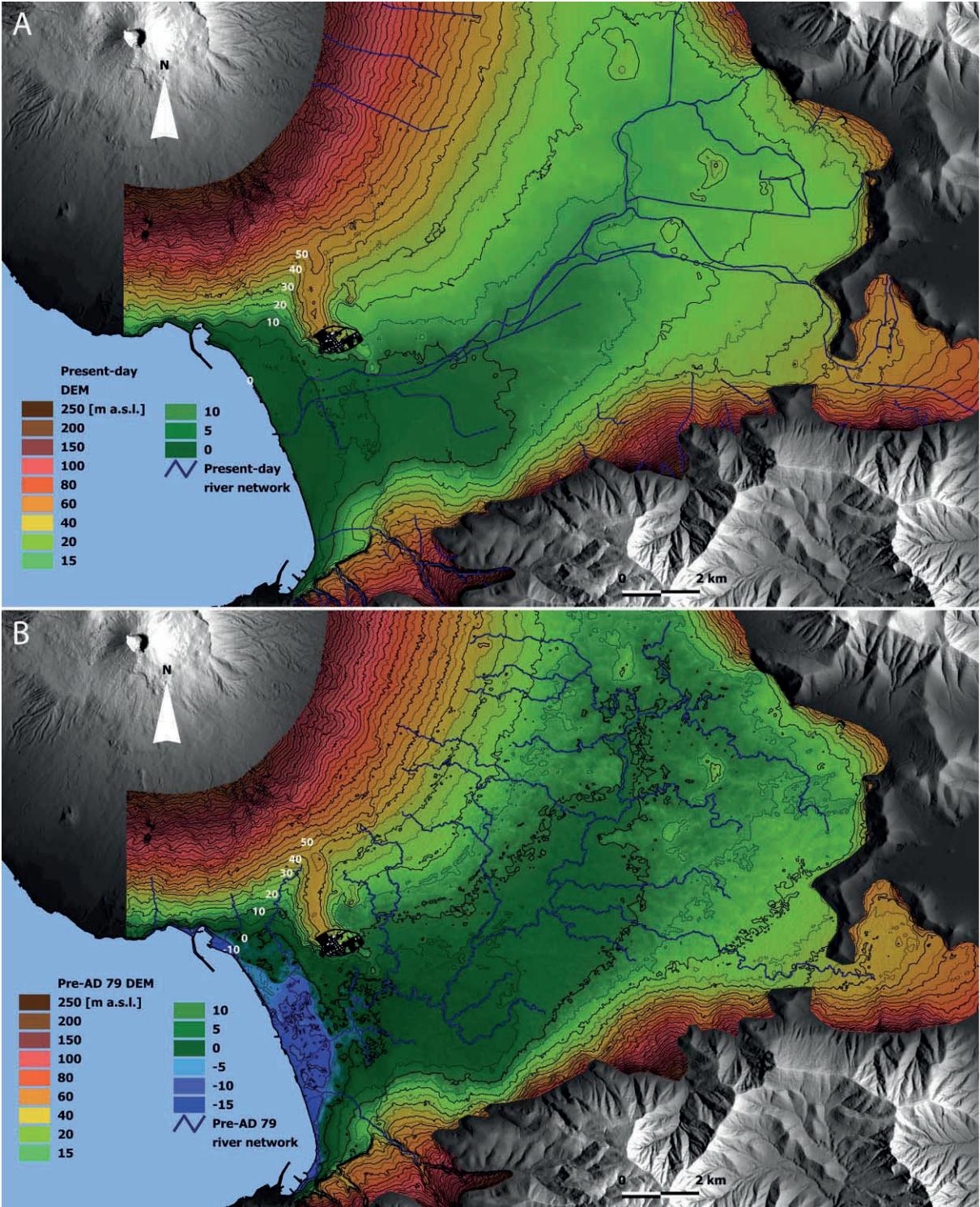
Figure 6. A: Drilling data on the classified pre-AD 79 layer. B: Inferred reconstruction of pre-AD 79 paleo-environmental and paleo-geomorphological features.
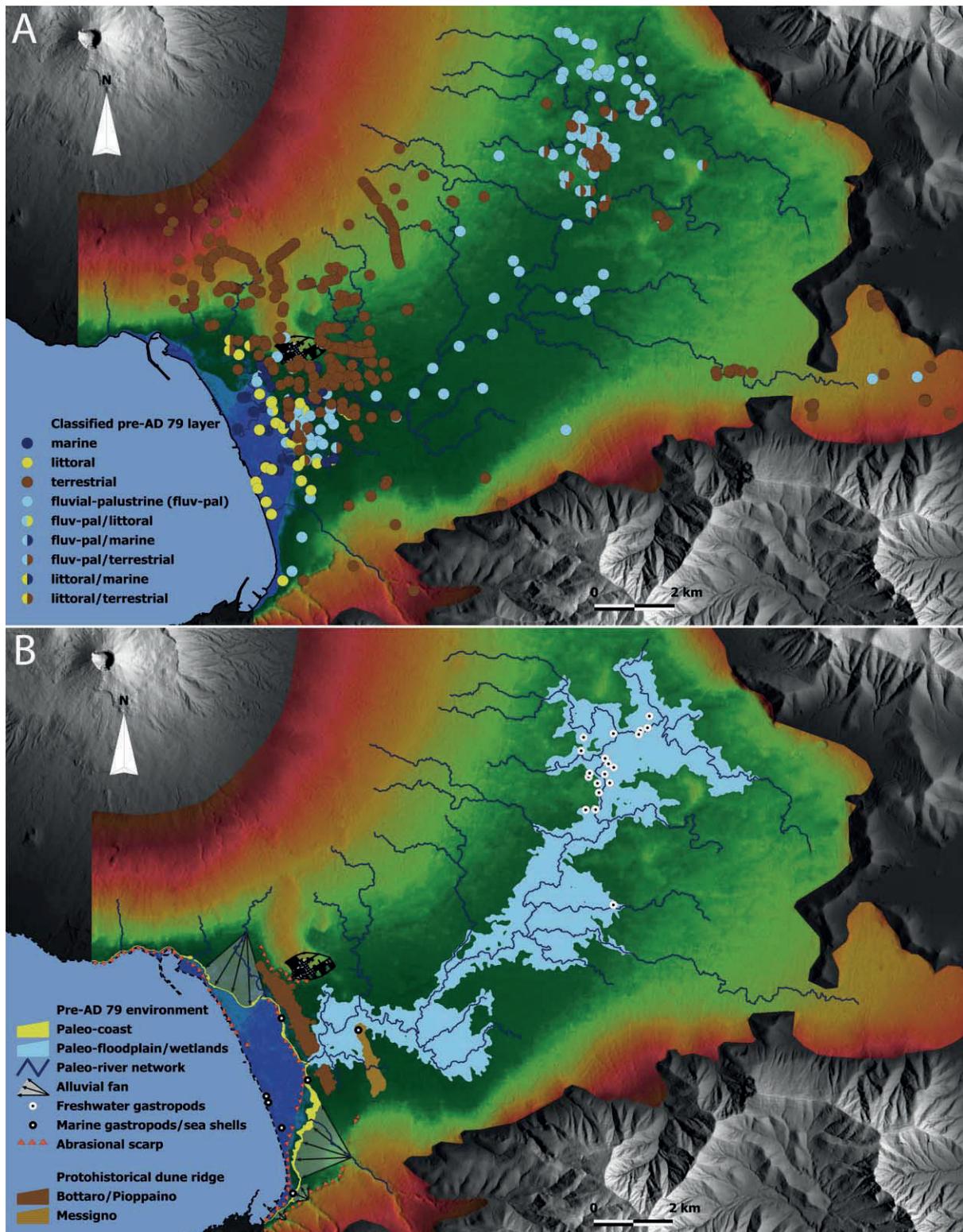
As Vogel and Märker (2010) have already stated the pre-AD 79 topography corresponds to the present-day topography since main topographic elements reappear. However, the pre-AD 79 paleo-surface is situated approximately 5.8 m

(mean) underneath the modern surface resulting in a wide area of the Tyrrhenian coast lying below the present-day sea level. The course of the fluvial network before AD 79 and today also have a lot of similarities even though especially the lower reaches of the Sarno River is regulated and canalized today whereas the paleo-Sarno River shows more natural fluvial patterns (Fig. 5). South of Pompeii the paleo-Sarno River flows around the more elevated protohistorical dune ridge of Messigno and cuts the dune ridge of Bottaro/Pioppaino before it enters the Tyrrhenian Sea about 1.5 km east of the present-day Sarno River (Vogel and Märker, 2010) (Fig. 6B).

The general drainage system of the pre-AD 79 Sarno River network can be considered dendritic. The contributing streams follow mainly the slope of the terrain whereas strong structural influences seem to be absent. However, Fig. 7A shows that small segments of the paleo-river network may also be subject to some kind of structural control as they repeatedly follow right angles that are orientated NE-SW and NW-SE. This would rather suggest a rectangular drainage system. In fact the right angles of the paleo-river network align with the two main fault systems in whose intersection the Sarno River plain is structurally located: (i) that of Somma-Vesuvius volcanic complex which is orientated NE-SW and (ii) that of the Apennines which is NW-SE trending (Del Pezzo et al., 1983; Balducci et al., 1985; Marzocchi et al., 1993; Bianco et al., 1997, Cella et al., 2007). Several hundreds of seismic events, mostly of volcano-tectonic type, are recorded each year in the Somma-Vesuvius area (Bianco et al., 1997; Del Pezzo et al., 2004). That probably can also be presumed for the time before AD 79. Consequently, seismic events amplify the underlying tectonic structure and thus, partly influence the course of the pre-AD 79 fluvial network. This results in segments of a rectangular drainage system. In contrast, the river tends to eliminate those structures due to fluvial erosion and accumulation during seismic quiescence which leads to a dendritic drainages system (Fig. 7A).

Figure 7. A: Pre-AD 79 DEM of the Sarno River plain and pre-AD 79 river network. The drainage system can be considered as dendritic with scattered rectangular segments that result from structural control (red). B: Paleo-geomorphological map of the Sarno River plain before AD 79.
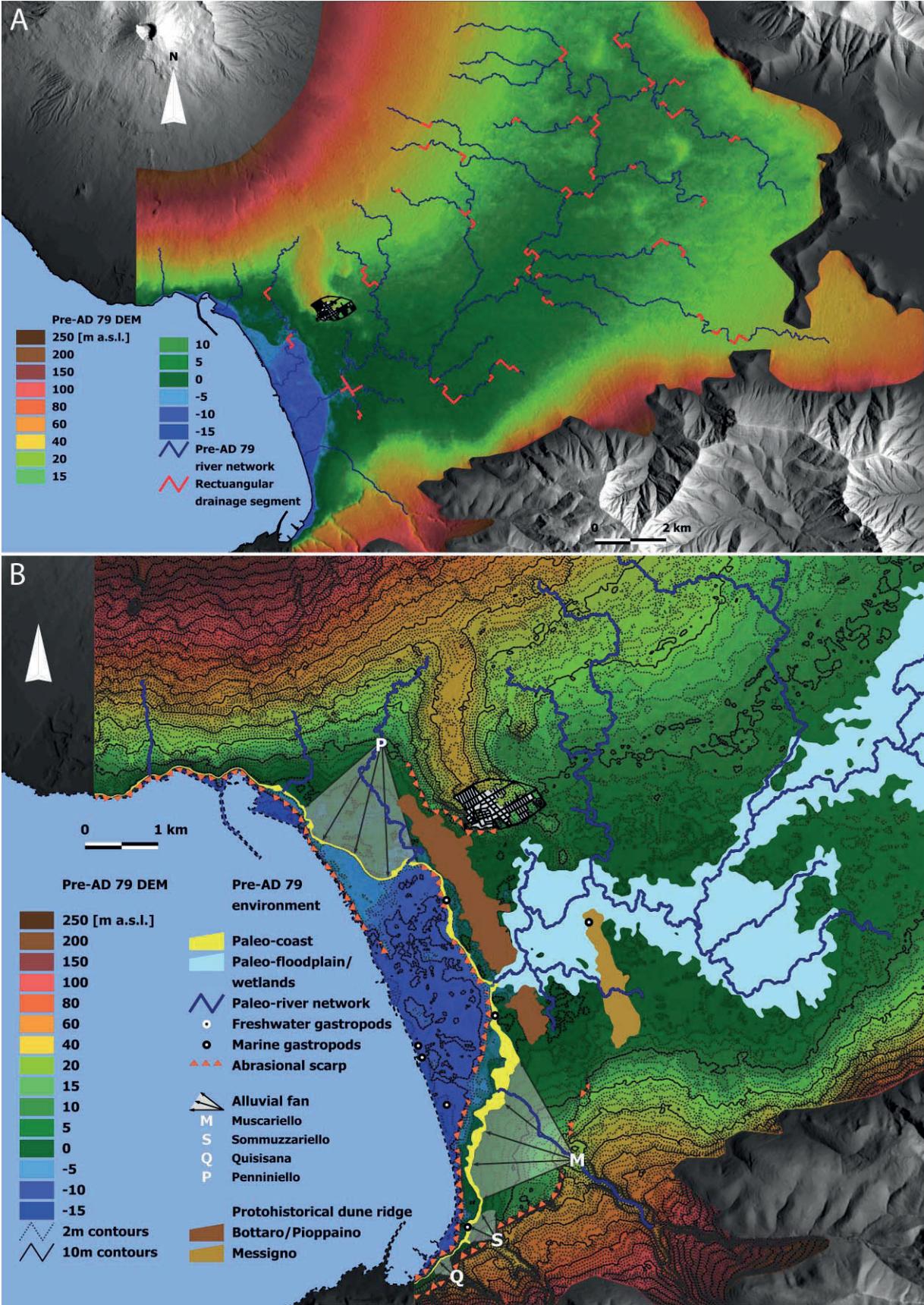
In the southwest of the Sarno River plain between the Tyrrhenian coast and the Lattari Mountains a big alluvial fan re-emerged on the new pre-AD 79 DEM. This was already identified by Vogel and Märker (2010) and named in the geomorphological map of Cinque (1991) 'conoide di Muscariello'. In the west there are the much smaller alluvial fans of Sommuzzariello and Quisisana (Cinque, 1991) (Fig. 7B). That these alluvial fans already existed before AD 79 is confirmed by Irollo (2005) who determined that the initial deposition of the 'conoide di Muscariello' occurred in the Upper Pleistocene (15-13 ka BP).

Due to the volcanic activity of Somma-Vesuvius and the resulting recurring accumulation of volcanic deposits in that area the coastline of the Sarno River plain continuously propagated westwards (Cinque et al., 1987; Livadie et al., 1990; Cinque, 1991). This is particularly evident in the protohistorical dune ridges of Messigno and Bottaro/Pioppaino that can be found approximately 3,000 m and 1,500 m inland from the present-day coast. Consequently, it can be presumed that during its early formation the 'conoide di Muscariello' extended directly into the Tyrrhenian Sea and was partly deposited underwater. In fact, stratigraphical investigations by Irollo (2005) illustrate both, marine/littoral and alluvional deposits suggesting a combination of fluvial and marine deposition. The paleo-Gragnano River, the main tributary of the 'conoide di Muscariello', before AD 79 flowed to the northwest and entered the sea in the north of the alluvial fan (Fig. 5B). The present-day 'Fosso di Gragnano' instead flows to the west and into the sea in the very southwest around 1,300 m away from its paleo-mouth before AD 79 (Fig. 5A). The relocation of the river channel might have been caused by the sudden large amount of sediments during the AD 79 eruption of Somma-Vesuvius or subsequent lahars. This may have led to the burial of the paleo-river channel of the 'Fosso di Gragnano' and thus to its relocation to the southwest.

Between the western slope of the Pompeiian hill and the southern slope of Somma-Vesuvius volcano another alluvial fan was identified which is fed by the main discharge of that area. Cinque (1991) refered to it as 'conoide di Penniniello'. It is striking that the southwestern, i.e. the presumably youngest part of the fan lies approximately 2 m higher than its central or southeastern part. This accumulation may have been caused by a high sediment load after an eruption of Somma-Vesuvius

that eventually forced the river to bend to the south instead of flowing straight to the southwest and directly entering the sea. The contour lines show clearly that the stream has already cut into its own deposits. The northern branch of the protohistorical dune ridge of Bottaro/Pioppaino most likely was dissected by fluvial erosion leaving only scattered traces of dunal deposits (Fig. 7B) due to the morphology of the 'conoide di Penniniello'.

The pre-AD 79 coastline, i.e. the coastline prior to the eruption of Somma-Vesuvius AD 79, was reconstructed according to the littoral deposits from the drilling data and the pre-AD 79 coastal topography. In its central part the ancient coast runs nearly parallel to the modern coast in a distance of 1,100 to 1,300 m inland. At the slopes of Somma-Vesuvius and the Lattari Mountains instead the paleo-coast and the modern coast are much closer to each other with distances between 50 to 150 m. Between the mountain slopes and the plain the alluvial fans of Muscariello and Penniniello result in a northwestwards and southwestwards propagation of the ancient coastline, respectively. Regarding the pre-AD 79 topography the pre-AD 79 coastline is mainly situated between the -2 m and -4 m contour lines in the north near Somma-Vesuvius and between the 0 and 1 m contour line in the south of the plain. This elevation unconformity of the pre-AD 79 littoral deposits can most likely be attributed to some neotectonic activity in the study area. Sigurdsson et al. (1985) and Livadie et al. (1990) also observed a deeper occurrence of the Roman littoral deposits in the north of the Sarno River plain at approximately -4 m a.s.l. which Pescatore et al. (2001) explained with a more rapid subsidence near Somma-Vesuvius in comparison with more distal areas.

Converging contour lines in the coastal area of the Sarno River plain may indicate abrasion terraces that can be related to marine erosion of different coastlines. Abrasional scarps at the foot of the Pompeiian hill and the Lattari Mountains derive from protohistorical coastlines (Cinque, 1991; Vogel and Märker, 2010). Along the pre-AD 79 coastline marine scarps can be found at the slopes of Somma-Vesuvius and in the central part of the coast (Fig. 7B).

Additional marine scarps between the pre-AD 79 and the present-day coastline refer to more recent processes (Fig. 7B). Due to the modeling approach, post-AD 79 processes have generated those features that are, by mistake, reflected in the pre-AD

79 topography. Consequently, they must be regarded as modeling artefacts. Those terrace features may be formed during post-AD 79 sealevels. As a result of Plinian and sub-Plinian eruptions of Somma-Vesuvius, e.g. AD 472 or 1631 (Rosi et al., 1993; Rolandi et al., 1998) excessive loads of volcanic sediments were produced that were subsequently redistributed by the river network and redeposited in the coastal area. Finally, this caused a further westward propagation of the coastline.

The floodplain of the paleo-Sarno River was reconstructed by combining the fluvial-palustrine deposits from the drilling data with the pre-AD 79 topography and the deduced pre-AD 79 paleo-river network. As Vogel and Märker (2010) already stated in the previous model the fluvial-palustrine deposits fit very well with the pre-AD 79 paleo-river network (Fig. 6A). They are characterized by the 1 to 2 m isolines of the 'vertical distance to channel network' index from the SAGA terrain analysis module (Olaya and Conrad, 2008).

Conclusion and outlook

A revised reconstruction of the pre-AD 79 topography of the Sarno River plain was carried out on the basis of an improved classification and regression model of Vogel and Märker (2010). The pre-AD 79 digital elevation model and the classified environmental characteristics of the pre-AD 79 layer derived from the drilling data was used to reconstruct paleo-environmental and paleo-geomorphological features of the Sarno River plain such as the paleo-coastline, the paleo-Sarno river and its floodplain, alluvial fans near the Tyrrhenian Sea as well as abrasion terraces of historical and protohistorical coastlines. However, as already stated by Vogel and Märker (2010) this reconstruction must be considered as a model of the pre-AD 79 conditions based on the hypothesis stated above. Especially neotectonic phenomena that occurred between AD 79 and today are only in part considered in the modeling approach, e.g. through the elevation of the pre-AD 79 littoral deposits.

The collection of additional stratigraphical data especially within areas of the Sarno River plain that are insufficiently covered by previous core drillings as well as the combination of the pre-AD 79 DEM with archaeological findings can enhance the paleo-environmental reconstruction of the Sarno River plain.

In a next project phase geomorphologically interesting landforms such as the alluvial fan of 'Muscariello' and the floodplain of the paleo-Sarno River will be studied in more detail using geophysical prospections to further verify the pre-AD 79 DEM and the applied methodology. Moreover, the pre-AD 79 DEM and paleo-environment will be utilized to further reconstruct the ancient cultural landscape of the Sarno River plain, e.g. the phenomenon of the Roman farms or the ancient road network.

Acknowledgments

References

Andronico D., Calderoni G., Cioni R., Sbrana A., Sulpizio R. and Santacroce R. 1995. Geological map of Somma-Vesuvius volcano. Per. Mineral. 64, 77-78.

Autorità di Bacino del Sarno 2003. Geological map, scale 1.10 000 (in Italian). CARG Project, Region Campania.

Balducci S., Vasellini M. and Verdiani G., 1985. Exploration well in the 'Ottaviano' Permit, Italy; 'Trecase 1'. In. Strub, A.S., Ungemach, P. (eds.) European Geothermal Update. Proc. 3rd Int. Seminar on the Results of EC Geothermal Energy Research, Reidel.

Beers T.W., Dress P.E. and Wensel L.C. 1966. Notes and observations. Aspect transformation in site productivity research. Journal of Forestry 64, 691-692.

Bianco F., Castellano M., Milano G., Ventura G. and Vilardo, G. 1997. The Somma-Vesuvius stress field induced by regional tectonics. evidences from seismological and mesostructural data. J. Volcanol. Geotherm. Res., 82, 199-218.

Breiman L., Friedman J., Olshen R. and Stone C. 1984. Classification and Regression Trees. Chapman and Hall, New York.

Carey S. and Sigurdsson H. 1987. Temporal variations in column height and magma discharge rate during the 79 A.D. eruption of Vesuvius. Geol. Soc. Am. Bull. 99, 303-314.

Cella F., Fedi M., Florio G., Grimaldi M. and Rapolla, A. 2007. Shallow structure of the Somma-Vesuvius volcano from 3D inversion of gravity data. J. Volcanol. Geoth. Res. 161, 303-317.

Cioni R., Marianelli P. and Sbrana A., 1992. Dynamics of the A.D. 79 eruption. Stratigraphic, sedimentological and geochemical data on the successions from the Somma-Vesuvius southern and eastern sectors. Acta Vulcanol. 2, 109-123.

Cinque A. 1991. The versilian transgression in the Sarno River plain, Campania (in Italian). Geogr. Fis. Dinam. Quat. 14, 63-71.

Civetta L., Galati R. and Santacroce R. 1991. Magma mixing and convective compositional layering within the Vesuvius magma chamber. B. Volcanol. 53, 287-300.

Civetta L., Di Vito M.A., De Lucia M. and Isaia R. 1998. Eruptive history of Somma-Vesuvius (in Italian). In. Guzzo, P., Peroni, R. (eds.), Archeol. Vulcanol. Campania. Naples, 9-16.

Delibrias G., Di Paola G.M., Rosi M. and Santacroce R. 1979. The eruptive history of Somma-Vesuvius volcanic complex reconstructed from pyroclastic successions of Monte Somma (in Italian). Rend. Soc. It. Mineral. Petrol 35, 411-438.

Del Pezzo E., Iannaccone G., Martini M. and Scarpa R., 1983. The 23 November 1980 southern Italy earthquake. Bull. Seismol. Soc. Am. 73, 187–200.

Del Pezzo E., Bianco F. and Saccorotti G. 2004. Seismic source dynamics at Vesuvius volcano, Italy. J. Volcanol. Geotherm. Res. 133, 23-39.

Dikau R. 1988. Entwurf einer geomorphographisch-analytischen Systematik von Reliefeinheiten. Heidelb. Geogr. Baust. 5, 1-45.

Di Maio G. and Pagano M. 2003. Considerations on the coast line and the modality of burial of ancient Stabia after the Vesuvian eruption AD 79 (in Italian). Riv. Studi Pomp. XIV, 197-245.

Di Vito M.A., Sulpizio R., Zanchetta G. and Calderoni, G. 1998. The geology of the South Western Slopes of Somma-Vesuvius, Italy, as inferred by borehole stratigraphies and cores. Acta Vulcanol. 10 (2), 383-393.

Fiorillo F. and Wilson R.C. 2004. Rainfall induced debris flows in pyroclastic deposits, Campania southern Italy). Eng. Geol. 75, 263-289.

Irollo G. 2005. The Holocene evolution of the coastal area between Naples and Stabia (Campania) based on geological and archaeological data (in Italian). Doctoral thesis. Faculty of Mathematical, Physical and Natural Science. University of Naples "Federico II", pp. 414.

Köthe R. and Lehmeier F. 1993. SARA – Ein Programmsystem zur Automatischen Reliefanalyse. Z. Angew. Geogr. 4, 11-21.

Lirer L., Munno R., Petrosino P. and Vinci A. 1993. Tephrostratigraphy of the AD 79 pyroclastic deposits in perivolcanic areas of Mt. Vesuvio (Italy). J. Volcanol. Geotherm. Res. 58, 133-149.

Lirer L., Vinci A., Alberico I., Gifuni T., Bellucci F., Petrosino P. and Tinterri R. 2001. Occurrence of inter-eruption debris flow and hyperconcentrated flood-flow deposits on Vesuvio volcano, Italy. Sedimentary Geology 139, 151-167.

Livadie C.A., Barra D., Bonaduce G., Brancaccio L., Cinque A., Ortolani F., Pagliuca S. and Russo F. 1990. Geomorphologic, neotectonic and volcanic evolution of the coastal plain of the Sarno River (Campania) related to the settlements before AD 79 eruption (in Italian). Pact 25-13, 237-256.

Luongo G., Perrotta A., Scarpati C. 2003. Impact of the AD 79 explosive eruption on Pompeii, I. Relations amongst the depositional mechanisms of the pyroclastic products, the framework of the buildings and the associated destructive events. J. Volcano. Geoth. Res. 126, 201-223.

Marzocchi W., Scandone R., Mulargia F. 1993. The tectonic setting of Mount Vesuvius and the correlation between its eruptions and the earthquakes of the Southern Appennines. J. Volcanol. Geotherm. Res. 58, 27–41.

Myles A., Feudale R., Liu Y., Woody N., Brown S. 2004. An introduction to decision tree modelling. J. Chemometr. 18, 275-285.

Ohlig C.P.J. 2001. De Aquis Pompeiorum. Das Castellum Aquae in Pompeji. Herkunft, Zuleitung und Verteilung des Wassers. In. De Waele, J.A.K.E. and Moormann, E.M. (eds.) Circumvesuviana, Vol. 4, 2001, pp. 483.

Olaya V. and Conrad O. 2008. Geomorphometry in SAGA. In. Hengl, T., Reuter, H.I. (eds.) Geomorphometry. Concepts, Software, Applications.

Pescatore T., Senatore M.R., Capretto G. and Lerro G. 2001. Holocene Coastal Environments near Pompeii before the A.D. 79 Eruption of Mount Vesuvius, Italy. Quaternary Res. 55, 77-85.

Pfeiffer T., Costa A. and Macedonio G. 2005. A model for the numerical simulation of tephra fall deposits. J. Volcanol. Geoth. Res. 140, 273-294.

Rolandi G., Maraffi S., Petrosino P. and Lirer, L. 1993a. The Ottaviano eruption of Somma-Vesuvio 8000 y B.P. a magmatic alternating fall and flow-forming eruption. J. Volcanol. Geoth. Res. 58, 43-65.

Rolandi G., Mastrolorenzo G., Barrella A.M. and Borrelli A. 1993b. The Avellino plinian eruption of Somma-Vesuvio 3760 y B.P- the progressive evolution from magmatic to hydromagmatic style. J. Volcanol. Geoth. Res. 58, 67-88.

Rolandi G., Petrosino P. and Geehin J. 1998. The interplinian activity at Somma-Vesuvius in the last 3500 years. J. Volcanol. Geotherm. Res. 82, 19-52.

Rosi M., Principe C. and Vecci R. 1993. The 1631 eruption of Vesuvius reconstructed from the review of chronicles and study of deposits. J. Volcanol. Geotherm. Res. 58, 151-182.

Rossano S., Mastrolorenzo G. and De Natale G. 1998. Computer simulations of pyroclastic flows on Somma-Vesuvius volcano. J. Volcanol. Geotherm. Res. 82, 113-137.

Santacroce R. 1987. Somma-Vesuvius. C.N.R., Quaderni de 'La Ricerca Scientifica' 114, Rome, pp. 251.

Sigurdsson H., Carey S., Cornell W. and Pescatore T. 1985. The eruption of Vesuvius in A.D. 79. Natl. Geogr. Res. 1, 332-387.

Sigurdsson H. 2002. Mount Vesuvius before the Disaster. In. Jashemski W.F. ed.. The Natural History of Pompeii. Cambridge University Press, 29-36.

Sigurdsson H. and Carey S. 2002. The Eruption of Vesuvius in A.D. 79. In. Jashemski W.F. (ed.) The Natural History of Pompeii. Cambridge University Press, 37-64.

Stefani G. and Di Maio G. 2003. Considerations on the coast line of AD 79 and to the ancient port of Pompeii (in Italian). Riv. Studi Pomp. XIV, 142-195.

Vogel S. and Märker, M. 2010. Reconstruction the Roman topography and environmental features of the Sarno River plain (Italy) before the AD 79 eruption of Somma-Vesuvius. Geomorphology 115, 67-77.

Zevenbergen L.W. and Thorne C.R. 1987. Quantitative Analysis of Land Surface Topography. Earth Surf. Proc. Land. 12, 47-56.

2.3   Characterization of the pre-AD 79 Roman paleosol south of Pompeii (Italy): Correlation between soil parameter values and paleo-topography

Sebastian Vogel[a,c,*] and Michael Märker[a,b]

[a] Heidelberg Academy of Sciences and Humanities c/o University of Tübingen, Rümelinstraße 19-23, 72070 Tübingen, Germany

[b] Department of Vegetation, Soil, Environment and Agroforestry Sciences, University of Florence, P.zzale Cascine 16, 50144 Florence, Italy

[c] German Archaeological Institute, Podbielskiallee 69-71, 14195 Berlin, Germany

* Corresponding author. Tel: +49 (0)30 187 711 358, Fax: +49 (0)30 187 711 168
E-mail address: sv@dainst.de (S. Vogel)

Characterization of the pre-AD 79 Roman paleosol south of Pompeii (Italy): Correlation between soil parameter values and paleo-topography

Sebastian Vogel [a,c,*], Michael Märker [a,b]

[a] Heidelberg Academy of Sciences and Humanities, c/o University of Tübingen, Rümelinstraße 19-23, 72070 Tübingen, Germany
[b] Department of Vegetation, Soil, Environment and Agroforestry Sciences, University of Florence, P.zzale Cascine 16, 50144 Florence, Italy
[c] German Archaeological Institute, Podbielskiallee 69-71, 14195 Berlin, Germany

ARTICLE INFO

ABSTRACT

The Plinian eruption of Somma-Vesuvius AD 79 that destroyed the ancient city of Pompeii, resulted in a nearly complete burial of the Sarno River plain. Hence, to a certain extent the pre-AD 79 Roman paleo-surface and paleosols of that entire landscape were conserved. To characterize the pre-AD 79 Roman paleosol and the paleo-topographical situation south of Pompeii, ten stratigraphic core drillings were conducted along two transects stretching W–E and N–S. At five locations the drillings yielded Roman paleosols that were described, sampled and analysed for soil physical and chemical parameters. Corresponding to the present-day topography of the study area, which is flat to slightly sloping, the Roman paleo-surface appears in a similar relative paleo-topographic position. It runs nearly parallel to the modern surface at a depth of 5.50 to 6.40 m. By comparing the paleosol's properties with its position along the transects a correlation between soil parameter values and paleo-topography is revealed. The spatial distribution of paleosol characteristics is a function of soil development in relation to elevation and distance from the paleo-floodplain of the paleo-Sarno River network. This is most evident for soil thickness, soil horizonation, total organic carbon (TOC) and phosphate content and to some extent for soil texture and oxalate-extractable Si (Si_{ox}) as a measure of allophane content. Near the paleo-Sarno River and its floodplain the Roman paleosols were 30 cm thick having an AC-profile and showed lower amounts of TOC and phosphates. In contrast, at higher elevation and longer distance from the paleo-River the paleosols were 60 cm thick, showed the development of a B-horizon, and had higher TOC and phosphate contents and partly a finer soil texture and higher amounts of Si_{ox}. Nevertheless, all five Roman paleosols were macroscopically isotropic, i.e. they were mostly very dark gray throughout the profile. Thus, and in accordance with $Al_{ox} + 0.5Fe_{ox} < 2\%$, at the time of the eruption AD 79, pedogenetically the Roman paleosol south of Pompeii is a relatively young soil. Subsequent to the eruption AD 79 at lower elevations the buried Roman paleosols have come under the influence of a seasonally fluctuating groundwater table. This caused redoximorphic features in the lower section of the AD 79 white pumice layer in terms of red Fe(III)-oxide accumulations and increased amounts of SO_4^{2-} in the underlying pre-AD 79 Roman paleosols.

© 2010 Elsevier B.V. All rights reserved.

1. Introduction

Paleosols are ancient soils that have developed in the geological past under a distinct paleo-environment characterized by the particular interplay of the soil-forming factors active prior to burial. Paleosols can be found within sedimentary sequences such as alluvium or volcanic successions. Since paleosols are geoarchives of a past soil-forming environment they contain evidence about the evolution of ancient landscapes including past land use, vegetation or geomorphological processes. Especially, when an ancient land surface is preserved underneath depositional strata such as volcanic ashbeds the ancient soilscape can be reconstructed in detail (Burggraf et al.,

1981; French, 2003; Gerrard, 1992; Retallack, 2001, 2005). Recurring volcanic deposition and subsequent pedogenesis create multi-layered stratigraphies that preserve the profiles and properties of the buried soils and provide highly useful information about past pedogenesis (Shoji and Takahashi, 2002). Even though, particular properties of volcanic soils contribute to a good preservation after burial, paleosols cannot be considered as strictly fossilized as their can undergo diagenetic alterations such as: (i) decomposition of soil organic matter, (ii) changes in soil color, (iii) soil compaction after burial or (iv) addition of nutrients from the leaching of overlying strata. In contrast, other soil properties such as soil horizons, texture, mineral composition, phosphate concentration or the depth functions of organic carbon and nitrogen are likely to remain preserved over longer periods of time (French, 2003; Retallack, 1998, 2001).

The explosive eruption of Somma-Vesuvius AD 79 that destroyed the ancient cities of Herculaneum and Pompeii resulted in a nearly

* Corresponding author. Tel.: +49 30 187 711 358; fax: +49 30 187 711 168.
E-mail address: sv@dainst.de (S. Vogel).

complete burial of the entire Sarno River plain to a certain extent conserving the pre-AD 79 Roman paleosols of a whole region. The important factors for their good preservation are that:

(i) AD 79 a large area of the south-eastern territory of Somma-Vesuvius was buried relatively homogeneously by pumice lapilli fallout and pyroclastic flow/surge deposits,

(ii) even after consolidation and redistribution of the pyroclastic material after their initial deposition, the volcanic deposits of AD 79 still reach a significant thickness of approximately 3.5 m (determined from 1186 stratigraphical core drillings),

(iii) the process of burial was nearly isochronous, i.e. it occurred in a very short period of time of only 19 h (Luongo et al., 2003),

(iv) the first eruptive phase consisted of 'cold' pumice lapilli fallout covering the Roman paleo-surface. Hence, the paleosol was protected from the heating effect that could have been caused by the hot ash of the later occurring pyroclastic surges.

The pre-AD 79 Roman paleosol can be clearly distinguished from other stratigraphic layers because of a sharp transition of the characteristic white pumice layer representing the initial phase of the AD 79 Plinian eruption overlying a dark colored soil. Hence, the soil material can be sampled by means of stratigraphic core drillings and analysed for their soil properties.

Pedological analyses of the paleosols of the Sarno River plain, are rather scarce, among them Foss (1988), Scudder et al. (1996) and Foss et al. (2002). Foss (1988) and Foss et al. (2002) investigated the morphological, physical and chemical properties of paleosols of the Pompeii area, which they dated between 1871 yr BP (AD 79) and 17,000 yr BP (~15,000 BC). They analysed the soil's solid phase sampled in quarries (Ottaviano, Terzigno, and Pozzelle) and archaeological excavations (Pompeii, Oplontis, Herculaneum, and Boscoreale) stating that volcanic depositions such as airborne pumice and ash, in general, result in an excellent preservation of paleo-surfaces. The stratigraphy of the deposits included numerous lithologic discontinuities indicating periods of both volcanic activity and pedogenesis. The volcanic deposits were interrupted by paleosols representing phases of biostasy. Hence, weathering of the parent material and an accumulation of soil organic matter could take place. The parent material of both the paleosols and the present-day soils were mainly composed of pumice, ash and volcanic glass along with some lithic fragments (Foss, 1988; Foss et al., 2002). Furthermore, especially the pre-AD 79 Roman paleosols contained archaeological artefacts such as nails, pieces of tile, building stones and other man-made objects. Altogether, Foss (1988) and Foss et al. (2002) distinguished four to five major episodes of volcanic activity and subsequent soil development, whereas the Plinian eruptions of AD 79, Avellino (1890–1630 BC) and Mercato (7070–6770 BC) (Civetta et al., 1998; Robinson, 2008; Rolandi et al., 1993a,b; Vogel et al., 1990) were most evident in their profiles. The associated paleosols mainly consisted of a humus-rich horizon (A) whereas some profiles also showed a weathered or cambic horizon (Bw) on top of the substratum (C). However, thinner volcanic depositions from minor eruptions were presumably incorporated into the plow layer (Ap) and thus could not be identified. Foss (1988) states that the different paleosols were comparable regarding their morphology within the stratigraphic sequence showing similar soil properties. Consequently, he postulated similar pedogenetic conditions before and after AD 79.

The Roman paleosols around Pompeii showed little disturbance, which was particularly evident in the well preserved humus-rich A-horizons. Furthermore, the paleosols were very similar to the modern soils of the Pompeii area apart from a higher pH and a higher nutrient content, i.e. the modern soils were moderately to slightly acid whereas the paleosols were alkaline throughout the profile (Foss, 1988). Thus, Foss (1988) and Foss et al. (2002) assumed this to be the result of bases (Mg^{2+}, Ca^{2+}) leached from the overlying volcanic sediments and recharging the surface horizons of the paleosols. Other modifications after burial were described by these authors as structural changes,

decomposition of soil organic matter and changes in soil color. Following the soil classification of the FAO, Foss (1988) classified the paleosols as well as the modern soils as Mollic Andosols.

Scudder et al. (1996) used ^{14}C dates and cultural artifacts to estimate the approximate age of the paleosols of Pompeii by its soil thickness. As the Roman paleosols were less than 30 cm thick in most locations, they argue that there was little volcanic activity for about 600 or 700 years prior to the eruption AD 79, which agrees with Sigurdsson and Carey (2002) who suggest circa 700 years of stability and pedogenesis. Scudder et al. (1996) also analysed extractable phosphorous (P) in the paleosol as an indicator of human activity. They found P contents that were higher than the background values, which they assume derived for instance from organic waste, manure or fertilizer.

The aim of this paper is to provide a characterization of the pre-AD 79 Roman paleosol, conserved beneath the AD 79 volcanic deposits of Somma-Vesuvius, following standard physical and chemical properties. Moreover, the paleo-topographical situation south of Pompeii has been determined. Following two toposequences of the pre-AD 79 Roman paleosol particular attention will be drawn to the correlation between soil parameter values and paleo-topographic position.

The terms pre-AD 79 Roman paleosol or Roman paleosol are used synonymously indicating the soil that developed until the AD 79 eruption of Somma-Vesuvio when it was buried by volcanic deposits. This soil primarily acquired its soil properties through pedogenesis prior to burial AD 79. However, some post-burial soil developments may have changed the original character of the Roman soil to a certain extent. Consequently, a soil physical and chemical characterization of the pre-AD 79 Roman paleosol intents to refer to the present-day appearance of the soil including both original soil parameters formed before burial AD 79 and potential post-burial changes, e.g. due to decomposition of soil organic matter, leaching of nutrients from the overlying deposits or groundwater fluctuations.

This work is part of the geoarchaeological research project 'Reconstruction of the ancient cultural landscape of the Sarno River plain' undertaken by the German Archaeological Institute in cooperation with the Heidelberg Academy of Sciences and Humanities/University of Tübingen (Seiler, 2008).

2. Research area

The research area is located in the Sarno River plain (Italy) southeast of the volcanic complex of Somma-Vesuvius and in the southern part of the Plio-Pleistocene graben structure of the Campanian plain (Fig. 1). In the south and in the east the plain is flanked by Mesozoic calcareous rocks of the Lattari and Sarno Mountains belonging to the Apennine Mountain chain. In the west, the plain opens to the Tyrrhenian Sea and is drained by the Sarno River network.

During our field campaign ten stratigraphic core drillings were conducted south of the archaeological site of ancient Pompeii in the location of Moreggine (Fig. 1). The research area is situated at the foot of the southern slope of the N–S stretching Pompeiian hill that is thought to represent either a tongue of lava from Somma-Vesuvius (Pescatore et al., 1999; Ward Perkins, 1984) or a remnant of an ancient volcanic caldera (Cinque and Irollo, 2004).

The drillings were placed along two transects spanning across approximately 950 m from north to south and 820 m from west to east. The former is to determine a catena of the paleo-pedological and paleo-topographical situations from the city wall of ancient Pompeii in the north to the Sarno River in the south. This transect crosses the modern Bottaro channel and the autostrada A3 Napoli-Salerno. The latter begins in the west near the protohistorical dune ridge of Bottaro/Pioppaino and the railway line Circumvesuviana extending eastwards into the Sarno River plain also crossing the Bottaro channel (Fig. 1).

Following the AD 79 paleo-environmental reconstruction of the Sarno River plain of Vogel et al. (2011) and Vogel and Märker (2010)
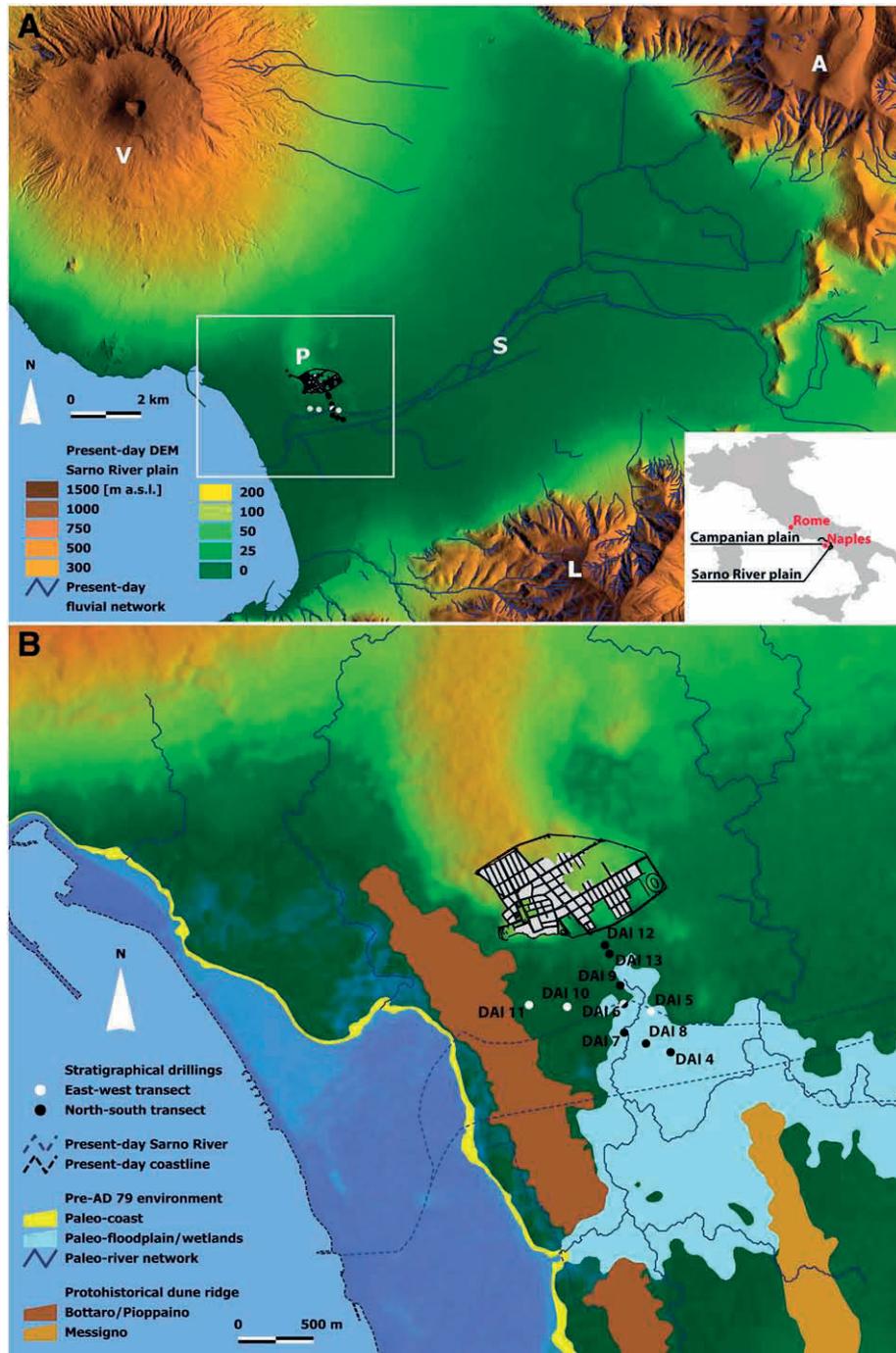
Fig. 1. A: present-day digital elevation model (DEM) of the Sarno River plain (white letters: A—Apennine (Sarno Mountains), L—Lattari Mountains, P—Pompeii, S—Sarno River, V—Somma-Vesuvius). B: location of stratigraphic core drillings south of the excavation of Pompeii with paleo-environmental conditions before AD 79 (Vogel et al., 2011). The small scale map of Italy shows the location of the Campanian plain and the Sarno River plain.

the southernmost drillings DAI 4, DAI 7 and DAI 8 having the lowest elevations are situated within the predicted floodplain of the paleo-Sarno River. There the Roman layer is dominated by fluvial-palustrine deposits. The Roman layers of the other sites were predicted to contain terrestrial deposits such as well drained soils.

3. Materials and methods

Due to the densely populated and urbanized study area and due to an approximate depth of the Roman paleo-surface between 5 and 10 m below the present-day surface the sampling of the paleosols had to be

done by means of mechanical stratigraphic core drillings. Furthermore, through stratigraphic drillings it is possible to sample the Roman paleosol in natural undisturbed stratigraphy ensuring minimum disturbance and maximum conservation. In contrast Foss (1988) and Foss et al. (2002) obtained soil samples from quarries and archaeological excavations, i.e. in exposures that have already been open since a certain period of time. Consequently, the investigated paleosols are likely to be more or less affected by recent weathering processes.

To gain a sufficient amount of undisturbed soil material a core of 15 cm in diameter was extracted by the stratigraphic drillings. After identifying the Roman paleosol underneath the volcanic deposits of

81

AD 79, it was described in the field and sampled every 10 cm. Munsell soil color was determined on moist samples. In the laboratory the air-dried soil samples were passed through a 2 mm sieve to remove the skeleton so as to get the fine earth fraction for the following soil physical and chemical analyses.

Soil pH was measured in 1 M $CaCl_2$ (DIN ISO 10390, 2005). The soil texture of the fine earth fraction was investigated by wet sieving and sedimentation following Stokes' law (1845) after dispersing the sample with 0.2 N Na-pyrophosphate. Soil texture classes were used according to the German DIN standard (DIN ISO 11277, 2002). Due to the presence of amorphous aluminium silicates in soils of volcanic origin and the associated difficulties to disperse the sample it is important to emphasize the particle size was only used in classes and on a relative scale (Mizota and Van Reeuwijk, 1989).

Total organic carbon (TOC) and total inorganic carbon (TIC) were determined by elementary analysis using the dry combustion reference method (DIN EN 13137, 2001). At first all carbon forms in the sample (total carbon, TC) were converted to CO_2 at 950 °C and measured by a non-dispersive infrared gas analyzer (NDIR). Then the sample was treated with hydrochloric acid (HCl) removing all inorganic carbon forms (TIC) and measured again for TOC. TIC was then calculated according to $TC = TOC + TIC$ (Schuhmacher, 2002; Tiessen and Moir, 1993).

Total nitrogen was determined photometrically using the modified method of Kjeldahl including the digestion of the organic compounds with sulfuric acid (H_2SO_4) and the distillation of ammonia (NH_3) with sodium hydroxide (NaOH) (DIN ISO 11261, 1997). Total phosphate-P was extracted using aqua regia (nitrochloric acid; 3:1 ratio of concentrated HCl and concentrated HNO_3) at 140 °C and analysed by ICP-OES (inductively coupled plasma-optical emission spectrometry) (DIN 38414 S12, 1986). Sulfate ions (SO_4^{2-}) were determined by complexo-metric titration with barium chloride ($BaCl_2$) (DIN 38405 D5, 1985).

Due to the weathering of volcanic glass, volcanic soils contain a complex colloidal fraction of allophane/imogolite, ferrihydrite or Al/Fe-humus complexes showing variable charge characteristics (Madeira et al., 2007; Nanzyo, 2002). Consequently, the cation exchange complex was characterised by determining the effective cation exchange capacity (CEC_{eff}) since it is measured at field pH. CEC_{eff} and the amount of exchangeable base cations (Ca^{2+}, Mg^{2+}, Na^+, K^+) were analysed photometrically by flame atomic absorption spectrometry (AAS) after sequential extraction with an unbuffered ammonium chloride solution (NH_4Cl). Additionally, the amounts of Al, Fe and Mn ions were analysed by AAS.

Due to their volcanic origin the Roman paleosols were tested for the presence and amounts of aluminium, iron and silicon associated with short-range-order or active amorphous constituents by means of extraction with acid oxalate (Al_{ox}, Fe_{ox}, Si_{ox}) (Arnalds and Kimble, 2001; Blakemore et al., 1981). Ferrihydrite percentages were determined by $Fe_{ox} \times 1.7$ (Parfitt and Childs, 1988). Si_{ox} is a measure of allophane content (Parfitt, 1990). Hence, Si_{ox} was used to detect relative changes in the allophane concentration. Moreover, $Al_{ox} + 0.5Fe_{ox}$ enables the classification of the soil along the weathering sequence of pyroclastic deposits (tephric soil material → vitric properties → andic properties) (FAO-ISRIC-IUSS, 2006).

4. Results

In the following section, the paleo-topographic situation before AD 79 is described based on the stratigraphical drilling data (Fig. 2). The results of the field and laboratory analyses are summarised in Tables 1, 2 and 3. Fig. 3 illustrates the part of the stratigraphic sequence of the drilling cores containing the Roman paleosols (red rectangle).

The stratigraphic sections of the N–S and W–E transect show that the present-day topography of the study area in the location of Moreggine is flat to slightly sloping having approximate inclinations of 0.09° (W–E) and 0.23° (N–S), respectively (Fig. 2). The same values can be applied to the Roman paleo-surface running nearly parallel to

the modern surface at a depth of 5.50 (DAI 9) to 6.40 m (DAI 6). Interpolated groundwater data provided by the Autorità di Bacino del Sarno show that, apart from DAI 12, the present-day mean annual groundwater table south of Pompeii lies at or above the Roman paleo-surface.

Physiographic features of the modern surface are the Bottaro channel near DAI 6 and the Sarno River south of DAI 4 (Figs. 1 and 2). Besides the drillings DAI 4, DAI 7 and DAI 8 the Roman paleo-layer can be characterized as terrestrial deposits. Five drillings contain Roman paleosols (DAI 5, DAI 6, DAI 9, DAI 11 and DAI 13) whereas in DAI 10 and DAI 12 the Roman layer is anthropogenically disturbed. In DAI 7 and DAI 8 the AD 79 pumice lapilli fallout is slightly rounded and surrounded by a matrix of mud. In DAI 4, fluvial sediments appear containing fluvial sand and gravel, pieces of travertine, rounded ceramic sherds and shells of turriculata freshwater gastropods.

The Roman paleosols south of Pompeii mainly consist of reworked pyroclastic material such as ash and lapilli. They are compacted, well drained and mostly have an irregular prismatic fracture. The soil skeleton contains fine lithic gravel, subrounded pumice and some-times pieces of travertine. It can also include ceramics and occasionally fragments of charcoal. The layer underneath the Roman paleosols consists either of fluvial deposits (DAI 5, DAI 9 and DAI 13) or protohistorical volcanoclastics (DAI 6 and DAI 11).

The Roman paleosols are between 30 (DAI 5, DAI 6) and 60 cm (DAI 11) thick and the Munsell soil color measured on moist samples is mostly very dark gray throughout the profile with no horizonation to be determined macroscopically. The soil texture of the fine earth fraction (<2 mm) is mainly sandy loam (Table 1). Only the paleosol of DAI 13 consists of silt loam. The soil skeleton (>2 mm) ranges from 3.4 (DAI 13) to 21.3% (DAI 11) whereas DAI 5 and DAI 13 show a distinct maximum of coarse material in the upper soil containing pumiceous particles from the overlaying AD 79 white pumice layer (Table 1).

The pH value of the paleosols upper horizon is mostly neutral or slightly alkaline ranging from 6.8 (DAI 9) to 7.8 (DAI 5). With rising depth pH increases in DAI 9. In DAI 5 and DAI 13 pH remains virtually constant, but it decreases in DAI 11. DAI 6 shows a distinct pH minimum of 4.7 (very strong acid) between 10 and 20 cm, which coincides with a strong sulfate (SO_4^{2-}) maximum in that horizon. The paleosols of DAI 5, DAI 6 and DAI 11 show increased amounts of SO_4^{2-} with a pronounced maximum of 131 (DAI 11) to 298 mg l^{-1} (DAI 6) in the middle section of the soil. In contrast, DAI 9 and DAI 13 contain no or almost no SO_4^{2-}.

Total organic carbon (TOC) is between 12 (DAI 9) and 41 g kg^{-1} (DAI 13) in the upper part of the paleosol generally decreasing with depth. Increased amounts of TOC in the substratum of DAI 5, DAI 9 and DAI 13 derive from humus-rich fluvial-palustrine deposits under-neath the Roman paleosols.

The concentration of nitrogen (N) in the top of the paleosol is between 0.6 (DAI 9) and 1.4 g kg^{-1} (DAI 11, DAI 13) following the trend of TOC. The C/N ratio is highest in the upper soil ranging between 20 (DAI 5, DAI 9) and 29 (DAI 13) whereas in DAI 13 it reaches a distinct maximum of up to 45 in the substratum. All five paleosols show low amounts of total inorganic carbon (TIC) of maximum 4 g kg^{-1} (DAI 5, DAI 9) and a rather fluctuating depth function, which seems to be partly connected to the distribution of exchangeable Ca^{2+}.

The effective cation exchange capacity (CEC_{eff}) of the Roman paleosols is highest in the upper section of the profile ranging from 8.3 (DAI 6) to 15.3 cmol$_c$ kg^{-1} (DAI 13). DAI 9 and DAI 13 have a second maximum of CEC_{eff} in the substratum, which coincides with increased amounts of TOC.

The base saturation is around 100% with no exchangeable Al^{3+} to be present. The cation exchange complex is considerably dominated by Ca^{2+}, followed by K^+, Na^+ and finally Mg^{2+}. The resulting mean cation saturations are: 39 (DAI 6) to 58% (DAI 13) for Ca^{2+}; 27 (DAI 9) to 34% (DAI 5, DAI 11) for K^+; 8 (DAI 13) to 22% (DAI 6) for Na^+ and 4 (DAI 13) to 10% (DAI 5) for Mg^{2+}. Apart from DAI 13 Ca^{2+} strongly decreases in the subsoil approximately reaching the amount of K^+.
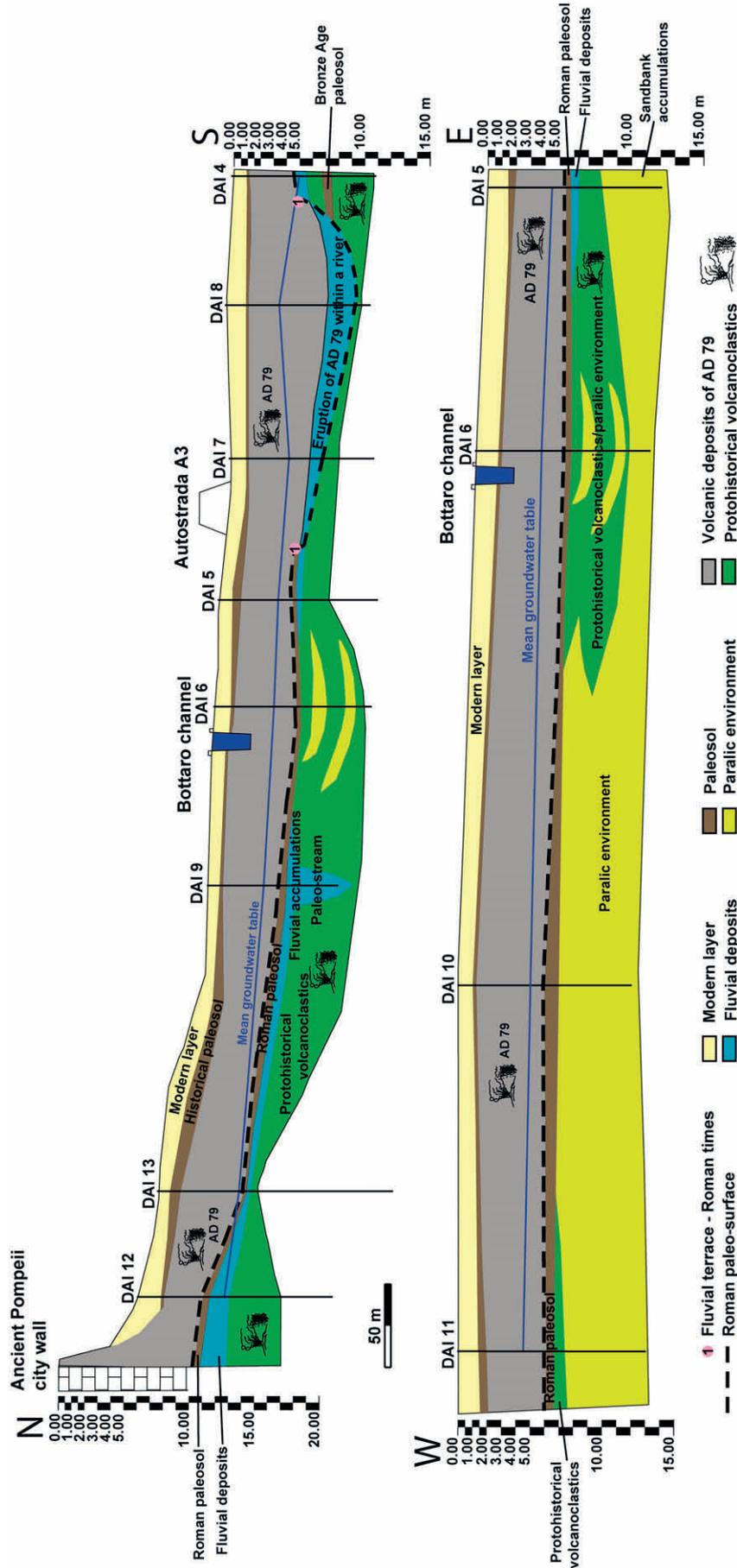
Fig. 2. Stratigraphic cross sections of the north–south and west–east transect, interpolated from the drillings south of Pompeii.

83

Table 1
Field description and soil physical parameters of the Roman paleosols.

Drilling	*DAI 5*
Easting	2477368
Northing	4510412
Elevation	5.7 m a.s.l.
Soil thickness	30 cm

Horizons	Depth[m]	Munsell color(moist)	Soil texture	Soil skeleton (>2 mm) [Mass-%]	Remarks
Ab	5.60–5.70	10 YR 3/1	Sandy loam	14	
ACb	5.70–5.80	10 YR 3/1	Sandy loam	7.2	Ceramics
Cb	5.80–5.90	10 YR 3/1	Sandy loam	9.6	Ceramics
Description	Roman paleosol of AD 79, cultivated, compacted, well drained, very dark gray, soil skeleton of fine gravel (mainly lithic), contains ceramic fragments				

Drilling	*DAI 6*
Easting	2477190
Northing	4510462
Elevation	6.1 m a.s.l.
Soil thickness	30 cm

Horizons	Depth[m]	Munsell color(moist)	Soil texture	Soil skeleton(>2 mm) [Mass-%]	Remarks
A1b	6.40–6.50	10 YR 2/1	Sandy loam	6.5	Ceramics
A2b	6.50–6.60	10 YR 3/1	Sandy loam	6.4	
Cb	6.60–6.70	10 YR 3/1	Sandy loam	7.4	Ceramics
Description	Roman paleosol AD 79, pyroclastic, cultivated, irregular prismatic fracture, weakly cohesive, compacted, well drained, black to very dark gray, contains scattered red and grey mottles, soil skeleton of fine gravel (lithic), contains ceramic fragments				

Drilling	*DAI 9*
Easting	2477169
Northing	4510589
Elevation	7.6 m a.s.l.
Soil thickness	30 cm

Horizons	Depth[m]	Munsell color(moist)	Soil texture	Soil skeleton(>2 mm) [Mass-%]	Remarks
Ab	5.50–5.60	10 YR 2/2	Sandy loam	7.9	
Bw1b	5.60–5.70	10 YR 3/1	Sandy loam	6.7	Travertine
BwCb	5.70–5.80	10 YR 3/1	Sandy loam	5.9	Travertine
2ACb	5.80–5.90	10 YR 2/2	Sandy loam	7.2	Travertine
2Cb	5.90–6.00	10 YR 3/1	Sand	14	
Description	Roman paleosol of AD 79, reworked and subrounded pumice and lithics, cultivated, compacted, very dark gray to very dark brown, irregular prismatic fracture, well drained, pseudo-hydromorph, contains charcoal, soil skeleton of lapilli and granules/tubules/aggregates of travertine				

Drilling	*DAI 11*
Easting	2476553
Northing	4510459
Elevation	7.7 m a.s.l.
Soil thickness	60 cm

Horizons	Depth[m]	Munsell color(moist)	Soil texture	Soil skeleton(>2 mm) [Mass-%]	Remarks
A1b	6.10–6.20	10 YR 2/1	Sandy loam	12.7	Ceramics
A2b	6.20–6.30	10 YR 3/1	Sandy loam	8.4	
Bwb	6.30–6.40	10 YR 2/1	Sandy loam	14.2	Ceramics
BwCb	6.40–6.50	10 YR 2/1	Sandy loam	21.3	
C1b	6.50–6.60	10 YR 3/1	Loamy sand	16.8	
C2b	6.60–6.70	10 YR 3/1	Loamy sand	18.4	
Description	Roman paleosol of AD 79 on reworked pyroclastics, irregular prismatic fracture, compacted, homogeneous, slightly plastic, black to very dark gray, contains scattered red and grey mottles, good presence of organic matrix, contains fragments of ceramic				

Drilling	*DAI 13*
Easting	2477090
Northing	4510802
Elevation	8.9 m a.s.l.
Soil thickness	50 cm

Horizons	Depth [m]	Munsell color (moist)	Soil texture	Soil skeleton (>2 mm) [Mass-%]	Remarks
A1b	6.10–6.20	10 YR 3/1	Silt loam	10.4	Ceramics
A2b	6.20–6.30	10 YR 3/1	Silt loam	4.6	Ceramics, Charcoal
ABwb	6.30–6.40	10 YR 3/1	Silt loam	3.4	Ceramics, Charcoal
Bwb	6.40–6.50	10 YR 3/1	Silt loam	4.7	Charcoal
BwCb	6.50–6.60	10 YR 3/1	Silt loam	7	Ceramics, Charcoal
2ACb	6.60–6.70	10 YR 3/1	Silt loam	7.6	
Description	Roman paleosol of AD 79 on fluvial deposits, pyroclastic, reworked ash, presence of subrounded pumice, compacted, pseudo-conchoidal fracture, very dark gray, contains charcoal and ceramic fragments (sigillata), contains small nuclei of travertine, mortar				

The phosphate (P) concentrations of the Roman paleosols vary from 1660 (DAI 6) to 4190 mg kg^{-1} DM (DAI 13) whereas high P values coincide with high amounts of TOC. The amounts of short-range-order or amorphous Al, Fe and Si compounds extracted by acid oxalate are relatively low. The elemental composition shows the order $Al_{ox}>Fe_{ox}>Si_{ox}$ and range from 0.1 to 0.9%. Al_{ox}, Fe_{ox} and Si_{ox} are mainly increased in the top of the paleosol showing high amounts of TOC whereas especially DAI 11 shows a maximum in the middle section of the soil profile. The same depth function can be applied for $Al_{ox} + 0.5Fe_{ox}$ ranging between 0.4 and 1.1%.

5. Discussion

Due to the good preservation of the Roman paleosols underneath the AD 79 volcanic deposits of Somma-Vesuvio the obtained data characterize the physical and chemical properties of the buried pre-AD 79 Roman paleosol. Moreover, the N–S and W–E transect show the corresponding paleo-topographical situation south of Pompeii that was interpolated from the stratigraphic drilling data (Fig. 2). Combining the paleo-topography with paleosol properties allows the evaluation the paleo-soil-landscape characteristics and its underlying processes.

According to the present-day level to slightly sloping topography of the study area south of Pompeii, the Roman paleosols appear in a similar relative paleo-topographic position, i.e. the Roman paleo-surface runs nearly parallel to the modern surface. This agrees with the statement of Stefani and Di Maio (2003) that the eruption AD 79 caused a coating on the ancient topography resulting in an analog shape of the two surfaces.

As mentioned earlier, the Roman paleo-layer of DAI 7 and DAI 8 is characterised by slightly rounded lapilli, which is surrounded by a matrix of mud. This corresponds with a swampy area of stagnant water or a river where the pumice fallout of AD 79 was either directly deposited or transported into. Furthermore, DAI 4, which is situated at higher elevation, contains fluvial sediments, pieces of travertine and shells of freshwater gastropods. This situation presumably relates to the fluvial network of the paleo-Sarno River and its floodplain. DAI 7 and DAI 8 might represent an old river arm that was filled with AD 79 volcanic deposits whereas DAI 4 represents an old fluvial terrace or

undercut slope. Accordingly, Vogel et al. (2011) and Vogel and Märker (2010) state that this area is dominated by fluvial-palustrine deposits (Fig. 1B) from the paleo-river network, which may be characterized by meanders, back waters and an extensive flood area. The Roman layer of the remaining seven drillings can be considered as terrestrial deposits. Five of them contained Roman paleosols (DAI 5, DAI 6, DAI 9, DAI 11 and DAI 13) whereas two were anthropogenically disturbed (DAI 10 and DAI 12).

The soil thickness of the Roman paleosols varies between 30 (DAI 5, DAI 6) and 60 cm (DAI 11) following the paleo-topographic position along the transects. In the south of the N–S transect and close to the paleo-floodplain of the paleo-Sarno River the paleosols are only 30 cm thick (DAI 5 and DAI 6). In the north, at higher elevations and longer distances from the paleo-river the Roman paleosols are thicker with 50 cm (DAI 13). Thus, on the N–S transect the spatial distribution of soil thickness is a function of elevation and distance from the paleo-floodplain of the paleo-Sarno River. The vicinity to fluvial-palustrine environments is also stressed by palynological analysis in the Roman paleosol of DAI 6 where pollen of marsh and aquatic plants were found (Di Maio, April 2008, written communication).

Due to its constant flat topography, on the W–E transect the soil thickness only increases with the distance from the paleo-floodplain. DAI 11 which is situated most distant from the paleo-floodplain, in the west of the transect, is 60 cm thick. In contrast, the paleosols near the paleo-floodplain in the east have a thickness of only 30 cm (DAI 5 and DAI 6).

The pre-AD 79 Roman paleosols are macroscopically isotropic with no horizonation to be visible. This is evidenced by the Munsell soil color on moist samples, which is mostly very dark gray throughout the profile. Consequently, corresponding with their thickness of only 30 cm DAI 5 and DAI 6 show an AC-profile. In contrast, DAI 11 and DAI 13 have a soil profile of 50 to 60 cm thickness and show the initial development of a B-horizon. Following Scudder et al. (1996) thicker paleosols with a more pronounced horizonation imply a longer duration of soil development, i.e. weathering and humus accumulation. In DAI 11 and DAI 13 this correlates with higher amounts of TOC in the top of the paleosol. Moreover, DAI 11 has a maximum of Fe_{ox} and Al_{ox} in the middle section of the soil, whereas DAI 13 shows a considerably finer soil texture. However, relatively thin soil profiles

Table 2
Soil chemical parameters of the Roman paleosols I (ND, not detectable).

Drilling	Depth [m]	pH (CaCl$_2$)	TOC [g kg^{-1}]	TIC [g kg^{-1}]	N [g kg^{-1}]	C/N	P [mg kg^{-1}]	CEC$_{eff}$ [cmol$_c$ kg^{-1}]	Eff. base saturation [%]	Exchangeable cations [cmol$_c$/kg]					SO$_4^{2-}$ [mg l^{-1}]
										K$^+$	Na$^+$	Ca^{2+}	Mg^{2+}	Al^{3+}	
DAI 5	5.60–5.70	7.79	21.9	0.5	1.1	19.9	1816	13.2	99.8	4.38	1.97	5.55	1.27	ND	51
	5.70–5.80	7.84	18.9	4.0	1.0	18.9	1713	12.3	100	3.97	1.85	5.50	1.20	ND	137
	5.80–5.90	7.81	19.4	ND	1.0	19.4	1711	11.7	100	4.36	1.79	4.38	1.19	ND	79
DAI 6	6.40–6.50	7.46	25.0	2.8	1.0	25.0	1661	8.3	100	2.62	1.14	4.07	0.51	ND	125
	6.50–6.60	4.73	17.1	2.6	1.0	17.1	1807	7.6	98.9	2.39	1.82	2.93	0.38	0.01	298
	6.60–6.70	6.06	8.3	1.0	0.6	13.8	1717	5.2	100	1.93	1.49	1.53	0.24	ND	24
DAI 9	5.50–5.60	6.77	12.1	2.3	0.6	20.2	2429	10.3	99.6	2.54	1.27	5.90	0.55	ND	ND
	5.60–5.70	7.12	10.8	0.1	0.6	18.0	2209	9.5	100	2.36	1.38	5.30	0.46	ND	ND
	5.70–5.80	7.29	9.3	4.0	0.6	15.5	2549	10.6	99.8	2.47	1.10	6.55	0.46	ND	ND
	5.80–5.90	7.40	11.2	1.7	0.6	18.7	2675	9.2	100	2.62	1.02	5.10	0.45	ND	ND
	5.90–6.00	7.47	2.1	1.7	0.2	10.6	2262	7.0	100	2.26	1.41	3.06	0.30	ND	ND
DAI 11	6.10–6.20	7.32	33.5	1.5	1.4	23.9	3256	10.7	99.5	3.58	1.28	5.20	0.59	ND	92
	6.20–6.30	7.36	27.9	2.3	1.4	19.9	3284	11.2	100	3.43	1.20	6.05	0.55	ND	104
	6.30–6.40	6.95	20.3	1.8	1.0	20.3	2231	7.6	100	2.79	1.17	3.14	0.47	ND	113
	6.40–6.50	6.34	16.8	2.5	1.0	16.8	1940	6.3	100	2.21	1.41	2.29	0.35	ND	131
	6.50–6.60	6.41	12.7	0.4	0.7	18.1	1908	4.8	100	1.68	1.23	1.65	0.24	ND	79
	6.60–6.70	6.23	6.6	1.0	0.6	11.1	1815	3.7	100	1.20	1.09	1.28	0.16	ND	53
DAI 13	6.10–6.20	7.46	41.0	ND	1.4	29.3	4187	15.3	99.7	4.66	1.22	8.45	0.93	ND	10
	6.20–6.30	7.46	40.8	2.7	1.3	31.4	4124	15.6	99.7	4.48	1.28	9.10	0.69	ND	10
	6.30–6.40	7.48	38.9	1.2	0.9	43.3	3910	13.4	100	4.27	1.12	7.50	0.51	ND	7
	6.40–6.50	7.50	32.8	0.9	0.8	41.0	4163	13.1	99.9	3.60	0.85	8.20	0.44	ND	7
	6.50–6.60	7.49	31.2	3.2	0.7	44.6	3019	13.8	99.9	3.79	1.30	8.30	0.40	ND	8
	6.60–6.70	7.54	33.3	0.8	0.8	41.6	3002	15.6	99.7	4.79	1.21	9.15	0.40	ND	14

Table 3
Soil chemical parameters of the Roman paleosols II.

Drilling	Depth [m]	Al_{ox} [%]	Fe_{ox} [%]	Si_{ox} [%]	$Al_{ox} + 0.5Fe_{ox}$ [%]	Ferrihydrite[a] [%]
DAI 5	5.60–5.70	0.38	0.56	0.2	0.66	0.95
	5.70–5.80	0.33	0.22	0.12	0.44	0.38
	5.80–5.90	0.34	0.19	0.11	0.44	0.32
DAI 6	6.40–6.50	0.44	0.72	0.27	0.81	1.23
	6.50–6.60	0.43	0.42	0.16	0.64	0.71
	6.60–6.70	0.38	0.22	0.14	0.49	0.38
DAI 9	5.50–5.60	0.27	0.25	0.12	0.4	0.43
	5.60–5.70	0.27	0.25	0.12	0.4	0.42
	5.70–5.80	0.27	0.26	0.12	0.4	0.44
	5.80–5.90	0.31	0.25	0.14	0.43	0.42
	5.90–6.00	0.23	0.36	0.1	0.41	0.61
DAI 11	6.10–6.20	0.59	0.26	0.27	0.72	0.43
	6.20–6.30	0.62	0.32	0.29	0.78	0.54
	6.30–6.40	0.84	0.33	0.42	1	0.57
	6.40–6.50	0.9	0.33	0.47	1.06	0.55
	6.50–6.60	0.69	0.29	0.37	0.84	0.49
	6.60–6.70	0.58	0.31	0.29	0.73	0.53
DAI 13	6.10–6.20	0.48	0.16	0.17	0.57	0.28
	6.20–6.30	0.39	0.08	0.13	0.43	0.13
	6.30–6.40	0.35	0.09	0.12	0.4	0.15
	6.40–6.50	0.34	0.11	0.12	0.39	0.19
	6.50–6.60	0.37	0.14	0.12	0.44	0.23
	6.60–6.70	0.38	0.14	0.15	0.45	0.24

[a] Ferrihydrite percentages determined by ammonium oxalate-extractable $Fe \times 1.7$ (Parfitt and Childs, 1988).

explained by the recurring volcanic activity of Somma-Vesuvius. Scudder et al. (1996) and Sigurdsson and Carey (2002) suggest 600 to 700 years of stability and pedogenesis prior to the AD 79 eruption whereas Andronico and Cioni (2002) assume the last eruption before AD 79 between 217 and 216 BC (AP6) (Rolandi et al., 1998; Stothers and Rampino, 1983). Furthermore, the pedogenetically young age of the paleosols may also result from the proximity of the study area to the erosional or depositional influence of the paleo-Sarno River and its floodplain. As mentioned earlier a close vicinity to the paleo-river network is evident in the drilling cores of DAI 4, DAI 7 and DAI 8. It is also emphasized by the substrate directly underneath the Roman paleosols of DAI 5, DAI 9 and DAI 13, which contain fluvial-palustrine deposits. Moreover, the stratigraphic sequence of DAI 9 suggests the presence of a protohistorical paleo-stream that was filled with fluvial accumulations. In fact, according to the reconstructed paleo-river network of Vogel et al. (2011), before AD 79, a paleo-stream may have existed close to DAI 9 (Fig. 1B). An archaeologically relevant question would be whether the Romans actively reclaimed land for instance by drainage of fluvial-palustrine soils. In fact, in several stratigraphic sequences within the Sarno River plain the Roman paleosols developed on top of fluvial-palustrine deposits or the Roman layer was characterized as an intermediate stage between terrestrial and fluvial-palustrine deposits. This question should be further evaluated; nevertheless, it is beyond the scope of this paper.

Due to the low elevation of the research area, its proximity to the Sarno River network as well as due to a subsequent rise of the groundwater table relative to AD 79, today the mean annual groundwater table south of Pompeii lies mostly at or above the Roman paleo-surface (Autoritá di Bacino del Sarno) (Fig. 2). Hence, the Roman paleosols are seasonally saturated by groundwater. This is documented by a total of

and an only initial soil horizonation in all five Roman paleosols imply that at the time of the eruption AD 79 pedogenetically the Roman paleosol south of Pompeii was a relatively young soil. This can be
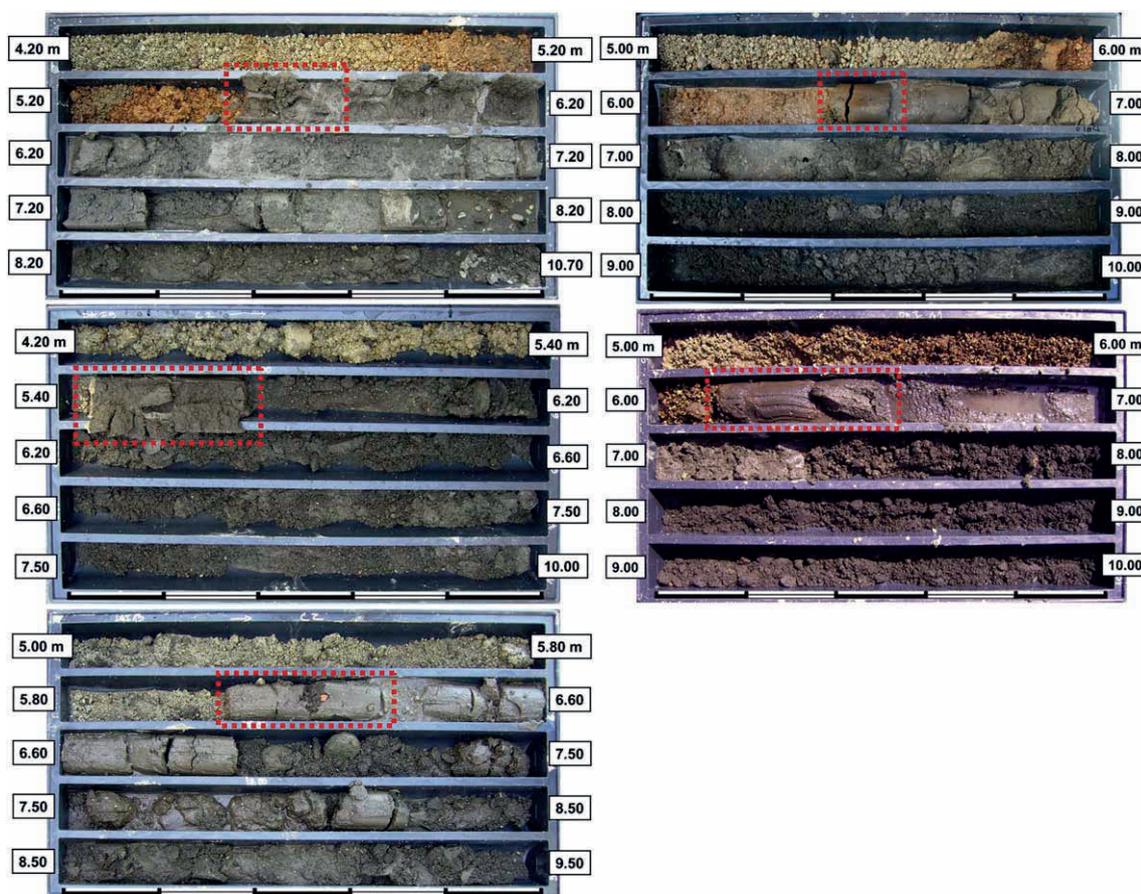

Fig. 3. Pre-AD 79 Roman paleosols (red rectangle) of DAI 5 (top left), DAI 6 (top right), DAI 9 (middle left), DAI 11 (middle right) and DAI 13 (bottom). Note the redoximorphic features in the white pumice layer above the Roman paleosols of DAI 5, DAI 6 and DAI 11.

seven stratigraphies (DAI 4, DAI 5, DAI 6, DAI 7, DAI 8, DAI 10 and DAI 11) showing redoximorphic features in the lower 60 (DAI 6) to 100 cm (DAI 5) of the AD 79 white pumice layer. These features become more intense towards the transition to the pre-AD 79 Roman paleo-surface (Fig. 3). The redoximorphic characteristics are recognized as red Fe oxide accumulations around the pumice. With rising groundwater table dissolved Fe ions reach the white pumice layer and are absorbed into its internal fine porous system. A drop of the water table then results in oxidising conditions in the macro pores between the pumice clasts, whereas in its interior reducing conditions are still predominant. This leads to a precipitation of Fe(III)-oxide, coating the pumiceous particles. In comparison to the obvious redoximorphology of the white pumice layer the Roman paleosols of DAI 6 and DAI 11 contain only scattered red and grey mottles, suggesting alternating oxidizing and reducing conditions. In contrast, the drillings DAI 9, DAI 12 and DAI 13 show no redoximorphology in the white pumice layer, indicating the absence of groundwater influence (Fig. 3). Indeed, DAI 12 and DAI 13 are located northernmost on the transect at the highest elevations.

As stated earlier, the distinct redoximorphology of the white pumice layer south of Pompeii seems to be caused by a seasonally fluctuating groundwater table. However, the pumice layer could also be subject to a perched water table. This situation was observed at the Villa dei Misteri north-east of Pompeii. The site is situated on the western slope of the Pompeiian hill in an elevation of 22 to 25 m a.s.l. Here, the Roman paleosol is not affected by groundwater. Nevertheless, scattered lenses of redoximorphic features were found in the lower section of the white pumice layer. This indicates the presence of a perched water table on top of the Roman paleo-surface due to seasonally fluctuating interflow/hypodermic preferential flow. A perched water table results from a strong decrease of permeability at the transition from the AD 79 white pumice layer to the pre-AD 79 Roman paleosol. The white pumice layer is highly permeable having a coarse texture and a pronounced system of macro pores. In contrast the paleosol shows a much finer soil texture, it is compacted due to the load of overlaying deposits and therefore less permeable. Hood infiltrometer measurements of saturated hydraulic conductivity (K_{sat}) of the Roman paleosol yielded values around 0.005 cm s^{-1}. On the other hand, K_{sat} of the white pumice layer was beyond instrumentation range of the hood infiltrometer (>0.01 cm s^{-1}). Hence, it was minimum one order of magnitude higher than in the Roman paleosol.

The topo-stratigraphic situation described earlier reveals that redoximorphology in the white pumice layer can be caused either by groundwater or perched water tables. However, due to the topographic situation and the available groundwater data we hypothesize a stronger influence of groundwater dynamics south of Pompeii.

It is noticeable that the pre-AD 79 Roman paleosols of DAI 5, DAI 6 and DAI 11 that show redoximorphic features within the AD 79 white pumice layer also have increased amounts of sulfate (SO_4^{2-}) with a pronounced maximum in the middle section of the soil. In contrast, the paleosols of DAI 9 and DAI 13 situated at higher elevations and showing no redoximorphology, contain no or almost no SO_4^{2-}. Furthermore, small amounts of Fe and Mn ions could be detected only within the middle section of DAI 6 showing the highest amounts of SO_4^{2-}. Accordingly, SO_4^{2-} may derive from the presence of groundwater. In soils that are subject to an oscillating water table increased amounts of sulfate can be caused under aerobic conditions by an oxidation of organic sulfur or inorganic sulfide to sulfate (Ahmad and Wilson, 1992; Nemeth et al., 1970). Geogenic sources of SO_4^{2-} are S-bearing minerals like pyrite (FeS_2) that are finely dispersed within the sediment (Russo and Punzo, 2004). Non-geogenic SO_4^{2-} may derive from saline residua of atmospheric precipitation due to volcanic eruptions, sulfurous volcanic effluents or anthropogenic sources (fertilization, industrial waste water).

Within the Roman paleosols of DAI 5, DAI 6 and DAI 11, SO_4^{2-} seems to be bound inorganically since it does not correlate with TOC. In volcanic soils sulfate tends to be adsorbed by the amorphous material. Even though $Al_{ox} + 0.5Fe_{ox} < 2\%$, showing a limited amount of amor-

phous material, in the paleosol of DAI 11 a maximum of SO_4^{2-} coincides with a maximum of Al_{ox} and Si_{ox} indicating some interaction with allophane. However, this is not the case for DAI 5 and DAI 6.

The parabolic distribution of SO_4^{2-} in DAI 5, DAI 6 and DAI 11, showing a maximum in the middle section of the profile, may derive from a higher permeability of the AD 79 pumice layer above and the protohistorical volcanoclastics (DAI 6, DAI 11) or fluvial deposits (DAI 5) underneath the Roman paleosol. This may result in a preferential groundwater flow within these layers and a reduction and translocation of SO_4^{2-}. In the middle section of the Roman paleosol on the other hand oxidizing conditions may remain longest leading to a relative accumulation of SO_4^{2-}.

The pH value of the paleosols surface horizon is neutral to slightly alkaline suggesting no soil acidity of H^+ and Al^{3+} to be active. This is also indicated by the effective base saturation of around 100%. Moreover, no exchangeable Al^{3+} could be determined. Thus, in the Roman paleosols, both pH and the effective cation exchange capacity (CEC_{eff}) are entirely determined by base cations.

Apart from DAI 9 the pH of the paleosols does not consistently increase with depth as can be commonly expected for unburied soils of non-arid climate (Blum, 2007; Scheffer and Schachtschabel, 2002). In DAI 6 and DAI 11 low pH values in the middle section of the paleosols are related to maxima of SO_4^{2-}. This is caused by the oxidation of sulfur or sulfide to SO_4^{2-} due to an oscillating groundwater table mentioned earlier. This leads to a production of H_2SO_4 and to an acidification of the paleosol (Ahmad and Wilson, 1992; Nemeth et al., 1970). At DAI 6 this is supported by the presence of small amounts of exchangeable Al and the lowest base saturation coinciding with the maximum of SO_4^{2-}.

The uniform distribution of pH values in DAI 5 and DAI 13 can be a result of post-burial alterations. In buried A-horizons the addition of organic matter has stopped. Hence, a decreased production of H^+ as a result of reduced microbial activity and oxidation of organic matter leads to a rising pH value. Furthermore, unburied A-horizons are normally heavily leached. In contrast, buried A-horizons can now be subject to ion accumulations from the overlaying deposits (Holliday, 2004). Consequently, in buried soils the depth function of the pH value can change after burial.

Even after almost 2000 years of burial the Roman paleosols south of Pompeii show moderate (DAI 5, DAI 9) to high (DAI 6, DAI 11, DAI 13) soil organic matter contents in the uppermost soil horizons.

This corresponds with Inoue (2001) who analyzed TOC of buried volcanic ash soils from 23,000 to 88 yr BP and found that they virtually maintained their original organic carbon concentrations. Main reasons for a high stability of soil organic matter (SOM) in volcanic soils under buried conditions he stated as follows (Inoue, 2001):

(i) predominance in SOM of humic acid with the highest degree of humification,
(ii) formation of stable Al/Fe-humus complexes and
(iii) reduced soil microbial activity.

Another reason for a decreased mineralization rate of the organic matter of the Roman paleosols south of Pompeii may be air exclusion due to the post-burial rise of the groundwater table. This may apply for DAI 5, DAI 6 and DAI 11. However, all five Roman paleosols were well drained at the time of sampling and no Fe and Mn ions were detected, indicating oxidizing conditions at least during the dry summer season.

DAI 11 and DAI 13 show the highest amounts of TOC. This corresponds to their paleo-topographic position, most distant from the paleo-floodplain, assuming longer time for pedogenesis and humus accumulation. DAI 5, DAI 9 and DAI 13 show a second maximum of TOC in the substratum. This results from the fact that the Roman paleosols of DAI 5, DAI 9 and DAI 13 developed on top of fluvial-palustrine deposits that are rich in organic carbon. The C/N ratio of the paleosol's upper soil ranges from 20 (DAI 5) to 29 (DAI 13). This confirms that microbial activity to decompose SOM is reduced. Furthermore, high C/N ratios are common in waterlogged situations, e.g. due to a high groundwater table. The highest

C/N ratio of 45 in the substratum of DAI 13 is also related to the subjacent humus-rich fluvial-palustrine deposits. If this layer contains undecomposed organic matter the C/N ratio of 45 can be explained.

In accordance with their volcanic nature and pyroclastic parent material the Roman paleosols should contain short-range-order minerals and/or organo-metallic complexes. Minerals like allophane, imogolite or ferrihydrite derive from rapid weathering of volcanic ejecta or glasses such as ash, tuff or pumice (Shoji et al., 1993, 1996). However, the amounts of acid oxalate-extractable Al, Fe and Si (Al_{ox}, Fe_{ox}, and Si_{ox}) are relatively low (Table 3). They are mainly increased in the upper soil showing high amounts of TOC, which suggests the presence of organo-metallic complexes. The Roman paleosols do not meet the established WRB criterion for andic properties of 2% or more $Al_{ox} + 0.5Fe_{ox}$. Instead it ranges between 0.4 and 1.1%, which rather refers to vitric properties (Shoji et al., 1993, 1996). Along with low amounts of ferrihydrite and Si_{ox} as a measure of the allophane content, this confirms the low weathering rate and relatively young age of the pre-AD 79 Roman paleosols south of Pompeii mentioned earlier. DAI 11 shows the highest amounts of Si_{ox} which may refer to a higher weathering rate most distant from the paleo-Sarno River.

The amounts of total inorganic carbon (TIC) in the Roman paleosols are generally low (Blum, 2007), even though the Apennine Mountain chain surrounding the Sarno River plain consists of carbonatic parent material. Moreover, in DAI 9 and DAI 13 pieces of travertine or mortar were present within the Roman paleosol. Compared to other Italian volcanic soils of a similar pH, the amount of exchangeable Ca^{2+} and its saturation is also relatively low, albeit dominating the cation exchange complex of the paleosols (see Buurman et al., 2007; Lulli, 2007). The depth functions of TIC and Ca^{2+} seem to be at least partly correlated, which indicates that both derive from $CaCO_3$. In soils with a pH between 6.5 and 8 the relationship between Ca^{2+} and carbonates (TIC) results from carbonate buffer reactions. Thereby, $CaCO_3$ is transformed into soluble $Ca(HCO_3)_2$ whereas HCO_3^- is washed out of the soil resulting in decreasing amounts of TIC (Blum, 2007; Scheffer and Schachtschabel, 2002). The amount of exchangeable K^+ and its saturation is comparably high (Lulli, 2007). Potassium predominantly derives from weathering of leucite-bearing potassic volcanic material of Somma-Vesuvius being part of the so-called 'Roman Comagmatic Region' (Cortini and Hermes, 1981; D'Addezio et al., 2005; Lulli, 2007; Turi and Taylor, 1976).

Volcanic soils belong to the most fertile soils, however, in comparison to other Italian volcanic soils the CEC_{eff} of the Roman paleosols is not considerably high (see Buurman et al., 2007; Lulli, 2007). This may be the results from the relative young age of the paleosols mentioned earlier. Furthermore, it cannot be excluded that CEC_{eff} of the Roman paleosols has changed due to the influence of post-burial groundwater dynamics. Since in general the CEC_{eff} is high in humus-rich horizons and in fine-grained substrate, within the Roman paleosols CEC_{eff} is positively correlated to TOC and highest in the silt loam of DAI 13.

Phosphates (P) are present in all organic materials such as plant tissue, excrements and bones. As they are released by organic decomposition processes, they mostly form immobile and insoluble chemical compounds with Ca, Fe and Al and thus become fixed within the soil's mineral fraction for very long periods of time. Furthermore, anthropogenic activity through organic inputs leads to an accumulation of phosphate in the soil, which can be detected even after 10^2–10^3 years (Crowther, 1997; Davidson and Wilson, 2006; Terry et al., 2000).

In accordance with elevated amounts of TOC, the paleosols of DAI 11 and DAI 13 have also increased amounts of P. Furthermore, the highest *P* value in DAI 13 may additionally result from the finer soil texture of the fine earth fraction. In all five paleosols, P is correlated with TOC suggesting a predominance of organic P. However, a second P maximum in the subsoil of DAI 13, coinciding with a minimum of TOC, show that a small portion of P must also be present in the mineral phase, e.g. as inorganic or sorbed P. At neutral pH and high calcium activity Ca^{2+} and P anions form insoluble inorganic Ca-phosphate.

Furthermore, in volcanic soils most important sorbents of P are allophane and ferrihydrite showing a high phosphate retention capacity (Fox and Xue-Yuan, 1986; Martínez-Cortizas et al., 2007; Parfitt, 1978). Even though the amounts of Si_{ox} and ferrihydrite are low a correlation with P can be identified.

Increased amounts of P in combination with TOC and CEC_{eff} in the top of the Roman paleosol is a measure of soil fertility (Davidson and Wilson, 2006). Hence, DAI 11 and DAI 13 can be considered more fertile than the other paleosols. This may result from a longer time of humus accumulation and pedogenesis as a function of the paleo-topographic position mentioned earlier.

Apart from soil fertility another important soil parameter for agricultural use is the effective soil depth or the vertical rooting space for plants. Especially DAI 5 and DAI 6 are only 30 cm thick, which per sé could limit root growth considerably. However, it can also be assumed that the original soil thickness of the Roman paleosols was somewhat higher as they may have been subject to consolidation due to the superimposed load of volcanic deposits since AD 79. Furthermore, since the strata below the Roman paleosols also consist of very loose and permeable material the plant's ability to propagate roots through the soil is not impeded. South of Pompeii the effective soil depth must have only been limited by a high groundwater table due to the vicinity of the paleo-Sarno River.

6. Conclusions and outlook

Ten stratigraphical core drillings were conducted and five Roman paleosols were analysed for soil physical and chemical parameters to carry out a characterization of the paleo-pedological and paleo-topographical situation south of Pompeii.

Following our hypotheses that the eruption AD 79 caused a good soil preservation environment our analyses have shown that many of the original features of the Roman paleosols may have been preserved. Among these features are soil horizons, texture, phosphate concentration, elemental composition or the depth functions of TOC and N.

Comparing the soil parameter values of the Roman paleosols with its paleo-topographic position a specific correlation was revealed. The spatial distribution of paleosol characteristics is a function of soil development due to the elevation and distance from the paleo-Sarno River and its floodplain. This relationship is most evident for soil thickness, soil horizonation, total organic carbon, phosphates and to some extent for soil texture and Si_{ox} as a measure of the allophane content. In the south of the N–S transect redoximorphology occurs in the AD 79 white pumice layer coinciding with high amounts of sulfate in the underlying pre-AD 79 Roman paleosols. This is probably caused by the influence of a seasonally fluctuating groundwater table subsequent to the eruption of AD 79.

Some soil properties may have been well preserved after burial especially due to particular characteristics of volcanic soils. However, other soil properties of the Roman paleosols do not necessarily reflect the ancient conditions because diagenetic alterations may have occurred after burial. In a next project phase this potential post-burial soil developments will be analysed. Hence, we will apply soil liquid and soil solid phase studies within the modern soil and the Roman paleosol of Pompeii in natural undisturbed stratification.

References

Ahmad, N., Wilson, H.W., 1992. Acid sulfate soils of the Caribbean region — their occurrence, reclamation, and use. Soil Science 153 (2), 154–164.

Andronico, D., Cioni, R., 2002. Contrasting styles of Mount Vesuvius activity in the period between Avellino and Pompeii Plinian eruptions, and some implications for assessment of future hazards. Bulletin of Volcanology 64, 372–391.

Arnalds, O., Kimble, J., 2001. Andisols of deserts in Iceland. Soil Science Society of America Journal 65, 1778–1786.

Blakemore, L.C., Searle, P.L., Daly, B.K., 1981. Soil Bureau analytical methods. A method for chemical analysis of soils. N.Z. Soil Bur. Sci. Report 10A. DSIRO.

Blum, W.E.H., 2007. Bodenkunde in Stichworten. Stuttgart 179.

Burggraf, D.R., White, H.J., Frank, H.J., Vondro, C.F., 1981. Hominid habitats in the Rift Valley, part 2. In: Rapp, G., Vondra, C.F. (Eds.), Hominid Sites. : Their Geologic Settings. Westview Press, Boulder, pp. 115–147.

Buurman, P., Bartoli, F., Basile, A., Füleky, G., Garcia Rodeja, E., Hernandez Moreno, J., Madeira, M., 2007. The physico-chemical data base. In: Arnalf, Ó., Bartoli, F., Buurman, P., Óskarson, H., Stoops, G., García-Rodeja, E. (Eds.), Soils of Volcanic Regions in Europe. Springer-Verlag, Berlin, Heidelberg.

Cinque, A., Irollo, G., 2004. Il "Volcano di Pompei": Nuovi dati geomorphologici e stratigrafici. Il Quaternario, Italian Journal of Quaternary Sciences 17 (1), 101–116.

Civetta, L., Di Vito, M.A., De Lucia, M., Isaia, R., 1998. Storia eruttiva del Somma-Vesuvio. In: Guzzo, P., Peroni, R. (Eds.), Archeologia e Vulcanologia in Campania, pp. 9–16. Naples.

Cortini, M., Hermes, O.D., 1981. Sr isotopic evidence for a multi-source origin of the potassic magmas in the Neapolitan Area, S. Italy. Contributions to Mineralogy and Petrology 77, 47–55.

Crowther, J., 1997. Soil phosphate surveys: critical approaches to sampling, analysis and interpretation. Archaeological Prospection 4, 93–102.

D'Addezio, G., Karner, D.B., Burrato, P., Insinga, D., Maschio, L., Ferranti, L., Renne, P.R., 2005. Faulted Middle Pleistozene Tephra Layer in the Val d'Agri Area, Southern Italy. Earth-prints Repository.

Davidson, D.A., Wilson, C.A., 2006. An Assessment of Potential Soil Indicators for the Preservation of Cultural Heritage. School of Biological and Environmental Science, University of Stirling.

DIN 38405 D5, 1985. German Standard Methods for the Examination of Water, Waste Water and Sludge, Anions (group D); Determination of Sulfate Ions (D5). Beuth-Verlag.

DIN 38414 S12, 1986. German Standard Methods for the Examination of Water, Waste Water and Sludge, Sludge and Sediments (group S); Determination of Phosphorus in Sludges and Sediments (S12). Beuth-Verlag.

DIN EN 13137, 2001. Characterization of Waste—Determination of Total Organic Carbon (TOC) in Waste, Sludges and Sediments. Beuth-Verlag.

DIN ISO 10390, 2005. Soil Quality—Determination of pH. Beuth-Verlag.

DIN ISO 11261, 1997. Soil Quality—Determination of Total Nitrogen — Modified Kjeldahl Method. Beuth-Verlag.

DIN ISO 11277, 2002. Soil Quality—Determination of Particle Size Distribution in Mineral Soil Material—Method by Sieving and Sedimentation. Beuth-Verlag.

FAO-ISRIC-IUSS, 2006. World Reference Base for Soil Resources. World Soil Resources Report 103. FAO-ISRIC-IUSS, Rome.

Foss, J.E., 1988. Paleosols of Pompeii and Oplontis. In: Curtis, R.L. (Ed.), Studia Pompeiana and Classica. Aristide D. Caratzas, Publisher, New Rochelle, N.Y.

Foss, J.E., Timpson, M.E., Ammons, J.T., Lee, S.Y., 2002. Paleosols of the Pompeii Area. In: Jashemski, W.F. (Ed.), The Natural History of Pompeii. Cambridge University Press, pp. 65–79.

Fox, R.L., Xue-Yuan, L., 1986. Proceedings of the International Symposium on Red Soils. Elsevier, Amsterdam.

French, C.A.I., 2003. Geoarchaeology in Action: Studies in Soil Micromorphology and Landscape Evolution. Routledge, London, New York, p. 291.

Gerrard, J., 1992. Soil Geomorphology: An Integration of Pedology and Geomorphology. Chapman and Hall, London.

Holliday, V.T., 2004. Soils in Archaeological Research. Oxford University Press. 448 pp.

Inoue, Y., 2001. Tephrochronological Studies on the Formation of Cumulative Andisols in Southern Kyushu, Japan. PhD Thesis. United Graduate School of Agricultural Science, Kagoshima University.

Lulli, L., 2007. Italian volcanic soils. In: Arnalf, Ó., Bartoli, F., Buurman, P., Óskarson, H., Stoops, G., García-Rodeja, E. (Eds.), Soils of Volcanic Regions in Europe. Springer-Verlag, Berlin, Heidelberg.

Luongo, G., Perrotta, A., Scarpati, C., 2003. Impact of the AD 79 explosive eruption on Pompeii, I. Relations amongst the depositional mechanisms of the pyroclastic products, the framework of the buildings and the associated destructive events. Journal of Volcanology and Geothermal Research 126, 201–223.

Madeira, M., Auxtero, E., Monteiro, F., García-Rodeja, E., Nóvoa-Munoz, J.C., 2007. Exchange complex properties of soils from a range of European volcanic areas. In: Arnalf, Ó., Bartoli, F., Buurman, P., Óskarson, H., Stoops, G., García-Rodeja, E. (Eds.), Soils of Volcanic Regions in Europe. Springer-Verlag, Berlin, Heidelberg.

Martínez-Cortizas, A., Nóvoa, J.C., Pontevedra, X., Taboada, T., García-Rodeja, E., Chesworth, W., 2007. Elemental composition of reference European volcanic soils. In: Arnalf, Ó., Bartoli, F., Buurman, P., Óskarson, H., Stoops, G., García-Rodeja, E. (Eds.), Soils of Volcanic Regions in Europe. Springer-Verlag, Berlin, Heidelberg.

Mizota, C., Van Reeuwijk, L.P., 1989. Clay Mineralogy and Chemistry of Soils Formed Under Volcanic Materials in Diverse Climatic Regions. Soil Monograph 2, ISRIC, Wageningen, The Netherlands, p. 185.

Nanzyo, M., 2002. Unique properties of volcanic ash soils. Glob. Environ. Res. 6 (2), 99–112.

Nemeth, K., Mengel, K., Grimme, H., 1970. The concentration of K, Ca and Mg in the saturation extract in relation to exchangeable K, Ca and Mg. Soil Science 109, 179–185.

Parfitt, R.L., 1978. Anionadsorption. Advances in Agronomy 30, 1–50.

Parfitt, R.L., 1990. Allophane in New Zealand — a review. Australian Journal of Soil Research 28, 343–360.

Parfitt, R.L., Childs, C.W., 1988. Estimation of forms of Fe and Al: a review and analysis of contrasting soils by dissolution and Moessbauer methods. Australian Journal of Soil Research 26, 121–144.

Pescatore, T., Senatore, M.R., Capretto, G., Lerro, G., Patricelli, G., 1999. Ricostruzione paleoambientale delle aree circostanti l'antica Città di Pompei, Campania, Italia) al Tempo dell'eruzione del Vesuvio del 79 d.C. Boll. Soc. Geol. It. 118, 243–254.

Retallack, G.J., 1998. Core concepts of paleopedology. Quaternary International 51 (52), 203–212.

Retallack, G.J., 2001. Soils of the Past: An Introduction to Paleopedology. Blackwell Science, p. 404.

Retallack, G.J., 2005. Palaeosols. Soil/Paleosols 203–208.

Robinson, M., 2008. La stratigrafia nello studio dell'archeologiche e protostorica a Pompei. In: Guzzo, P.G., Guidobaldi, M.P. (Eds.), Nuove ricerche archeologiche nell'area vesuviana scavi 2003–2006. Atti del Convegno Internazionale, Roma, pp. 125–136. 1–3 febbraio.

Rolandi, G., Maraffi, S., Petrosino, P., Lirer, L., 1993a. The Ottaviano eruption of Somma-Vesuvio, 8000 y B.P. a magmatic alternating fall and flow-forming eruption. Journal of Volcanology and Geothermal Research 58, 43–65.

Rolandi, G., Mastrolorenzo, G., Barrella, A.M., Borrelli, A., 1993b. The Avellino plinian eruption of Somma-Vesuvio, 3760 y B.P. the progressive evolution from magmatic to hydromagmatic style. Journal of Volcanology and Geothermal Research 58, 67–88.

Rolandi, G., Petrosino, P., McGeehin, J., 1998. The interplinian activity at Somma-Vesuvius in the last 3,500 years. Journal of Volcanology and Geothermal Research 82, 43–65.

Russo, M., Punzo, I., 2004. I minerali del Somma-Vesuvio. In: AMI (Ed.), Cremona, Italy, p. 320.

Scheffer, F., Schachtschabel, P., 2002. Lehrbuch der Bodenkunde. . Heidelberg.

Schuhmacher, B.A., 2002. Methods for the Determination of Total Organic Carbon in Soils and Sediments. Ecological Risk Assessment Support Center, U.S. Environmental Protection Agency, Washington, DC, p. 25.

Scudder, S.J., Foss, J.E., Collins, M.E., 1996. Soil science and archaeology. Advances in Agonomy 57, 1–76.

Seiler, F., 2008. Rekonstruktion der antiken Kulturlandschaften des Sarno-Beckens. Ein multidisziplinäres Kooperationsprojekt mit Partnern aus Naturwissenschaften und Altertumswissenschaften in Deutschland, Italien und England. In: Guzzo, P.G., Guidobaldi, M.P. (Eds.), Nuove ricerche archeologiche nell'area vesuviana (scavi 2003–2006). Convegno Internazionale, Roma, pp. 485–490. 1.–3. Februar.

Shoji, S., Takahashi, T., 2002. Environmental and agricultural significance of volcanic ash soils. Glob. Environ. Res. 6 (2), 113–135.

Shoji, S., Nanzyo, M., Dahlgren, R.A., 1993. Volcanic Ash Soils — Genesis, Properties and Utilization. Elsevier, Amsterdam–London–New York–Tokyo, p. 288.

Shoji, S., Nanzyo, M., Dahlgren, R.A., Quantin, P., 1996. Evaluation and proposed revision of criteria for Andosols in the World Reference Base for Soil Resources. Soil Science 161 (9), 604–615.

Sigurdsson, H., Carey, S., 2002. The eruption of Vesuvius in AD 79. In: Jashemski, W.F. (Ed.), The Natural History of Pompeii. Cambridge University Press, pp. 37–64.

Stefani, G., Di Maio, G., 2003. Considerazioni sulla linea di costa del 79 d.C. e sul porto dell'antica Pompei. Rivista di Studi Pompeiani XIV, pp. 142–195.

Stothers, R.B., Rampino, M.R., 1983. Volcanic eruptions in the Mediterranean before A.D. 630 from written and archaeological sources. Journal of Geophysical Research 88, 6357–6371.

Terry, R.E., Hardin, P.J., Houston, S.D., Jackson, M.W., Nelson, S.D., Carr, J., Parnell, J., 2000. Quantitative phosphorus measurement: a field test procedure for archaeological site analysis at Piedras Negras, Guatemala. Geoarchaeology: An International Journal 15, 151–166.

Tiessen, H., Moir, J.O., 1993. Total and organic carbon. In: Carter, M.E. (Ed.), Soil Sampling and Methods of Analysis. Lewis Publishers, Ann Arbor, MI, pp. 187–211.

Turi, B., Taylor Jr., H.P., 1976. Oxygen isotope studies of potassic volcanic rocks of the Roman Province, Central Italy. Contributions to Mineralogy and Petrology 55, 1–31.

Vogel, S., Märker, M., 2010. Reconstructing the Roman topography and environmental features of the Sarno River Plain (Italy) before the AD 79 eruption of Somma-Vesuvius. Geomorphology 115, 67–77.

Vogel, J.S., Cornell, W.C., Nelson, D.E., Southon, J.R., 1990. Vesuvius/Avellino, one possible source of seventeenth century BC climatic disturbances. Nature 344, 534–537.

Vogel, S., Märker, M., Seiler, F., 2011. Revised modeling of the post-AD 79 volcanic deposits of Somma-Vesuvius to reconstruct the pre-AD 79 topography of the Sarno River plain (Italy). Geologica Carpathica 1/2011.

Ward Perkins, J.B., 1984. Note di topografia e urbanistica. In: Zevi, F. (Ed.), a cura di Pompei 79, pp. 25–39. Napoli.

2.4   Analysis of post-burial soil developments of the pre-AD 79 Roman paleosol near Pompeii (Italy)

Sebastian Vogel[a,c],* and Michael Märker[a,b]

[a] Heidelberg Academy of Sciences and Humanities c/o University of Tübingen, Rümelinstraße 19-23, 72070 Tübingen, Germany

[b] Department of Vegetation, Soil, Environment and Agroforestry Sciences, University of Florence, P.zzale Cascine 16, 50144 Florence, Italy

[c] German Archaeological Institute, Germany. Podbielskiallee 69-71, 14195 Berlin, Germany

* Corresponding author. Tel: +49 (0)30 187 711 358, Fax: +49 (0)30 187 711 168
E-mail address: sv@dainst.de (S. Vogel)

Abstract

The explosive eruption of Somma-Vesuvius volcanic complex AD 79 almost completely buried the ancient landscape around Pompeii to some extent conserving the Roman paleosols of the Sarno River plain. To estimate post-burial soil developments of the pre-AD 79 Roman paleosol accociated with decomposition of soil organic matter or leaching of nutrients from the overlying strata detailed soil liquid and solid phase analysis were carried out. At Villa Regina (Boscoreale, Italy) an in situ soil moisture and soil water monitoring was conducted within the pre-AD 79 Roman paleosol in undisturbed stratification to analyse soil water flow from the volcanic deposits above. The results show that a soil water flow down to the Roman paleosol in a depth of 8 m takes place. The soil liquid phase of the Roman paleosol shows a distinct chemical composition of cations and anions to be transported through the soil profile. Soil water was extracted from the paleosol in a four months period between December 2008 and April 2009 when the soil moisture of the paleosol exceeded 24.5 %. This restricts the potential influence of post-burial soil development by nutrient transport to the rainy winter season.

To estimate the influence of the soil water flow on the mineral soil properties of the Roman paleosol the soil solid phase of the paleosol and the modern soil at the same topographic location were analyzed and compared. Taking the modern soil as a reference for an unburied volcanic soil distinct differences were revealed compared to the Roman paleosol. Thus, the following post-burial changes of the pre-AD 79 Roman paleosol were identified:

(i) Leaching of nutrients (Ca^{2+}, Mg^{2+}) from overlying deposits into the paleosol led to a higher pH value and effective cation exchange capacity.

(ii) After burial the accumulation of soil organic matter (SOM) stopped. Instead SOM began to gradually decompose resulting in low amounts of organic carbon and nitrogen in the paleosols.

(iii) Since additionally the buried A-horizons are recently subject to ion accumulations from the overlying strata former topsoil eluvial horizons gradually turn into subsoil illuvial horizons.

(iv) The bulk density of the paleosol is increased due to soil compaction as a result of the superimposed load of the overlying post-AD 79 deposits.

(v)   Lower amounts of ammonium-oxalate extractable Fe, Al and Si refer to a reduced weathering rate of the paleosols after burial.

Finally, a model of the present-day mean annual groundwater table of the Sarno River plain indicate that one has to distinguish the Sarno River plain into two different zones of potential post-burial soil developments: (i) the inner parts of the plain where after AD 79 the Roman paleosol has come under the influence of a rising mean groundwater table and (ii) the more elevated parts of the plain where the Roman paleosol is still part of the unsaturated vadose zone and more likely influenced vertically or laterally by infiltration water or hypodermic flow, respectively. Consequently, the mechanism of post-burial soil development being active in the Roman paleosol strongly depends on its paleo-topographic situation.

Introduction

Paleosols are geoarchives of a past soil formation since diverse mechanisms of burial can contribute to a preservation of original soil properties. Consequently, paleosols can be utilized for investigating the paleo-pedological and paleo-environmental conditions before burial. However, a critical use of paleosol characteristics in interpreting paleo-environments must be applied because pronounced diagenetic processes, i.e. post-burial soil developments, can take place, such as (Retallack, 1998, 2001; French, 2003):

(i)   decomposition of soil organic matter (SOM),

Within well drained terrestrial soils SOM is decomposed after burial by aerobic microorganisms. That can be detected by a change in the Munsell soil color towards brighter values (higher chroma). However, the general depth function of the SOM concentration of the paleosol stays mostly unaltered.

(ii)   leaching of nutrients from the overlying strata,

In highly permeable substrate seepage water can lead to a dislocation of bases from the upper layers into the paleosol.

(iii)   soil compaction after burial,

The superimposed load of the overlying deposits can cause soil compaction and a reduction of pore space.

Due to the probability of post-burial soil developments detailed field descriptions and laboratory analyses are necessary to understand both past and present pedogenetic processes that lead to the present-day appearance and properties of a paleosol (Scudder et al., 1996). Combined soil solid and liquid phase studies are powerful tools to study post-burial soil developments. If the analysis of the soil solid phase provides good information about the factors and processes that influence a soil since the beginning of pedogenesis, soil liquid phase chemistry helps to understand active pedogenic processes.

The soil liquid phase represents the major phase for soil chemical reactions that interacts and communicates with the entire stratigraphy. (Litaor, 1988; Campbell et al.,1989; Bierman et al., 1995; Cecchini et al., 2002; Derome, 2002; Ugolini and Dahlgren, 2002; Porebska, 2004). It can be categorized into: (i) pellicular (adsorbed) water, (ii) capillary (porous) water and (iii) gravitational water (Snakin et al., 2001). Gravitational water particularly represents the mobile fraction of soil water percolating through the soil profile either vertically by infiltration or laterally by hypodermic flow (interflow). Consequently, measuring the chemical composition of the gravitational water most notably reflects the active redistribution and mobility of substances within the soil profile by vertical or lateral transport processes (Wolt, 1994; Snakin et al., 2001; Scheffer and Schachtschabel, 2010). Hence, the analysis of the soil liquid phase within a buried paleosol enables the identification of those processes that are recently active and are likely to influence the paleosols solid phase properties after burial. Finally, by combining soil liquid and solid phase studies an estimate about post-burial soil developments can be made.

The explosive eruption of Somma-Vesuvius AD 79 almost completely buried the ancient landscape of the Sarno River plain to some extent conserving the Roman paleosols. Foss (1988) and Foss et al. (2002) investigated the pre-AD 79 Roman paleosol in the Pompeii area and stated that they showed little disturbance or destruction. The paleosols were very similar to the modern soils suggesting a similar environment for soil development before and after AD 79. Regarding the geological material the paleosols developed in pumice and ash analog to the present-day soils in Pompeii and Oplontis (Foss, 1988). However, the Roman paleosols had a higher pH and a higher nutrient content, i.e. the modern soils were moderately to slightly

acid whereas the paleosols were alkaline throughout the profile (Foss, 1988). Thus, Foss (1988) and Foss et al. (2002) presumed this to be the result of bases (Ca^{2+}, Mg^{2+}) leaching from the overlying volcanic sediments and recharging the surface horizons of the paleosols.

The objective of this study is to analyse post-burial soil developments of the pre-AD 79 Roman paleosol near Pompeii such as decomposition of soil organic matter or leaching of nutrients from the overlying strata. Consequently, detailed soil liquid and solid phase analyses of the Roman paleosol and the modern soil near Pompeii were carried out. Special attention is given to verify Foss' hypothesis of nutrient transport by soil water flow from the overlying volcanic deposits into the Roman paleosol.

Research area

The soil liquid and solid phase analyses were carried out at and around the archaeological excavation of Villa Regina (Boscoreale). This Roman farm (villa rustica) is situated in the Sarno River plain (Campania, Italy) southwest of Somma-Vesuvius volcanic complex and around 1.3 km northwest of ancient Pompeii. During the explosive eruption of Somma-Vesuvius AD 79 the Villa Regina was buried by pumice lapilli fallout and pyroclastic flow/surge deposits of approximately 2.5 m. This is overlain by volcanoclastics from later eruptions and, during phases of volcanic quiescence, intercalated fluvial deposits or soil material. This results in a total thickness of post-AD 79 deposits of around 8 m lying on top of the pre-AD 79 paleo-surface. The villa was excavated 1978-1980 (De Caro, 1994). The elevation of the Roman paleo-surface at that location is approximately 16 m a.s.l.. Topographically, the Villa Regina is situated in a longitudinal depression between the western slope of the Pompeiian hill in the east and the southern slope of Somma-Vesuvius in the northwest. Consequently, the discharge of this area is converging. This is stressed by recurring fluvial deposits that are evident in the post-AD 79 stratigraphy of Villa Regina as well as the paleo-channel network and the topographic wetness index deduced from the pre-AD 79 digital elevation model of the Sarno River plain (Vogel and Märker, 2010; Vogel et al., 2011) (Fig. 1). Thus, topographically the probability for soil water flow to take place down to the Roman paleosol in a depth of 8 m is relatively high at the location of Villa Regina.

The climate of the study area is Mediterranean with almost 70 % of the annual precipitation falling between October and March and a pronounced dry summer season. On a longterm average the mean annual precipitation is 865 mm whereas November is the wettest month with 129 mm and July is dryest with 16 mm. The mean annual temperature is 17.4 °C. The hottest month is August with a mean temperature of 25.7 °C whereas January is coolest with 9.6 °C (Osservatorio Meteorologico, Università di Napoli Federico II, from 1870 to today).

According to groundwater data of the Autorità di Bacino del Sarno the Roman layer of the Boscoreale area is not influenced by a high groundwater table. Thus, the Roman paleosol is part of the unsaturated vadose zone and soil water within the soil profile rather derives vertically from infiltration water or laterally from hypodermic flow.

Figure 1. Paleo-topographic location of the Villa Regina with surrounding soil sampling sites (A) and topographic wetness index deduced from the pre-AD 79 digital elevation model of Vogel et al. (2011) (B).
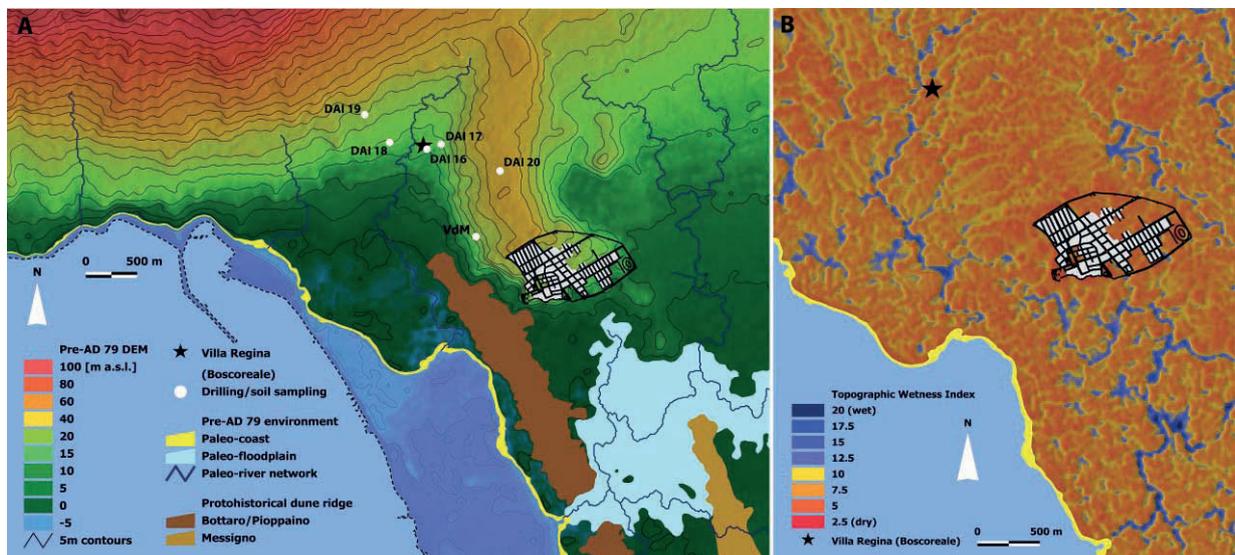
Methodology

To meet the objectives of this study, i.e. the assessment of post-burial soil developments of the pre-AD 79 Roman paleosol near Pompeii, we subdevided the analysis methodologically into the following three parts: (i) soil liquid phase analysis, (ii) soil solid phase analysis and (iii) groundwater table.

Soil liquid phase analysis

A soil hydrological monitoring system was installed within the paleosol in natural stratification to determine if the pre-AD 79 Roman paleosol is subject to soil water flow from the overlying volcanic deposits either vertically by percolation or laterally by hypodermic flow. Soil moisture and soil liquid phase was studied in situ by means of frequency domain reflectometry (FDR) and tension lysimeters (suction cups), respectively. Tension lysimeters were used since this methodology predominantly samples the mobile fraction of soil water that moves through inter-aggregate pores or preferential flow channels and thus reflects the chemical transport within the soil (Wolt, 1994). Due to the depth of the Roman paleosol of about 8 m a vertical installation from the present-day surface was not feasible. Consequently, the installation was implemented laterally inside the natural undisturbed stratification of the side walls of the archaeological excavation of Villa Regina, (Fig. 2).

Figure 2. Schematic view of the experimental setup using suction cups and soil moisture sensors (SM200) (A). The study site is situated at the northern edge of the archaeological excavation of Villa Regina (Boscoreale) (B). A roof was build to protect the installation from precipitation water entering the excavation (C).
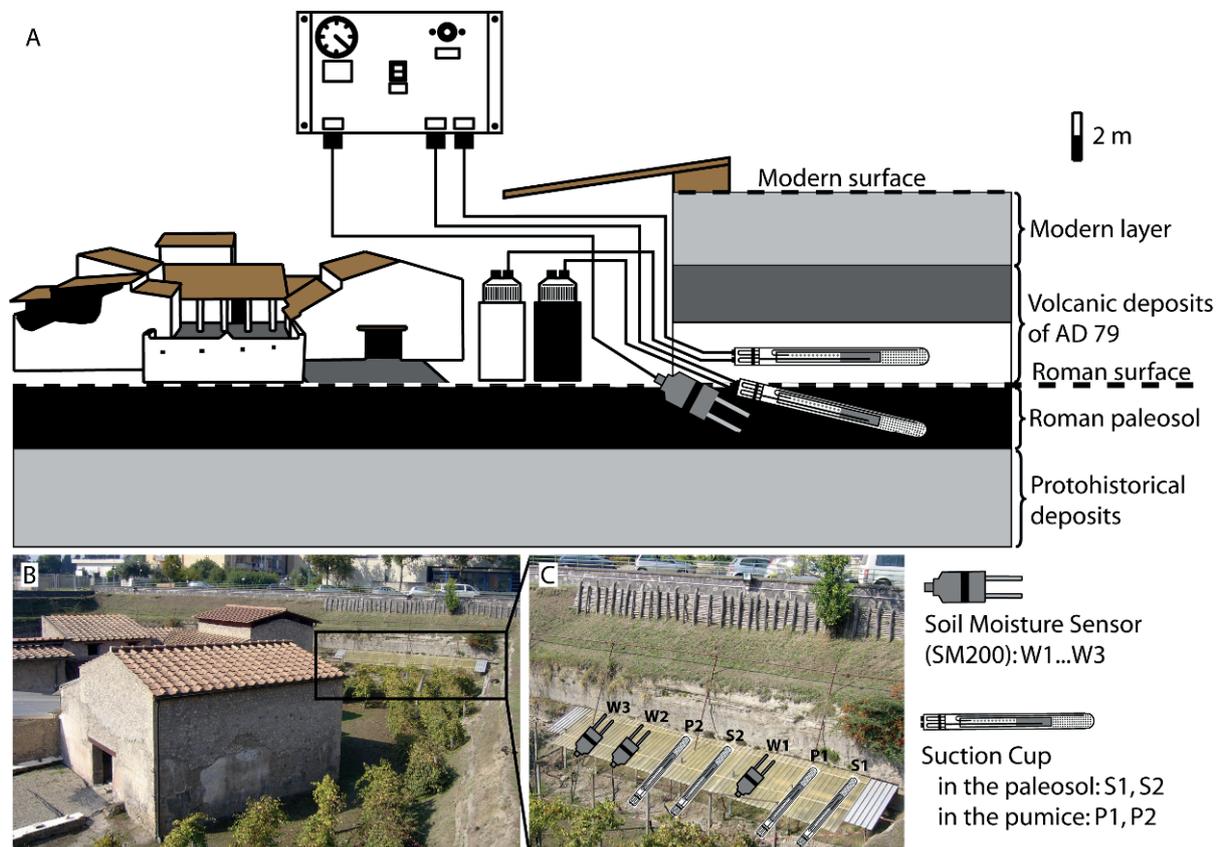
Altogether four sampling systems were installed, two within the lower section of the white pumice layer representing the first phase of the AD 79 eruption of Somma-Vesuvius and two within the Roman paleosol underneath. In the white pumice layer soil water will be sampled that moves either vertically by infiltration from the present-day surface down to the Roman paleosol or laterally by interflow upon the Roman paleo-surface. The soil liquid phase sampled in the Roman paleosol represents the soil water that has entered the paleosol, interacts with the mineral soil constituents and potentially influences the paleosol's solid phase properties.

The composition of the soil liquid phase may not directly refer to specific chemical processes active in the Roman paleosol. Nevertheless, the net effect of recent transport of nutrients into the Roman paleosol, is manifested in the concentration of substances in the soil water extract (Wolt, 1994). Consequently, the primary objective of the given sampling design is to determine if a soil water flow to the Roman paleosol occurs. Moveover, we provide data of the general trends in the soil liquid phase chemistry, i.e. the occurrence of certain ions in the lysimeter solution at the point of sampling (Grossmann and Moss, 1994; de Vries and Leeters, 1994; Wolt, 1994; Manderscheid and Matzner, 1995).

Due to the depth of the Roman paleosol of around 8 m below the present-day surface and the absence of interactions with present-day plant roots the composition of the soil liquid phase within the Roman paleosol is expected to be less heterogeneous compared to the rooting zone of the modern soil. This may also be favoured by the relative homogeneity of the AD 79 white pumice layer overlying the Roman paleosol. Consequently, even four sampling systems are expected to yield qualitative data on the soil liquid phase chemistry of the sampling area.

To install the suction cups holes were drilled laterally into the white pumice layer and the Roman paleosol. In the paleosol the suction cups were installed in a slurry of the paleosol material that was extracted during the drilling. This ensures an optimal contact between the instrument and the surrounding soil and a minimum of disturbance. After the installation the drilling hole was backfilled to prevent external water from seeping down the hole to the suction cup. In the white pumice layer a silica slurry of fine sand was used, having a low adsorption capacity. Thus, the influence of the slurry material on the soil liquid phase was minimized.

To extract the soil liquid phase a transient tension (vacuum) of 550 mbar (pF 2.7) was established biweekly to the suction cups by evacuation with an external pump. Due to a slight decrease of tension during the two weeks between the evacuations an applied tension of 550 mbar enables the sampling of the soil liquid phase at or below field capacity. Even though the gradient generated by the suction cups will not exclusively act on macropores but to some extent also on smaller pores (Grossmann and Udluft, 1991) the applied tension predominantly samples the mobile soil water fraction. The approximate pore diameter that is drained at a certain soil water potential can be calculated by means of the law of capillary rise or the Young-Laplace equation:

$$r = \frac{2\gamma \cos\alpha}{hpg},$$

where r is the radius of the capillary tube, γ the surface tension of water, α the contact angle, h the water potential, p the density of water and g the gravitational acceleration (Scheffer & Schachtschabel, 2010). Hence, applying a tension of 550 mbar and assuming complete wettability (α =0) of the substrate the suction cups extract water from soil pores from a minimum diameter of 5.4 µm which corresponds to intermediate and large sized pores.

Through the introduction of oxygen into the soil during the installation of the suction cups the biological activity of the paleosol may have been stimulated causing a mobilization of nutrients. This can influence the composition of the soil liquid phase directly after installation (Grossmann, 1988). That is why, the obtained lysimeter solution was rejected for the first weeks after installation. The suction cups were installed 1.5 m inside the stratigraphy to prevent the suction cups from being influenced by water entering the soil profile from the open excavation side of Villa Regina. Furthermore, the installation was carried out on the upslope part of the excavation assuring that rain water directly entering the excavation is flowing away from the installation. Additionally, the entire installation was canopied over its whole length (Fig. 2).

Due to high air temperatures especially during the summer season we used suction cups that collect the solution in their interior. That has the advantage that the extracted water stays cool and protected from sunlight until the sampling takes

place, minimising chemical transformations within the lysimeter solution. Due to its specific adsorption characteristics the filter material of the suction cup may have a pronounced influence on the composition of the sample. Consequently, the investigation of a certain analyte requires a particular filter material. As this study focusses on dissolved inorganic substances we used polyamide filters (Litaor, 1988; Grossmann, 1988; DVWK, 1990; Haberhauer, 1997; Spangenberg et al., 1997; Tischner et al., 1998).

The composition of the soil liquid phase was monitored over a period of 20 months to cover the variability throughout the year. The autumn and winter period is studied twice. This period is believed to be most relevant because the precipitation maximum and a relatively low evapotranspiration between October and March is likely to cause soil water flow down to the Roman paleosol. The soil liquid phase in the suction cups was controlled biweekly, sampled, transported to the laboratory and immediately analysed for pH. Within 24 h of sample collection the soil water extract was analysed for major cations (Ca^{2+}, Mg^{2+}, K^+, Na^+) and anions (SO_4^{2-}, HPO_4^{2-}, NO_3^-, Cl^-) because of their importance with respect to soil fertility and nutrient conditions. Furthermore, we analysed Al^{3+} because of its relevance in terms of the acidity status and plant physiology (Al-toxicity) (Hendershot and Courchesne, 1991; Wolt, 1994; Fillion et al., 1999; Derome, 2002; Roman et al., 2002; Strahm et al., 2005).

Since the composition and amount of the soil liquid phase sampled by the tension lysimeters varies with soil water content, additionally, three soil moisture sensors (SM200) where installed within the Roman paleosol measuring the volumetric water content (Θ) every six hours. The SM200 soil moisture sensor is a frequency domain reflectometer (FDR) measuring Θ indirectly by determining the permittivity of the soil (Delta-T Devices Ltd, 2006).

The soil liquid phase of the vadose zone strongly depends on water deriving from precipitation. To get a rough estimate of how the precipitation regime interacts with the soil moisture of the Roman paleosol and its soil water chemistry throughout the year, meteorological data were collected from the Campania Region. It may not be possible to relate a single precipitation event to the soil water sampled in the Roman paleosol at a depth of 8 m. Nevertheless, especially the time between the first precipitations in autumn and the first response in the soil moisture and the first soil

water sampling will be of particular interest. Moreover, the first soil water flow after the dry summer season is expected to have a strong influence on the composition of the soil liquid phase in terms of higher element concentrations that are leaching into the Roman paleosol.

Soil solid phase analysis

To estimate post-burial soil developments of the pre-AD 79 Roman paleosol the soil solid phase of both the Roman paleosol and the modern soil were sampled at the same topographic location, analyzed for their physical and chemical soil properties and compared. Thereby, the modern soil was taken as a reference for an unburied volcanic soil. Foss (1988) stated that the environment for soil development before and after AD 79 was similar since the paleosols as well as the modern soils around Pompeii showed similar soil properties. Regarding the geological material the paleosol developed from pumice and ash analog to the present-day soil (Foss, 1988). The volcanic material of Somma-Vesuvius is characterized by a silica-undersaturated, potassium-rich composition abundantly containing leucite ($KAlSi_2O_6$) and K-feldspar ($KAlSi_3O_8$) (Piochi et al., 2006). The particular chemical composition of volcanic deposits may vary throughout the different eruptions of Somma-Vesuvius. However, for the comparison between the modern soil and the pre-AD 79 paleosol we hypothesize a similar chemism of the soil substrate regarding the analyzed soil solid phase properties. Consequently, considering the results of the soil liquid phase study and the approximate soil age major differences between the modern soil and the paleosol were utilized to estimate post-burial changes. We hypothesize that post-burial soil changes in the pre-AD 79 Roman paleosol are above all associated with nutrient transport from the overlying strata or decomposition of soil organic matter. Consequently, at the comparison special attention was given to the pH value, carbonate content, cation exchange capacity and soil organic matter (SOM) content of the soils. In general the topsoil is characterized by high SOM content and nutrient turnover rates as well as of major soil chemical reactions due to plant roots and microorganisms. Hence, the topsoils were considered for the comparison between the modern soil and the pre-AD 79 Roman paleosol.

Five mechanical stratigraphical core drillings were carried out around Villa Regina along a NW-SE transect crossing the longitudinal depression between the Pompeiian hill and Somma-Vesuvius. The drillings DAI 18 and DAI 19 are situated in the northwest at the footslope of Somma-Vesuvius whereas DAI 16 and DAI 17 are located at the footslope of the Pompeiian hill. DAI 20 is situated on top of the Pompeiian hill in the southeast. Additional soil samples were taken further south towards Pompeii at the Villa dei Misteri (VdM) at the southwestern slope of the Pompeiian hill (Fig. 1).

After the stratigraphical core drillings were conducted the modern soil and the pre-AD 79 Roman paleosol were identified and described in the field. In four stratigraphies a modern soil and a pre-AD 79 paleosol could be found (DAI 16, DAI 18, DAI 20 and VdM). The soil solid phase was sampled on a regular basis of every 10 cm and the following soil physical and chemical parameters were analysed in the laboratory:

(i)   soil pH measured in 1 M $CaCl_2$ (DIN ISO 10390),

(ii)   soil texture of the fine earth fraction by wet sieving and sedimentation following Stokes' law (1845) after dispersing the sample with 0.2 N Na-pyrophosphate (DIN ISO 11277). Due to the presence of amorphous aluminium silicates in volcanic soils and the arising difficulties to disperse the sample the particle size was only used in classes and on a relative scale (Mizota and Van Reeuwijk, 1989),

(iii) total organic carbon (TOC) and total inorganic carbon (TIC) by elementary analysis using the dry combustion reference method (DIN EN 13137),

(iv)   total nitrogen using the modified method of Kjeldahl (DIN ISO 11261),

(v)   effective cation exchange capacity (CEC_{eff}) and the amount of exchangeable base cations by sequential extraction with unbuffered ammonium chloride,

(vi)   ammonium-oxalate extractable Fe, Al and Si by flame atomic absorption spectrometry (AAS) and inductively coupled plasma atomic emission spectrometry (ICP-AES).

Groundwater table

Subsequent to the eruption of Somma-Vesuvius AD 79 there was a relative rise of the groundwater table in the Sarno River plain. Consequently, in many parts of the inner plain, although terrestrial before AD 79, the Roman paleosol has come under the influence of groundwater which may also have considerably effected the soil properties. The effect of this phenomenon is not focus of the present study. However, the approximate area of the Sarno River plain where the Roman paleosol is either part of the unsaturated vadose zone or recently influenced by groundwater was determined. Hence, the depth of the mean annual groundwater table was modeled from more than 5,600 groundwater observation points provided by the Autorità di Bacino del Sarno. Thereafter, the groundwater table was subtracted from the pre-AD 79 digital elevation model (DEM) of the Sarno River plain (Vogel and Märker, 2010; Vogel et al., 2011) to determine the area where the present-day groundwater table lies above the pre-AD 79 Roman surface and influences the Roman paleosol.

Vogel and Märker (2010) and Vogel et al. (2011) delineated the floodplain and wetlands related to the pre-AD 79 paleo-Sarno River by means of fluvial/palustrine deposits from stratigraphical core drillings. In general, wetlands can be characterized by a water table that stands at or near the terrain surface for a sufficient period of the year to allow the development of palustrine deposits (Brinson, 1993). Consequently, the reconstructed paleo-floodplain can be considered as the area where, before AD 79, the mean groundwater table was at or near the Roman surface (Fig. 3). To calculate the approximate rise of the groundwater table since AD 79 the mean 'vertical distance to channel network' index (SAGA terrain analysis module) was deduced from the pre-AD 79 DEM for the two groundwater levels standing at the Roman surface, i.e. today and before AD 79.

Results and discussion

Groundwater table

The subtraction of the modeled present-day mean annual groundwater table (Autorità di Bacino del Sarno) from the pre-AD 79 DEM (Vogel and Märker, 2010) reveals that a large area of the inner Sarno River plain is effected by a groundwater table lying at or above the pre-AD 79 paleo-surface (Fig. 3). Altogether this comprises

an area of around 75 km² or around 37 % of the entire Sarno River plain. Hence, there must have been a considerable rise of the groundwater table after the AD 79 eruption of Somma-Vesuvius.

The relative change of the groundwater table since AD 79 was calculated using the mean 'vertical distance to channel network' index of the groundwater level standing at the Roman surface today and before AD 79. By comparing the two values a rise of the mean annual groundwater level of the Sarno River plain since AD 79 by approximately 1.8 m was revealed. Considering this groundwater rise since AD 79 the Sarno River plain can be divided into two different zones of potential post-burial soil developments: (i) the lower areas of the inner Sarno River plain where after AD 79 the Roman paleosol has come under the influence of a rising mean groundwater table and (ii) the more elevated areas of the Sarno River plain where the Roman paleosol is still part of the unsaturated vadose zone and more likely influenced by vertical or lateral soil water flow. This demonstrates that the mechanism of post-burial soil developments being active in the Roman paleosol is by no means uniform for the entire Sarno River plain but strongly depends on paleo-topography and paleo-landscape position.

Figure 3. Model of the present-day mean annual groundwater table above the pre-AD 79 paleo-surface. The 0m-isoline incorporates the area where the groundwater table is at the pre-AD 79 paleo-surface (blue colors). Accordingly, the contour line of the pre-AD 79 flood plain approximately describes the 0 m-isoline before AD 79.
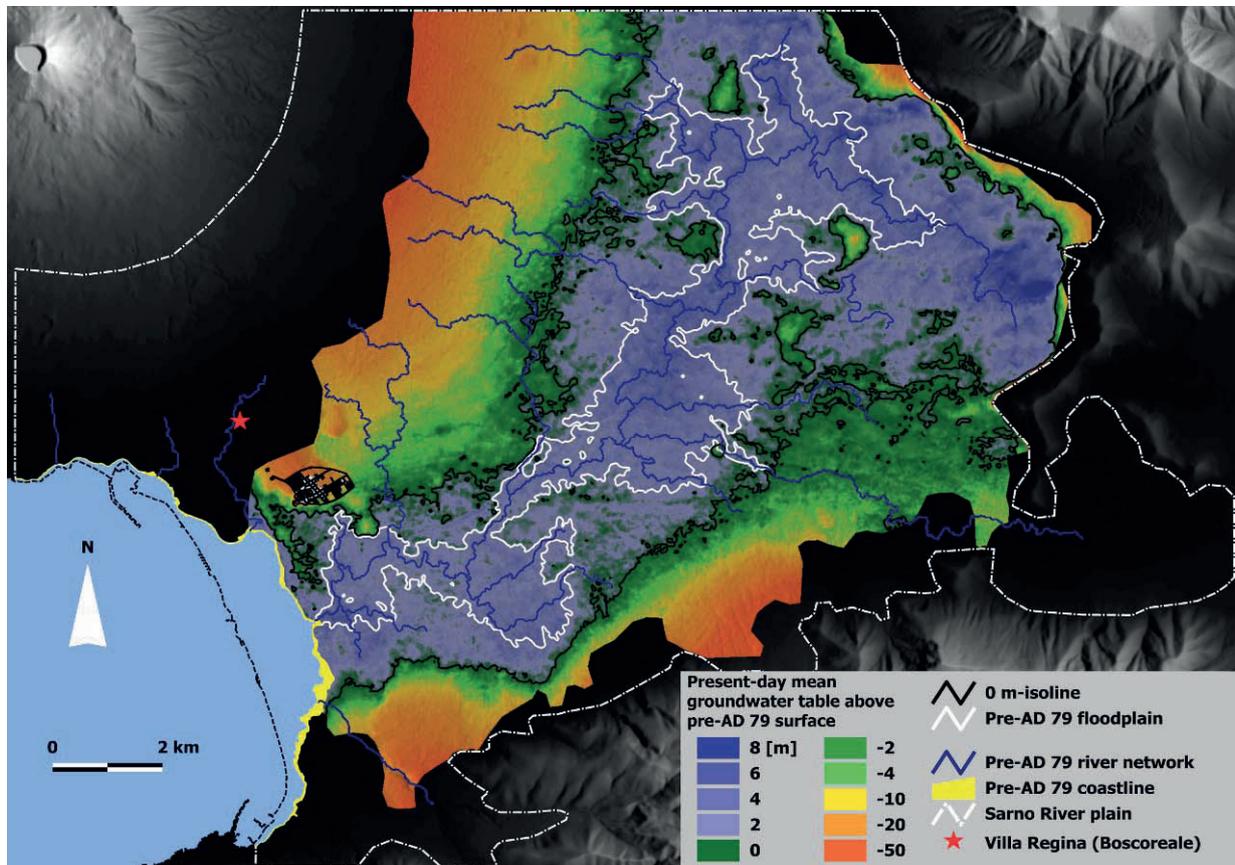
Soil liquid phase analysis

Fig. 4 shows the soil moisture (Θ) of the Roman paleosol at Villa Regina and the precipitation regime for the study period 2008/2009. At the beginning of the study period in October 2008 the Roman paleosol was still dry from the preceding summer season. This is supported by a constant and low initial Θ of around 22 %. First single rainfall events started in September 2008 whereas the main rainy season with more regular precipitation began in early November 2008. However, it took until the beginning of December for a first response of Θ in the Roman paleosol. Thus, the infiltration water needed approximately 30 days to percolate from the present-day surface to the Roman paleosol in a depth of 8 m. That delay results from the fact that overlying volcanic ash layers, pumice and volcanic soils have a large water retention capacity (Shoji and Takahashi, 2002; Sahin et al., 2005). Moreover, in unsaturated layered soil profiles soil water movement is not necessarily strictly vertical but

considerably influenced by the stratification effect. Especially less permeable fine grained layers, like ash layers interbedded in highly permeable pumice layers tend to induce unsteady flow patterns. Water is held in the fine material and does not percolate further down into coarser material until the former layer is saturated. When the water potential of the two strata reach the same value the water movement is again controlled by the gravitational potential (Fiorillo and Wilson, 2004; Javaux and Vanclooster, 2004).

The phase of rewetting of the Roman paleosol after the dry summer season lasts from early December until February 2009 when Θ continuously increases to its maximum of 25.8 %. The main rainy season ended mid February with more sporadic rainfall events until the end of April. From mid March and again with a delayed response of around 30 days Θ started to decrease, at first rather slightly still remaining above 25 % and more explicitly from the end of April. Then Θ decreases to its minimum of 13.6 % in the end of September. The soil moisture data reveal that the Roman paleosol at Villa Regina was at no time of the year water saturated.

Figure 4. Soil moisture (Θ) of the Roman paleosol at Villa Regina (Boscoreale) and precipitation chart of Napoli-Osservatorio Meteo D.G.V. for the study period 2008/2009. The grey section indicates the period soil water could be extracted from the Roman paleosol.
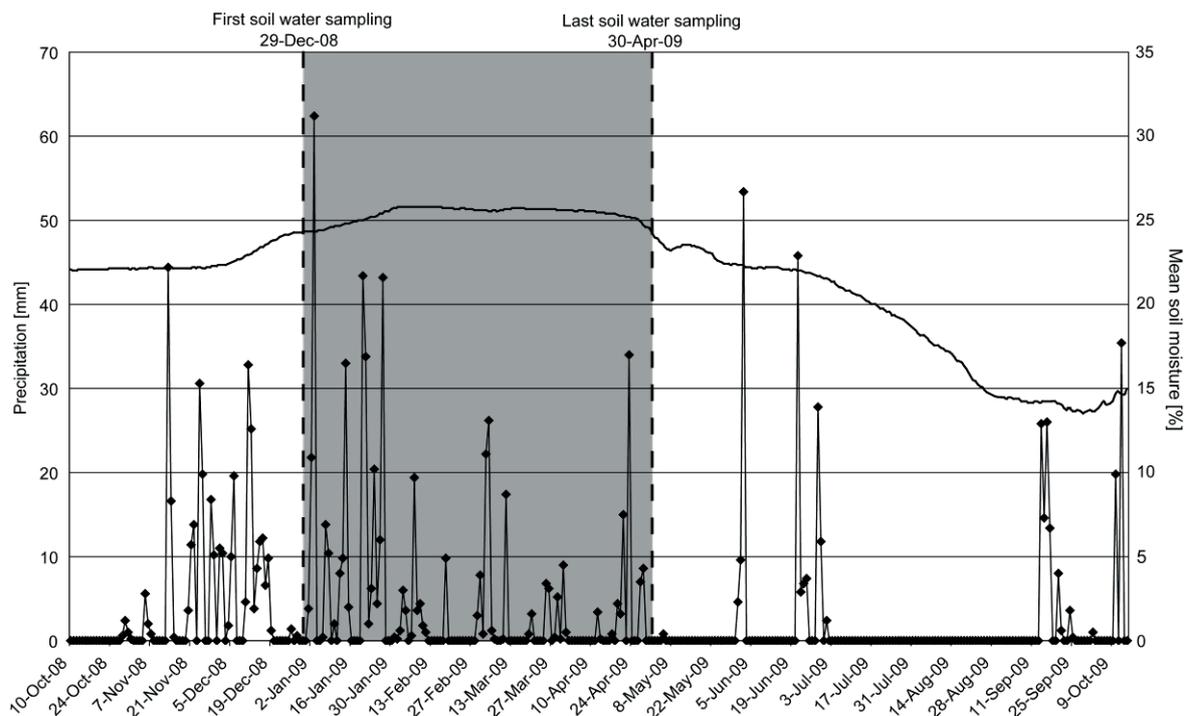
The first soil liquid phase was extracted by the suction cups at the end of December, another 30 days after Ө started to increase. By the time of the first soil water sampling Ө was 24.3 %. Henceforward, soil liquid phase could be sampled biweekly from the Roman paleosol until the end of April 2009. By the end of the sample period Ө had decreased to 24.5 %. Thus, the Roman paleosol requires an approximate soil moisture of more than about 24.5 % for mobile gravitational water to be available and extracted by the suction cups with an applied tension of 550 mbar. In contrast, when Ө decreases below 24.5 % the matric potential attracting the soil water to the mineral soil particles increases and exceeds the tension of the suction cups. Thus, the suction cups can no longer extract soil water from the paleosol.

The exchange of ions occurring between the soil solid and soil liquid phase depends on the presence of water in the soil. Furthermore, ion transport within the soil profile depends on the presence of mobile macropore water (Wolt, 1994; Blum, 2007). Since the suction cups predominantly sample the mobile soil water fraction percolating through the profile a soil water flow from the overlying volcanic deposits into the Roman paleosol was detected. However, it only took place in a period of about 120 days between the end of December 2008 and the end of April 2009 when the soil moisture exceeded 24.5 %.

In contrast to the Roman paleosol no soil water could be extracted from the AD 79 white pumice layer directly above. Nevertheless, the suction cups did not completely dry out since they could more or less sustain their tension (vacuum) for the two weeks sample period. This may be caused by the bimodal structure of the white pumice layer. On one hand it has a very coarse texture with a lot of macropores between the pumice clasts. On the other hand each pumiceous particle consist of a very fine internal porous system. Thus, the water may not move homogeneously through the pumice layer. In the macropores between the pumice it randomly follows preferential flow paths until it is absorbed by the pumiceous particles showing a high water retention capacity (Sahin et al., 2005). Consequently, the first infiltration water reaching the white pumice layer after a dry summer season is easily absorbed by the pumice. At unsaturated conditions the water movement in the pumice layer presumably takes place only within the particles and via the contact areas between them. Hence, there may be almost no gravitational water flow within

the macropores between the pumice clasts until the particles reach saturation point. Thus, no mobile soil water was extracted by the suction cups. After all, the relatively high air humidity in the pumice layer may have prevented the suction cups from running dry and losing their vacuum (Wessel-Bothe, 2008, oral communication).

Another reason why it may have not been possible to extract soil water from the white pumice layer could be due to an abrupt change of conductivity at the transition from the fine pores of the pumice particles to the bigger pores of the sand slurry around the suction cups that cannot be overcome by the tension applied (Wessel-Bothe, 2008, oral communication). This change of conductivity could have been reduced if finer material was used for the slurry, such as silt. However, in comparison to sand, silt has a relatively high adsorption capacity. Thus, the slurry material could have a considerable unintentional effect on the composition of the soil water extract.

In summery even if the suction cups could not extract water from the white pumice layer at the point of sampling, it does not necessarily mean that there is no water present in the white pumice layer and percolating through it. The fact that soil water could be extracted from the Roman paleosol underneath proves that water flow does take place, either vertically by infiltration or laterally by interflow. Interflow on top of the Roman paleo-surface can also result in a wet paleosol but a dry pumice layer directly above when upslope water percolates through the pumice and laterally enters the paleosol. The contributing upstream area of the point of sampling, i.e. the upslope region that drains into that point, is approximately 4,000 m^2 and extends from the northwest to the northeast of Villa Regina. Interflow can be caused by the strong decrease of permeability at the transition from the white pumice layer to the Roman paleosol. Hood infiltrometer measurements of saturated hydraulic conductivity (K_{sat}) yielded K_{sat} values of around 0.005 cm s^{-1} for the Roman paleosol. In contrast, K_{sat} of the white pumice layer was beyond instrumentation range of the hood infiltrometer (> 0.01 cm s^{-1}). Hence, it was minimum one order of magnitude higher than in the Roman paleosol.

The pH value of the soil liquid phase represents the active acidity of the Roman paleosol (Mengel and Kirkby, 2001). With a mean pH value of 7.5 the soil water extract is slightly alkaline, varying only marginally throughout the year (Tab. 1,

Fig. 5). The soil water extract is colorless indicating no presence of dissolved organic carbon. The mean cation concentrations are: 42.9 mg/l for Ca^{2+}, 35.6 mg/l for K^+, 23.3 mg/l for Na^+ and 5.7 mg/l for Mg^{2+} whereas the mean anion concentrations are: 60.5 mg/l for Cl^-, 23.4 mg/l for NO_3^- and 22.7 mg/l for SO_4^{2-}. The mean calculated electrical conductivity (EC_{calc}) at 25°C is 441 µS/cm (Tab. 1). Ca^{2+} is the dominant cation in the soil water extract. The dominant anion balancing the cation charge is Cl^- followed by NO_3^- and SO_4^{2-}. The Cl^- concentration even exceeds that of Ca^{2+}. Despite the dominance of Cl^-, the relatively low EC_{calc} of the soil water extract reveals that the Roman paleosol can be considered non-saline (Schoeneberger et al., 2002). However, due to the relative vicinity of the study area to the Tyrrhenian Sea high amounts of Cl^- and Na^+ in the lysimeter extract may result from dry deposition of sea water aerosols during onshore winds eventually leading to a gradual salinization of the soil (Scheffer & Schachtschabel, 2010). NO_3^- may rather derive from anthropogenic sources. This corresponds with finding of Adamo et al. (2007) who found increased amounts of nitrates in aquifers of the Sarno River plain due to intensive agricultural use.

Only the first two soil water extracts at the beginning of the sample period contained small amounts of Al^{3+} whereas later on no Al^{3+} could be detected. The absense of free Al^{3+} ions indicates that no soil acidification is active within the Roman paleosol which agrees with the slightly alkaline pH of the soil water. No HPO_4^{2-} ions could be determined in the soil water extract as it is only weakly soluable and usually strongly retained by the soil solid phase (Wolt, 1994). Furthermore, the phosphate retension in a soil is pH-dependent leaving it more soluable at a slightly to moderately acid pH value. At alkaline pH on the other hand its solubility is reduced by the formation of Ca-phosphates (Welp et al., 1983).

Table 1. Chemical properties of the soil water extract of the Roman paleosols and the soil moisture (Θ) at the date of sampling (sample period 2008/2009) (ND, not detectable).

Date of sampling	29-Dec 2008	14-Jan 2009	26-Jan 2009	9-Feb 2009	24-Feb 2009	9-Mar 2009	23-Mar 2009	6-Apr 2009	15-Apr 2009	30-Apr 2009	Arithmetic mean
pH	7.7	7.6	7.5	7.8	7.6	7.6	7.2	7.3	7.7	7.4	**7.5**
EC$_{calc}$ [μS cm^{-1}] at 25°C	526.2	433.0	388.1	405.6	398.2	401.9	463.7	464.4	465.0	459.7	**440.6**
Θ [%]	24.3	24.8	25.4	25.8	25.4	25.6	25.7	25.6	25.4	25.5	**25.3**
Cations [mg l^{-1}]											
Ca^{2+}	41.1	40.4	38.2	38.3	38.1	39.3	48.0	48.0	48.6	48.7	**42.9**
K$^+$	45.6	39.3	37.1	33.8	32.9	32.8	33.7	33.7	33.6	33.8	**35.6**
Na$^+$	24.5	25.1	23.1	19.8	20.5	21.6	24.1	24.2	24.8	25.0	**23.3**
Mg^{2+}	5.1	4.8	4.4	5.3	5.1	5.2	6.6	6.6	6.7	6.8	**5.7**
Al^{3+}	0.3	0.1	ND	ND	ND	ND	ND	ND	ND	ND	**-**
Anions [mg l^{-1}]											
Cl$^-$	75.3	53.5	43.8	58.8	56.2	55.2	67.0	67.1	65.2	63.4	**60.5**
NO$_3^-$	44.3	27.1	20.9	19.5	19.3	19.1	20.8	20.8	21.7	20.2	**23.4**
SO$_4^{2-}$	33.2	24.2	23.2	21.0	20.8	21.2	20.9	21.0	21.4	20.6	**22.7**
HPO$_4^{2-}$	ND	ND	ND	ND	ND	ND	ND	ND	ND	ND	**-**

<u>Figure 5</u>. PH value and course of the soil liquid phase chemistry of the Roman paleosol before and after the correction with the soil moisture (Θ) at the date of sampling. Sampling period 2008/2009.
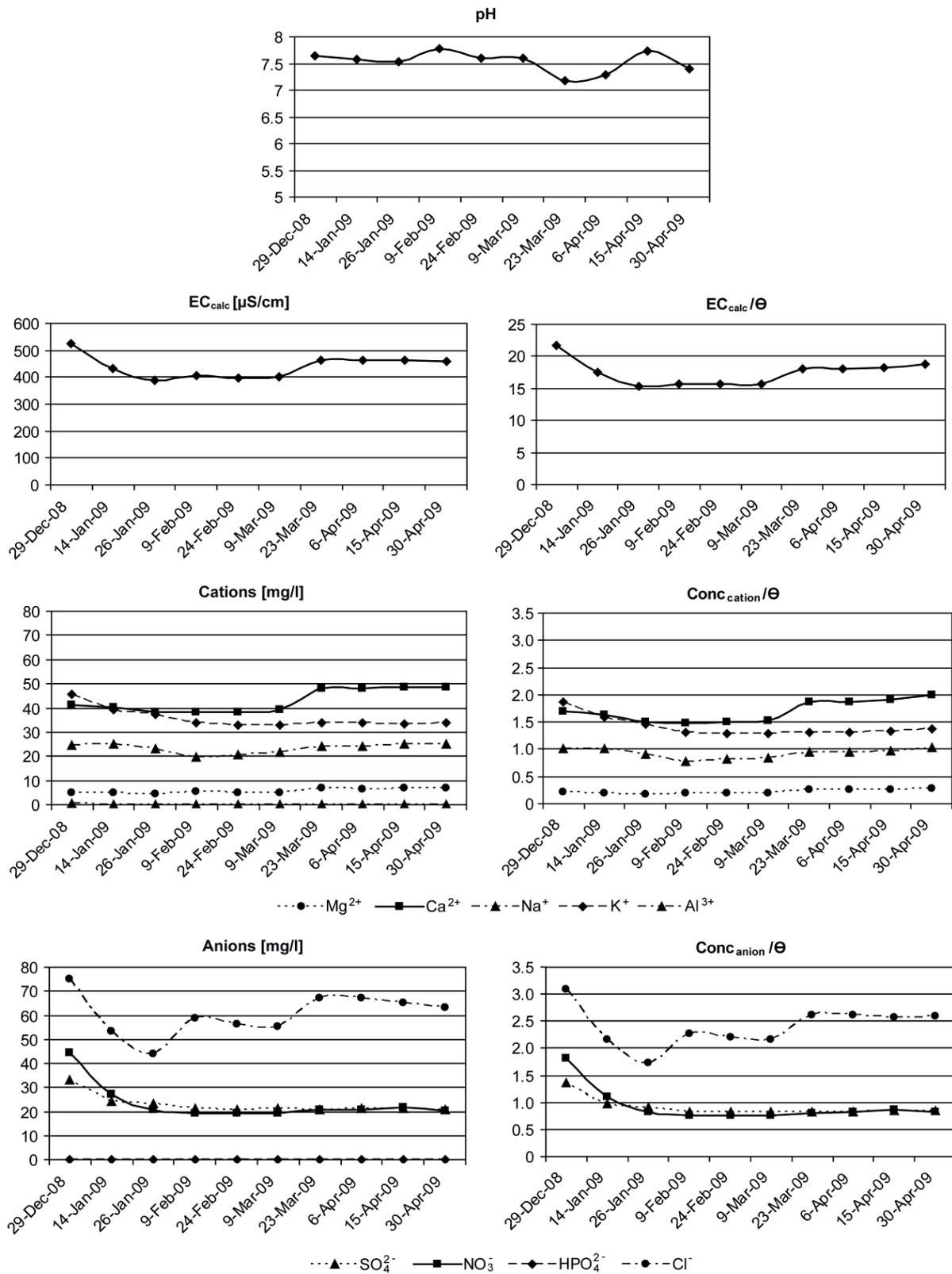
The amount of water available in the soil has a distinct influence on the liquid phase chemistry in terms of concentration or dilution effects during dry or wet conditions,

respectively (Mengel and Kirkby, 2001). Consequently, to gain a corrected course of the soil water composition, EC_{calc} and the cation and anion concentrations were devided by the soil moisture (Θ) of the Roman paleosol at the date of sampling. Due to the relative small variation of Θ during the sample period of only 1.5 % the course of soil water composition does not change significantly. However, especially the change in Θ at the beginning and the end of the sample period is noticeable in EC_{calc}/Θ (Fig. 5).

EC_{calc}/Θ has its maximum at the first soil solution sample end of December 2008. Then it decreases for the first four weeks until the end of January 2009 and stagnates until the beginning of March. Then it increases, remains static and slightly increases at the very end of the sample period. The increased EC_{calc}/Θ during the first weeks of soil water sampling is caused by increased ion concentrations. This can be explained by the 'first flush effect' that can occur at the beginning of the rainy season when the first infiltration water reaches the Roman paleosol after a dry summer season. An accumulation of ions during summer then results in higher element concentrations in the soil water extract. Arthur and Fahey (1993) observed the same effect but associated with snowmelt instead of precipitation water. At the initial stages of snowmelt the solute concentrations in the soil solution were also high and declined rapidly in the first four to six weeks (Arthur and Fahey, 1993).

It is striking that the 'first flush effects' is much stronger for the anions than for the cations. This may be due to the fact that volcanic soils have a high fraction of variable charge (Madeira et al., 2007). Consequently, at a slightly alkaline pH value the exchange sites are predominantly negatively charged resulting in a high cation exchange capacity and a negligable anion exchange capacity (Nanzyo et al., 1993). Hence, cations tend to be adsorbed to the surface of the soil colloids whereas anions are leached out of the profile with the mobile soil water. In the middle of the rainy winter season EC_{calc}/Θ reaches a minimum because of ions continuously leaching from the soil (De Pascale and Barbieri, 1997). Thereafter, EC_{calc}/Θ increases at the end of march and slightly at the end of April on account of an increase of Ca^{2+}, Cl^- and partly of Na^+. This is caused by the inversion of the 'first flush effect', i.e. the decline of ion leaching from the soil due to a smaller amount of mobile soil water and the starting accumulation at the end of the rainy season (De Pascale and Barbieri, 1997).

However, this effect is much less pronounced compared to the beginning of the sample period presumably due to the precipitation that does not stop abruptly at the end of the rainy season and due the delayed response of Θ in the Roman paleosol.

Beyond the elevated ion concentrations at the beginning and the end of the sample period no significant seasonal variation could be detected. The concentration of Mg^{2+} even stays constant during the entire sample period. This may be due to the following reasons:

(i)   In the Roman paleosol in a depth of about 8 m plants are absent. Thus, there is no influence on the soil water composition by nutrient uptake and ion secretion of plant roots.

(ii) The mobile soil water fraction predominantly sampled by tension lysimeters has much shorter contact times with the soil solid phase then the capillary water resulting in lower ion concentrations and less seasonality (Wolt, 1994).

(iii) The shortness of the sample period of about 120 days, i.e. the time soil water could be extracted from the paleosol, inhibits the detection of seasonal variations in the soil water composition.

During the winter season of 2009/2010 the above described characteristics of the soil water chemistry of the Roman paleosol recur. The ion concentration is increased at the beginning, then decreases to its minimum and re-increases at the end of the sample period (Tab. 2, Fig. 6). The first lysimeter sample was taken at the beginning of February 2010 about 30 days later than 2009. This is caused by the Roman paleosol having a much lower initial soil moisture (Θ) in the summer of 2009 (13.6 %) in comparison to 2008 (22 %) (Fig. 5). Furthermore, in the first half of the rainy season from October to January 2008/2009 there were a total of 735 mm of precipitation in comparison to only 492 mm in 2009/2010. Consequently, 2009/2010 the process of rewetting of the soil substrate until percolation takes place and Θ of the Roman paleosol is sufficiently high for soil water to be sampled by the suction cups took much longer. Altogether, due to less precipitation 2009/2010 the period of soil water sampling lasted only 100 days in comparison to 120 days 2008/2009.

In autumn 2009 all three soil moisture sensors failed as they probably lost their attachment to the substrate due to soil shrinkage during the dry summer season. Consequently, the ion concentrations could not be corrected with Θ which would

have even amplified the course of soil water chemistry to a certain extent as could be seen for 2008/2009 (Fig. 6).

Table 2. Chemical properties of the soil water extract of the Roman paleosols at the date of sampling (sample period 2009/2010) (ND, not detectable).

Date of sampling	2-Feb 2010	18-Feb 2010	2-Mar 2010	18-Mar 2010	1-Apr 2010	15-Apr 2010	29-Apr 2010	13-May 2010	Arithmetic mean
pH	7.4	7.8	7.7	7.7	7.8	7.8	7.8	7.8	**7.7**
EC_{calc} [µS cm^{-1}] at 25°C	528.2	495.3	465.0	470.1	478.2	498.9	489.3	502.1	**490.9**
Cations [mg l^{-1}]									
Ca^{2+}	50.3	46.3	40.2	40.8	41.3	45.7	46.0	46.8	**44.7**
K^+	46.7	42.3	39.7	40	41	40.7	40.5	40.8	**41.5**
Na^+	18.3	20.4	21.4	21.9	22	23.8	22.5	24.6	**21.9**
Mg^{2+}	6.9	7	6.7	6.72	6.75	6.8	6.7	6.8	**6.8**
Al^{3+}	0.2	0.1	ND	ND	ND	ND	ND	ND	**-**
Anions [mg l^{-1}]									
Cl^-	70.3	60.2	58.3	58.7	60.2	62.3	61.5	61.9	**61.7**
NO_3^-	38.7	39.6	37.5	37.9	38	38.4	39.0	38.7	**38.5**
SO_4^{2-}	32.7	33.5	30.8	31.1	32	32.5	31.6	31.8	**32.0**
HPO_4^{2-}	1.1	0.7	0.5	0.5	0.6	0.7	0.6	0.7	**0.68**

Figure 6. PH value and course of the soil liquid phase chemistry of the Roman paleosol. Sampling period 2009/2010.
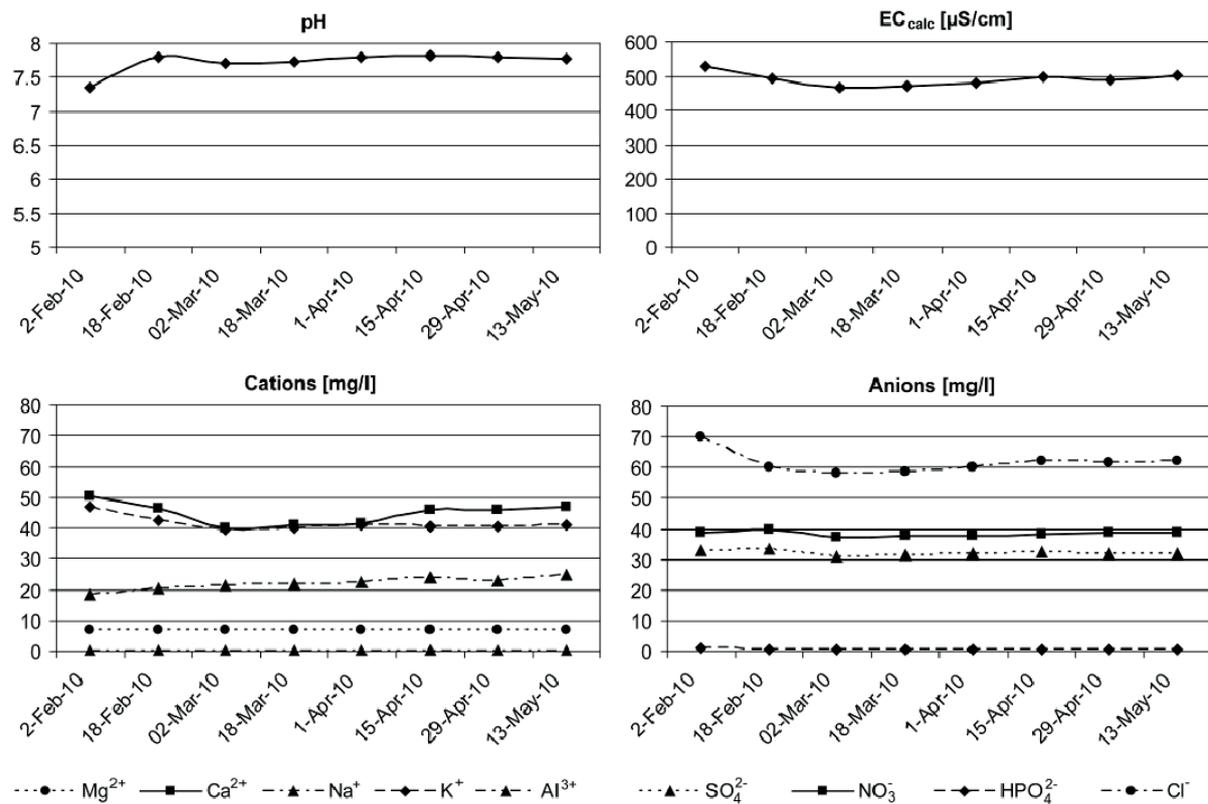
Soil solid phase analysis

From the relative position of the Roman paleosol and the modern soil within the stratigraphy a rough estimation of their approximate soil age was made. The age of the Roman paleosol ranges between 300 and 700 years which is inferred from the time of volcanic quiescence prior to the AD 79 eruption of Somma-Vesuvius (see Stothers and Rampino, 1983; Rolandi et al., 1998; Scudder et al., 1996; Sigurdsson, 2002). However, the exact age of the modern soils is not entirely clear. It can be estimated between a minimum of 64 years and a maximum of 1,940 years as they are underlain either by the pumice lapilli fallout of the 1944 eruption of Somma-Vesuvius (DAI 16, VdM) or reworked ash layers deriving from the final stage of the AD 79 eruption (DAI 18, DAI 20).

The results of the soil solid phase analysis show distinct characteristics that distinguish the topsoils of the Roman paleosol from the modern soil at the same topographic location (Tab. 3). The Roman paleosols have a pH value that is approximately 0.5 pH units higher compared to the modern soils which corresponds

with the observations of Foss (1988) and Foss et al. (2002). The paleosol is neutral to slightly alkaline whereas the modern soil is moderately acid to neutral. The lower pH value of the modern soil probably results from the active accumulation and decomposition of soil organic matter (SOM) producing organic acids as well as from nutrient uptake and proton release of plant roots. Moreover, percolating soil water tends to leach basic cations from the upper horizons of the modern soil which further decreases the pH value. In contrast, according to the results of the soil liquid phase study, the Roman paleosol is rather subject to post-burial nutrient input by leaching from the overlying deposits which increases the pH value. However, as described above this process takes only place during four months of the year in the rainy winter season when mobile soil water is present. Furthermore, the pH decreasing influence of plants and active accumulation of SOM is missing in the paleosols. It is noticeable that the pH of the paleosols often does not consistently increase with depth as can be seen for most of the modern unburied soils. In the Roman paleosols the former A-horizons are recently subject to ion accumulations from the overlying strata. Hence, after burial boundaries between zones of leaching and accumulation can gradually blur (Holliday, 2004).

Table 3. Soil solid phase properties of the pre–AD 79 Roman paleosol and modern soil near Pompeii.

Site	Soil	Soil texture	pH (CaCl$_2$)	CaCO$_3$ [%]	TOC [%]	N [%]	C/N	CEC$_{eff}$ [cmol$_c$ kg^{-1}]	eff. base saturation [%]	Exchangeable cations [cmol$_c$ kg^{-1}]				Al$_{ox}$ [%]	Fe$_{ox}$ [%]	Si$_{ox}$ [%]	Al$_{ox}$+0.5Fe$_{ox}$ [%]
										K$^+$	Na$^+$	Ca^{2+}	Mg^{2+}				
DAI16	modern soil	loamy sand	6.03	0.71	1.16	0.11	10.19	13.84	100	2.07	4.87	5.22	1.71	0.78	0.67	0.58	1.11
	pre–AD 79 paleosol	sandy loam	7.13	0.79	0.89	0.08	11.25	13.96	100	2.03	1.32	9.47	1.17	1.09	0.41	0.72	1.30
DAI18	modern soil	sandy loam	7.41	3.08	0.80	0.05	17.13	6.54*	100	1.90	1.04	3.27*	0.34	0.87	0.83	0.85	1.28
	pre–AD 79 paleosol	sandy loam	7.53	1.62	0.34	0.01	25.65	17.16*	100	1.63	0.66	13.85*	1.07	0.35	0.29	0.14	0.50
DAI20	modern soil	sandy loam	7.38	1.26	0.73	0.06	12.97	18.82*	100	3.02	0.89	13.18*	1.78	1.24	0.93	1.23	1.70
	pre–AD 79 paleosol	sandy loam	7.58	5.22	0.98	0.03	34.77	19.00*	100	3.05	0.83	13.37*	1.81	0.55	0.37	0.22	0.73
VdM	modern soil	sandy loam	7.21	0.32	0.80	0.08	9.81	21.22	100	3.28	0.56	16.01	1.42	0.94	0.87	0.77	1.38
	pre–AD 79 paleosol	sandy loam	7.72	0.40	0.31	0.03	10.33	22.22	100	2.21	0.83	17.71	1.51	0.28	0.29	0.11	0.43

*in soil samples containing >1% CaCO$_3$ the analysis of CEC$_{eff}$ can cause a dissolution of CaCO$_3$ which may result in increased values of CEC$_{eff}$ and exchangeable Ca^{2+} (thus, CEC$_{eff}$ rather equates to CEC$_{pot}$)

In soils of neutral to slightly alkaline pH values, there is a close relationship between $CaCO_3$ and Ca^{2+} ions that derive from carbonate buffer reactions (Scheffer and Schachtschabel, 2010; Blum, 2007). To neutralize the supply of H^+ ions to the soil carbonate dissociates and HCO_3^- and Ca^{2+} ions leach out of the profile. Consequently, the modern soil contains lower amounts of carbonate and Ca^{2+}. The Roman paleosol on the other hand shows a higher content of carbonate and Ca^{2+} indicating a relative accumulation. From both the soil liquid and solid phase study it can be seen that Ca^{2+} is the dominant cation to be present in the mobile soil water and the mineral soil respectively.

The effective cation exchange capacity (CEC_{eff}) is slightly higher in the Roman paleosols in comparison to the modern soils above all due to higher amounts of exchangeable Ca^{2+}. This confirms the post-burial transport of nutrients into the paleosol. It is noticeable that DAI 18 shows the highest differences in CEC_{eff} and Ca^{2+} between the Roman paleosol and the modern soil. A possible explanation for that derives from the topographical situation of DAI 18 at the footslope of Somma-Vesuvius (Fig. 1A). Hence, the contributing upslope area of that location is much bigger in comparison to DAI 16 and VdM which are situated on the footslope of the Pompeiian hill. Therefore, besides the vertical water movement through the soil, a more pronounced lateral hypodermic flow can be expected for DAI 18, e.g. on top of the pre-AD 79 paleo-surface. In total this may result in a stronger translocation of nutrients down to the Roman paleosol of DAI 18. In contrast, DAI 20 shows only slightly higher values of CEC_{eff} and Ca^{2+} in the Roman paleosol. DAI 20 is situated on top of the Pompeiian hill (Fig. 1A). Thus, the vertical component of soil water movement most likely predominates at DAI 20 whereas hypodermic flow is negligible resulting in less total nutrient transport into the Roman paleosol.

With regard to the exchangeable cations it is noticeable that the Roman paleosols contain more Ca^{2+} and Mg^{2+} ions but less K^+ and Na^+ ions than the modern soils. This suggests that above all Ca^{2+} and Mg^{2+} is adsorbed to the exchange sites of the soil after entering the paleosol through the mobile soil water. K^+ and Na^+ on the other hand although also present in the soil water extract seem to be washed out of the profile since they play a minor role in the cation exchange complex of the paleosols. This is caused by a higher attraction of Ca^{2+} and Mg^{2+} by the exchange

sites due to their higher valance in comparison to K^+ and Na^+. This corresponds to Foss (1988) and Foss et al. (2002) who presumed that especially Ca^{2+} and Mg^{2+} leach from the overlying volcanic sediments and recharge the surface horizons of the paleosols.

It is striking that the range of values of CEC_{eff} and the exchangeable cations is considerably wider for the modern soils than for the paleosols. The modern soils are subject to active processes of SOM and nutrient turnover such as accumulation and decomposition of SOM and ion uptake and segregation by plant roots. All those processes considerably influence the cation exchange complex hence resulting in a higher variation of CEC_{eff}. In the Roman paleosols on the other hand the accumulation of SOM and the influence of plants has stopped after burial resulting in a rather similar CEC_{eff} compared to the modern soils.

Due to the neutral to slightly alkaline pH value of the Roman paleosol the surface charge of the soil colloids is predominantly negative. Thus, adsorption of anions such as Cl^-, NO_3^- or SO_4^{2-} to the exchange sites of the soil is negligible. The mobile soil water containing these anions pass the paleosol without the anions being attached to the exchange sites of the soil solid phase. Consequently, they are leached out of the soil profile.

Both the Roman paleosols and the modern soils have very low to low soil organic matter (SOM) contents. However, the paleosols show slightly lower amounts of SOM than the modern soils. This is due to the fact that with burial AD 79 the accumulation of SOM within the paleosol has stopped and started to gradually decompose. Taking into account that the modern soils of DAI 16 and the Villa dei Misteri (VdM) are only 64 years old in comparison to an expected age of some hundred years of the Roman paleosols the decomposition of SOM in the paleosol can be considered substantial. Vogel and Märker (2010) analysed the pre-AD 79 Roman paleosol south of Pompeii that showed moderate to high SOM contents in the uppermost soil horizons. One reason for that they assumed to be a risen groundwater table since AD 79 south of Pompeii that temporarily results in air exclusion in the Roman paleosol and a decreased mineralization of SOM. In contrast, the soil moisture and groundwater data at Villa Regina reveal that at higher elevations the Roman paleosol is unsaturated throughout the year which may result in a successive decomposition of

SOM subsequent to burial AD 79 and hence, today to very low or low amounts of SOM.

According to organic carbon the Roman paleosols also contain lower amounts of nitrogen than the modern soils. The resulting C/N ratio on the other hand is higher in the paleosols than in the modern soils. This is related to the mode of decomposition of SOM in the paleosols. Crowther et al. (1996) who studied post-burial change in a humic rendzina soil in England states that shortly after burial the decomposition rate may be high due to the breakdown of more readily decomposable components of SOM. However, over time the decomposition rate decreases when more resistent components predominate the SOM. This may result in a higher C/N ratio in the paleosols than in the modern soils were the accumulation of easily decomposable SOM is still active.

Apart from DAI 16 the Roman paleosols have lower amounts of ammonium-oxalate extractable Fe, Al and Si than the modern soils. That means that the modern soils contain more short-range-order minerals and/or organo-metallic complexes due to active weathering of pyroclastic parent material. Consequently, weathering within the Roman paleosol must have slowed down after burial presumably due to the reduced presence of water in the paleosol of only four months during the year. Shoji and Takahashi (2002) state that soil burial by ash deposition strikingly reduces the effect of climate and organisms on the buried soil which significantly lowers their weathering rate.

Bulk density is an indicator of soil compaction. The mean bulk density of the Roman paleosol (VdM) is 1.36 g/cm³ which is not considerably high and perse would not indicate soil compaction. However, in comparison to the modern soil having approximately 1.13 g/cm³ it is slightly increased which can be attributed to the superimposed load of the overlying post-AD 79 deposits.

Conclusions

The combination of the present-day mean groundwater table of the Sarno River plain (Autorità di Bacino del Sarno) and the pre-AD 79 DEM (Vogel et al., 2011) revealed that one has to distinguish the Sarno River plain into two different zones in terms of potential post-burial soil developments: (i) at around 37 % of the Sarno River plain

since AD 79 the Roman paleosol is influenced by a rise of the mean groundwater table of approximately 1.8 m and (ii) at the remaining 63 % the Roman paleosol is still part of the unsaturated vadose zone and more likely influenced vertically by infiltration water or laterally by interflow. Consequently, the mechanism of potential post-burial soil development being active in a Roman paleosol is not uniform for the entire Sarno River plain but strongly depends on the paleo-topographic situation.

The soil moisture and soil liquid phase study at the archaeological excavation of Villa Regina demonstrated that recently soil water flow down to the Roman paleosol in a depth of 8 m takes place. Consequently, on its way percolating through the stratigraphy this soil water can dissolve ions from the overlying volcanic deposits, incorporate them into the Roman paleosol and influence its solid phase properties since burial AD 79. However, mobile soil water was only extracted from the paleosol in a four months period when the soil moisture exceeded 24.5 %. This restricts the potential influence of post-burial soil development by nutrient transport to the rainy winter season. The soil liquid phase of the Roman paleosol shows a distinct chemical composition. At the beginning and the end of the sample period increased ion concentrations could be determined that can be explained by the 'first flush effect' and its inversion.

Through the combination of the soil liquid phase study with comparison of the soil solid phase of the pre-AD 79 Roman paleosol and the modern soil at the same topographic location post-burial soil changes were estimated. Between the pre-AD 79 Roman paleosol and the modern soil distinct differences exist regarding their soil solid phase properties that point to the following post-burial changes in the pre-AD 79 Roman paleosol:

(i)   Leaching of nutrients (Ca^{2+}, Mg^{2+}) from overlying deposits into the paleosol led to a higher pH value and effective cation exchange capacity. However, the results from the soil water and soil moisture study restrict the annual soil water flow to a four months period during the rainy winter season.

(ii) After burial the accumulation of soil organic matter (SOM) has stopped. Instead SOM has began to gradually decompose resulting in low amounts of organic carbon and nitrogen in the paleosols.

(iii)   Since the buried A-horizons are recently subject to ion accumulations from the overlying strata through soil water flow former topsoil eluvial horizons gradually turn into subsoil illuvial horizons.

(iv)   The bulk density of the paleosol is increased due to soil compaction as a result of the superimposed load of the overlying post-AD 79 deposits.

(v)   Lower amounts of ammonium-oxalate extractable Fe, Al and Si indicate a reduced weathering rate of the paleosols after burial.

Although this study lags in comprehensive representative data to be able to draw conclusions on post-burial soil developments for the entire Sarno River plain the obtained results correspond with the findings of Foss (1988) and Foss et al. (2002). They assumed higher pH values and higher nutrient contents of the Roman paleosol, in comparison to the modern soil, are the result of bases leaching from the overlying sediments into the paleosol. Furthermore, the comparison between the pre-AD 79 Roman paleosol and the modern soil is based on the hypothesis that the chemical composition of the parent soil substrate is similar regarding the analysed soil parameters.

Detailed insights were gained into the occurrence of mobile soil water within the Roman paleosol and into the nature of post-burial soil developments. In the future, those post-burial changes have to be taken into account when the Roman paleosols is characterized and interpreted with respect to is ancient conditions and its ancient agricultural potential. However, as stated above, the described results are only valid for around 63 % of the Sarno River plain where the Roman paleosol is still part of the unsaturated vadose zone. From the Roman paleosols south of Pompeii Vogel and Märker (2010) describe some soil alterations due the post-burial rise of the groundwater table, i.e. redoximorphic features in the white pumice layer and increased amounts of sulphate in the underlying paleosols. To determine the influence of the risen groundwater table on the Roman paleosol in more detail chemical analysis of the groundwater within the Roman paleosols should be carried out.

Acknowledgments

References

Adamo, N., Imperatrice, M.L., Mainolfi, P., Onorati, G. and Scala, F., 2007. Acqua - Il monitoraggio in Campania. 2002 – 2006. ARPAC, Napoli, pp. 257.

Arthur, M.A. and Fahey, T.J., 1993. Controls on Soil Solution Chemistry in a Subalpine Forest in North-Central Colorado. Soil Sci. Soc. Am. J. 57, 1122-1130.

Bierman, P.M.; Rosen, C.J.; Bloom, P.R. and Nater; E. A., 1995. Soil solution chemistry of sewage-sludge incinerator ash and phoshate fertilizer amended soil. Journal of environmental quality, vol. 24, no. 2, pp. 279-285.

Blum, W.E.H.,, 2007. Bodenkunde in Stichworten. Stuttgart, 179 pp.

Bradford, G.R.; Bair, F.L. and Hunsaker, V., 1971. Trace and major element contents of soil saturation extracts. Soil Sci. 112, 225-230.

Brinson, M.M., 1993. A Hydrogeomorphic Classification for Wetlands. Wetlands Research Program, Technical Report WRP-DE-4, pp. 79.

Campbell, D.J. and Beckett, P.H.T., 1988. The soil solution in a soil treated with digested sewage sludge. J. Soil Sci. 39, 283-298.

Campbell, D.J.; Kinniburgh, D.G. and Beckett, P.H., 1989. The soil solution chemistry of some Oxfordshire soils: temporal and spatial variability. Journal of Soil Science, Vol. 40, 321-329.

Cecchini, G.; Carnicelli, S.; Mirabella, A.; Mantelli, F. and Sanesi, G., 2002. Soil conditions under a Fagus silvatica CONECOFOR stand in Central Italy: an integrated assessment through combined solid phase and solution studies. Journal of Limnology, Vol. 61, 36-45.

Crowther, J.; Macphail, R.I. and Cruise, G.M., 1996. Short-Term, Post-Burial Change in a Humic Rendzina Soil, Overton Down Experimental Earthwork, Wiltshire, England. Geoarchaeology 11(2), 95-117.

De Caro, S., 1994. La villa rustica in località Villa Regina a Boscoreale. In: Bretschneider G. (ed.) Pubblicazioni scientifiche del Centro di studi della Magna Grecia. Terza serie, pp. 241.

De Pascale, S. and Barbieri, G., 1997. Effect of soil salinity and top removeal on growth and yield of broad bean as green vegetable. Sci. Hortic. 71, 147-165.

de Vries, W. and Leeters, E.E.J.M., 1994. Effects of acid deposition on 150 forest stands in the Netherlands. Chemical composition of the humus layer, mineral soil and soil solution. DLO Winand Staring Centre for Integrated Land, Soil and Water Research. Rep. 69.1, Wageningen, The Netherlands, 84 p.

Delta-T Devices Ltd, 2006. User Manual for the SM200 Soil Moisture Sensor. SM200-UM-1.1, pp. 36.

Derome, J., 2002. Submanual on Soil Solution Collection and Analysis. ICP Forest Manual Part III, Expert Panel on Soil, 111-161.

DIN 38405 D5, 1985. German standard methods for the examination of water, waste water and sludge; anions (group D); determination of sulfate ions (D5). Beuth-Verlag.

DIN 38414 S12, 1986. German standard methods for the examination of water, waste water and sludge; sludge and sediments (group S); determination of phosphorus in sludges and sediments (S12). Beuth-Verlag.

DIN EN 13137, 2001. Characterization of waste-Determination of total organic carbon, TOC) in waste, sludges and sediments. Beuth-Verlag.

DIN ISO 10390, 2005. Soil quality-Determination of pH. Beuth-Verlag .

DIN ISO 11261, 1997. Soil quality-Determination of total nitrogen - Modified Kjeldahl method. Beuth-Verlag.

DIN ISO 11277, 2002. Soil quality-Determination of particle size distribution in mineral soil material-Method by sieving and sedimentation. Beuth-Verlag.

Dohrmann, R. & Kaufhold, S., 2009. Three new, quick CEC methods for determining the amounts of exchangeable calcium cations in calcareous clays. Clay Minerals Society 57(3), 338-352.

DVWK, 1990. Gewinnung von Bodenwasserproben mit Hilfe der Saugkerzenmethode. Berlin, Bd. Merkblatt 217.

French, C., 2003. Geoarchaeology in Action. Studies in Soil Micromorphology and Landscape Evolution. Routledge, London.

Fillion, N.; Probst, A. and Probst, J.L., 1999. Dissolved organic matter contribution to rainwater, throughfall and soil solution chemistry. Analusis, Vol. 27, No. 5.

Fiorillo, F. and Wilson, R.C., 2004. Rainfall induced debris flows in pyroclastic deposits, Campania (southern Italy). Engineering Geology 75, 263-289.

Foss, J.E., 1988. Paleosols of Pompeii and Oplontis. In: Curtis, R.L., (ed.) Studia Pompeiana and Classica, Aristide D. Caratzas, Publisher,New Rochelle, N.Y.

Foss, J.E., Timpson, M.E., Ammons, J.T. and Lee, S.Y., 2002. Paleosols of the Pompeii Area. In: Jashemski W.F., (ed.) The Natural History of Pompeii. Cambridge University Press, 65-79.

Grossmann, J., 1988. Physikalische und chemische Prozesse bei der Probenahme von Sickerwasser mittels Saugsonden. Diss. Institut für Wasserchemie und Chemische Balneologie der Technischen Universität München, pp. 147.

Grossmann, J. and Moss, R., 1994. Variability of water quality in a spruce stand. Journal of Plant Nutrition and Soil Science 157, 47-51.

Grossmann, J. and Udluft, P., 1991. The extraction of soil water by the suction-cup method: A review. Journal of Soil Science 42, 83-93.

Haberhauer, G., 1997. Adsorptionsverhalten von Saugkerzenmaterialien. 7.Gumpensteiner Lysimetertagung, BAL Gumpenstein, 27-31.

Hendershot, W.H. and Courchesne, F., 1991. Comparison of soil solution chemistry in zero tension and ceramiccup tension lysimeters. Journal of Soil Science, Vol. 42, 577-583.

Javaux, M. and Vanclooster, M., 2004. In Situ Long-Term Chloride Transport through a Layered, Nonsaturated Subsoil. 2. Effect of Layering on Solute Transport Processes. Vadose Zone Journal 3, 1331-1339.

Litaor, M. I., 1988. Review of soil solution samplers. Water Resource Research, Vol. 24, 727-733.

Manderscheid, B. and Matzner, E., 1995. Spatial and temporal variation of soil solution chemistry and ion fluxes through the soil in a mature Norway spruce (Picea abies (L.) Karst.) stand. Biogeochemistry, Vol. 30, 99-114.

Mengel, K. and Kirkby, E.A., 2001. Principles of plant nutrition. Kluwer academic publishers, Netherlands.

Mulder, J. and Cresser, M.S., 1994. Soil and Soil Solution Chemistry. In: Moldan, B. and Cerny, J. (eds.) Biogeochemistry of Small Catchments: A Tool for Environmental Research. John Wiley and Sons Ltd., 107-131.

Nanzyo, M.; Dahlgren, R. and Shoji, S., 1993. Chemical characteristics of volcanic ash soils. In: Shoji, S.; Nanzyo, M. and Dahlgren , R. (eds.) Volcanic ash soils – genesis, properties and utilization. Developments in Soil Science 21, Elsevier, Amsterdam, 145-188.

Piochi, M.; De Vivo, B. and Ayuso, R.A., 2006. The magma feeding system of Somma-Vesuvius (Italy) strato-volcano: new inferences from a review of geochemical and Sr, Nd, Pb and O isotope data. In: De Vivo, B. (ed.) Vesuvius, Campi Flegrei and Ignimbrites. Elsevier, Amsterdam, 183-204.

Porebska, G.; Sienkiewicz, J. and Ostrowska, A., 2004. Indicatory Properties of Soil Solutions in the Characteristics of Forest Site Quality. Polish Journal of Environmental Studies, Vol. 13, No. 5, 557-563

Retallack, G.J., 1998. Core Concepts of Paleopedology. Quaternary International, Vols. 51/52, 203-212.

Retallack, G.J., 2001. Soils of the Past, An Introduction to Paleopedology. Blackwell Science.

Roman, R.; Caballero, R. and Bustos, A., 2002. Variabilità of Soil Solution Ions in Fallowland Fields in Central Spain. Edafologia, Vol. 9 (2), 161-172.

Sahin, U.; Ors, S.; Ercisli, S.; Anapali, O. and Esitken, A., 2005. Effect of pumice amendment on physical soil properties and strawberry field growth. Journal of Central European Agriculture 6(3), 361-366.

Scheffer, F. and Schachtschabel, P., 2010. Lehrbuch der Bodenkunde. Spektrum Akademischer Verlag GmbH, Heidelberg, Berlin.

Schoeneberger, P.J.; Wysocki, D.A.; Benham, E.C. and Broderson, W.D., 2002. Field book for describing and sampling soils. Version 2.0. Natural Resources Conservation Service, National Soil Survey Center, Lincoln, NE, pp. 228.

Schofield, R.K., 1955. Can a precise meaning be given to "available" soil phosphorous? Soil and Fertilizers 18, 373-375.

Scudder, S.J.; Foss, J.E. and Collins, M.E., 1996. Soil science and archaeology. Advances in Agonomy, Vol. 57, 1-76.

Seiler, F., 2008) Rekonstruktion der antiken Kulturlandschaften des Sarno-Beckens. Ein multidisziplinäres Kooperationsprojekt mit Partnern aus Naturwissenschaften und Altertumswissenschaften in Deutschland, Italien und England, in Guzzo, P.G.; Guidobaldi M.P. (ed.) Nuove ricerche archeologiche nell'area vesuviana (scavi 2003-2006), Convegno Internazionale, Roma 1.-3. Februar 2007, 485-490.

Shoji, S. and Takahashi, T., 2002. Environmental and Agricultural Significance of Volcanic Ash Soils. Glob. Environ. Res. 6(2), 113-135.

Snakin, V.V.; Prisyazhnaya, A.A. and Kovács-Láng, E., 2001. Soil liquid phase composition. Elsevier.

Spangenberg, A.; Cecchini, G. and Lamersdorf, N., 1997. Analysing the performance of a micro soil solution sampling device in a laboratory examination and a field experiment. Plant and Soil, Vol. 196, 59-70.

Strahm, B.D.; Harrison, R.B.; Terry, T.A.; Flaming, B.L.; Licata, C.W. and Petersen, K.S., 2005. Soil solution nitrogen concentrations and leaching rates as influenced by organic matter retention on a highly productive Douglas-fir site. Forest Ecology and Management 218, 74–88.

Tischner, T.; Nutzmann, G. and Pothig, R., 1998. Determination of soil water phosphorus with a new nylon suction cup. Bulletin of freshwater ecology and inland fisheries, 61, Nr. 3, 325-332.

Ugolini, F.C. and Dahlgren, R.A., 2002. Soil Development in Volcanic Ash. Global Environmental Research, Vol. 6, Part 2, 69-82.

Vogel, S. and Märker, M., 2010. Reconstruction the Roman topography and environmental features of the Sarno River plain (Italy) before the AD 79 eruption of Somma-Vesuvius. Geomorphology 115, 67-77.

Vogel, S.; Märker, M. and Seiler, F., 2011. Revised modeling the post-AD 79 volcanic deposits of Somma-Vesuvius to reconstruct the pre-AD 79 topography of the Sarno River plain (Italy). Geologica Carpathica 1/2011.

Welp, G.; Herms, U. and Brümmer, G., 1983. Einfluß von Bodenreaktion, Redoxbedingungen und organischer Substanz auf die Phosphatgehalte der Bodenlösung. Journal of Plant Nutrition and Soil Science 146, 38-52.

Wolt, J., 1994. Soil solution chemistry. Application to environmental science and agriculture. John Wiley and Sons, Inc.

Zabowski, D. and Ugolini, F.C., 1990. Lysimeter and centrifuge soil solution: Seasonal differences between methods. Soil Science Society of America Journal, Vol. 54, 1130-1135.

Curriculum vitae

Sebastian Vogel

Born January 15, 1977 in Berlin (Germany); German citizenship

Education

Oct. 2009 – present	PhD, Eberhard Karls University of Tübingen, Department of Geography.
Oct. 1998 – Sep. 2005	Diploma in Geoecology, University of Potsdam.
Sep. 2001 – June 2002	University of Plymouth (U.K.), ERASMUS exchange program.
June 1996	Abitur, Walter Felsenstein Gymnasium Berlin.

Academic Positions & Research Experience

Aug. 2009 – present	Research assistant, Heidelberg Academy of Sciences and Humanities.
Feb. 2007 – July 2009	Research assistant, German Archaeological Institute, Berlin.
Okt. 2005 – Nov. 2006	Research assistant, University of Potsdam, Department of Geoecology.

Conference Presentations

Seiler, F.; Märker M.; Kastenmeier, P.; Vogel, S.; Esposito, D.; Heussner, U.; Boni, M.; Balassone, G.; Di Maio, G.; Joachimski, M.; Robinson, M., 2010. Multi disciplinary approach on the reconstruction of the ancient cultural landscape of the Sarno River Plain before the eruption of Somma-Vesuvius AD 79. Giornate di studio, Scienze naturali e archeologia. Il paesaggio antico: interazione uomo/ambiente ed eventi catastrofici, Napoli 14−16 ottobre 2010. Poster Presentation.

Vogel, S. and Märker, M., 2010. Reconstructing the paleo-topography and paleo-environmental features of the Sarno River plain (Italy) before the AD 79 eruption of Somma-Vesuvius volcanic complex. European Geosciences Union General Assembly, EGU 2010, Vienna, Austria, 2nd-7th May 2010. Oral Presentation.

Vogel, S. and Märker, M., 2010. Determining a detailed course of the ancient aquaeducts serving Pompeii (Italy) using a model of the pre-AD 79 paleo-topography. XXXVIII Conference on Computer Applications and Quantitative Methods in Archaeology. CAA 2010, 6th-9th April 2010. Poster Presentation.

Vogel, S and Märker, M., 2009. Reconstructing the Roman topography and environmental features of the Sarno River Plain (Italy) before the AD 79 eruption of Somma-Vesuvius. Joint Symposium of ROCEEH and BiK-F, Human Expansions and Global Change in the Pleistocene - Problems and Methods, 16th - 19th November 2009 Senckenberg Forschungsinstitut und Naturmuseum Frankfurt, Germany. Poster Presentation.

Vogel, S. and Märker, M., 2009. Reconstruction of the pre-Eruption AD 79 Paleo-topography and Paleo-environment of the Sarno River basin using Stratigraphical Core Drillings and Data Mining Technologies. 13th Congress Regional Committee on Mediterranean Neogene Stratigraphy (RCMNS) 'Earth System Evolution and the Mediterranean Area from 23Ma to the Present' Naples (Italy), 2nd-6th September 2009. Oral Presentation.

Vogel, S. and Märker, M., 2009. Reconstruction of the A.D. 79 Paleo-surface of the Sarno River basin using Data Mining Technologies and Classification and Regression Methods. International Meeting 'Geoarchaeology in Central Europe' Dresden (Germany), 30th April-2nd May 2009. Oral Presentation.

Heck, V. and Vogel, S., 2008. Rectification of Historic Royal Air Force Aerial Photos and Generation of an Orthophotomosaic of the Sarno River Basin. International Congress 'Historic maps and imagery for modern scientific applications' Bern (Switzerland), 28th-30th November 2008. Oral Presentation.

Vogel, S. and Märker, M., 2007. Reconstruction ot the A.D. 79 Paleo-surface of the Sarno River basin using Data Mining Technologies and Classification and Regression Methods-Preliminary results. International congress 'People/environ-ment relationships from the Mesolithic to the Middle Ages: recent geo-archaeological findings in Southern Italy' Salerno (Italy), 4th-7th September 2007. Poster Presentation.

Erklärungen gem. §§ 5 Abs. 2 und 6 Abs. 2 der Promotionsordnung der Mathematisch-Naturwissenschaftlichen Fakultät zum Antrag auf Zulassung zum Promotionsverfahren

Bitte nur die zutreffenden Erklärungen ankreuzen, Nichtzutreffendes streichen

☐ Ich erkläre hiermit, dass ich die zur Promotion eingereichte Arbeit selbständig verfasst, nur die angegebenen Quellen und Hilfsmittel benutzt und wörtlich oder inhaltlich übernommene Stellen als solche gekennzeichnet habe.

☐ Eine Erklärung über etwaige Promotionsverfahren (bisherige, abgebrochene oder abgeschlossene) oder entsprechende Prüfungsverfahren ist nicht beigefügt, da keiner der oben genannten Sachverhalte zutrifft. *(Gegebenenfalls eine Erklärung beifügen, wann und wo, in welchem Fach und mit welchem Ergebnis.)*

☐ Die vorgelegte Dissertation ist noch nicht ganz oder teilweise veröffentlicht worden und sie ist noch nicht ganz oder teilweise als Dissertation oder sonstige Prüfungsarbeit eingereicht worden. *(Gegebenenfalls eine Erklärung beifügen, wann und wo, in welchem Fach und mit welchem Ergebnis.)*

☐ Ich erkläre, dass mir die Gelegenheit zum vorliegenden Promotionsverfahren nicht kommerziell vermittelt wurde. Ich erkläre insbesondere, dass ich keine Organisation eingeschalten habe, die gegen Entgelt Betreuer für die Anfertigung von Dissertationen sucht oder die für ihn die ihm obliegenden Pflichten hinsichtlich der Prüfungsleistungen ganz oder teilweise erledigt.

☐ Eine Erklärung über strafrechtliche Verurteilungen, Disziplinarmaßnahmen und anhängige Straf- und Disziplinarmaßnahmen ist nicht beigefügt, da keiner der oben genannten Sachverhalte zutrifft. *(Gegebenenfalls eine Erklärung über strafrechtliche Verurteilungen, Disziplinar-maßnahmen und anhängige Straf- und Disziplinarverfahren, soweit die Auskunftspflicht nicht durch § 51 des Bundeszentralregistergesetzes ausgeschlossen ist, beifügen.)*

☐ Die Dissertation oder Teile der Dissertation sind Teil einer oder mehrerer Gemeinschaftsarbeiten, meine Beiträge wurden in eigener Verantwortung selbständig abgefasst. Eine Erklärung ist beigefügt über den Rahmen der gemeinschaftlichen Arbeit, die Namen der Mitarbeiter und deren Anteil an dem Gesamtprojekt und die Bedeutung meiner eigenen Beiträge für die Gemeinschaftsarbeit. *(Diese Erklärung muss vom Promotionskomitee (also den Betreuern) hinsichtlich aller Veröffentlichungen bei denen mehrere Autoren mitgewirkt haben, bestätigt werden.)*

_____   _____

Datum, Name in Blockschrift   Unterschrift